DEVELOPMENT OF INDICES FOR AGRICULTURAL DROUGHT MONITORING USING A SPATIALLY DISTRIBUTED HYDROLOGIC MODEL

A Dissertation

by

BALAJI NARASIMHAN

Submitted to the Office of Graduate Studies of
Texas A&M University
in partial fulfillment of the requirements for the degree of

DOCTOR OF PHILOSOPHY

August 2004

Major Subject: Biological and Agricultural Engineering

DEVELOPMENT OF INDICES FOR AGRICULTURAL DROUGHT MONITORING USING A SPATIALLY DISTRIBUTED HYDROLOGIC MODEL

A Dissertation

by

BALAJI NARASIMHAN

Submitted to Texas A&M University
in partial fulfillment of the requirements
for the degree of

DOCTOR OF PHILOSOPHY

Approved as to style and content by:

Raghavan Srinivasan (Co-Chair of Committee)	Binayak Mohanty (Co-Chair of Committee)
Patricia Haan (Member)	Anthony Cahill (Member)
Gerald Riskowski (Head of Department)	

August 2004

Major Subject: Biological and Agricultural Engineering

ABSTRACT

Development of Indices for Agricultural Drought Monitoring Using a Spatially Distributed Hydrologic Model. (August 2004)

Balaji Narasimhan, B.E., Tamil Nadu Agricultural University, India;

M.S., University of Manitoba, Canada

Co-Chairs of Advisory Committee: Dr. Raghavan Srinivasan
Dr. Binayak Mohanty

Farming communities in the United States and around the world lose billions of dollars every year due to drought. Drought Indices such as the Palmer Drought Severity Index (PDSI) and Standardized Precipitation Index (SPI) are widely used by the government agencies to assess and respond to drought. These drought indices are currently monitored at a large spatial resolution (several thousand km^2). Further, these drought indices are primarily based on precipitation deficits and are thus good indicators for monitoring large scale meteorological drought. However, agricultural drought depends on soil moisture and evapotranspiration deficits. Hence, two drought indices, the Evapotranspiration Deficit Index (ETDI) and Soil Moisture Deficit Index (SMDI), were developed in this study based on evapotranspiration and soil moisture deficits, respectively. A Geographical Information System (GIS) based approach was used to simulate the hydrology using soil and land use properties at a much finer spatial resolution ($16km^2$) than the existing drought indices.

The Soil and Water Assessment Tool (SWAT) was used to simulate the long-term hydrology of six watersheds located in various climatic zones of Texas. The simulated soil water was well-correlated with the Normalized Difference Vegetation Index NDVI ($r \sim 0.6$) for agriculture and pasture land use types, indicating that the model performed well in simulating the soil water.

Using historical weather data from 1901-2002, long-term weekly normal soil moisture and evapotranspiration were estimated. This long-term weekly normal soil moisture and evapotranspiration data was used to calculate ETDI and SMDI at a spatial resolution of 4km × 4km. Analysis of the data showed that ETDI and SMDI compared well with wheat and sorghum yields ($r > 0.75$) suggesting that they are good indicators of agricultural drought.

Rainfall is a highly variable input both spatially and temporally. Hence, the use of NEXRAD rainfall data was studied for simulating soil moisture and drought. Analysis of the data showed that raingages often miss small rainfall events that introduce considerable spatial variability among soil moisture simulated using raingage and NEXRAD rainfall data, especially during drought conditions. The study showed that the use of NEXRAD data could improve drought monitoring at a much better spatial resolution.

DEDICATION

I dedicate this dissertation to my family, especially to my parents A.V. Narasimhan and Alamelumangai Narasimhan. They have encouraged and supported me in many different ways in pursuing the doctoral degree. Without their many sacrifices, unflinching support, and encouragement it would not have been possible for me to complete this Ph.D. degree.

ACKNOWLEDGEMENTS

I would like to express my most sincere appreciation and gratitude to my major advisor, Dr. Raghavan Srinivasan for his patience, guidance, encouragement, constant enthusiastic support, and many kindnesses extended during the seemingly interminable period of this research. I would like to express my sincere appreciation for all the help and suggestions by my co-chair, Dr. Binayak Mohanty. I would also like to thank Dr. Patricia Haan and Dr. Anthony Cahill for serving as members of my advisory committee and for their help and suggestions. I would also like to thank Dr. Dale Whittaker for his help and encouragement during the early stages of my doctoral program.

I would like to extend my sincere thanks to these people who have helped in my dissertation in many ways:

- Dr. Mauro Di Luzio, Black Research Center, for modifying the ArcView SWAT extension to fit the needs of my project
- Dr. Jeff Arnold, Grassland Soil and Water Research Laboratory, for his help and advice while calibrating the SWAT model
- Ms. Nancy Simmons for her help in modifying the SWAT source code
- Ms. Susan Neitsch for her help in modifying the baseflow filter routine and useful tips while calibrating the model
- Dr. Rajaraman Jayakrishnan and Dr. Ramesh Sivanpillai for their constructive comments on my dissertation proposal

- Ms. Kim Twiggs for editing this manuscript
- My teachers Dr. K. Alagusundaram, and Dr. Santhana Bosu, Tamil Nadu Agricultural University for inspiring me to pursue a doctoral degree
- My colleagues Sabu Paul and Jennifer Hadley for their help and support

This research was supported by the Texas Higher Education Co-ordination Board's (THECB) Advanced Technology Program (ATP), project number 000517-0110-2001 titled, "A Real-Time Drought Assessment and Forecasting System for Texas Using GIS and Remote Sensing". The research effort was also partly funded by Texas Forest Service (TFS) and Texas Water Resources Institute (TWRI).

Finally I would like to thank my wife Sowmya for her love, care, affection, and constant encouragement which gave me the ability to withstand the setbacks experienced along the way and the energy needed to successfully complete the dissertation.

TABLE OF CONTENTS

CHAPTER Page

LIST OF FIGURES

FIGURE Page

FIGURE Page

LIST OF TABLES

TABLE Page

TABLE Page

CHAPTER I

INTRODUCTION

Overview

Drought is a normal, recurrent climatic feature that occurs in virtually every climatic zone around the world, causing billions of dollars in loss annually for the farming community. According to the U.S. Federal Emergency Management Agency (FEMA), the United States loses $6-8 billion annually on average due to drought (FEMA 1995). During the 1998 drought, the state of Texas alone lost a staggering $5.8 billion (Chenault and Parsons 1998), which is about 39% of the $15 billion annual agriculture revenue of the state (Sharp 1996). Bryant (1991) ranked natural hazard events based on various characteristics, such as severity, duration, spatial extent, loss of life, economic loss, social effect, and long-term impact and found that drought ranks first among all natural hazards. This is because, compared to other natural hazards like flood and hurricanes that develop quickly and last for a short time, drought is a creeping phenomenon that accumulates over a period of time across a vast area, and the effect lingers for years even after the end of drought (Tannehill 1947). Hence, the loss of life, economic impact, and effects on society are spread over a long period of time, which makes drought the worst among all natural hazards. In spite of the economic and the social impact caused by drought, it is the least understood of all natural hazards due to

---

This dissertation follows the style and format of *Transactions of the American Society of Agricultural Engineers*.

the complex nature and varying effects of droughts on different economic and social sectors (Wilhite 2000).

Drought Definition

Although deviation from the normal amount of precipitation over an extended period of time is broadly accepted as the cause for drought, there is no one, universally accepted definition for drought. This is because different disciplines use water in various ways and thus use different indicators for defining and measuring drought. Wilhite and Glantz (1985) analyzed more than 150 such definitions of drought and then broadly grouped those definitions under four categories: meteorological, agricultural, hydrological and socio-economic drought.

- Meteorological drought: A period of prolonged dry weather condition due to precipitation departure.
- Agricultural drought: Agricultural impacts caused due to short-term precipitation shortages, temperature anomaly that causes increased evapotranspiration and soil water deficits that could adversely affect crop production.
- Hydrological drought: Effect of precipitation shortfall on surface or subsurface water sources like rivers, reservoirs and groundwater.
- Socioeconomic drought: The socio economic effect of meteorological, agricultural and hydrologic drought associated with supply and demand of the society.

Based on the defined drought criteria, the intensity and duration of drought is expressed with a drought index. A drought index integrates various hydrological and meteorological parameters like rainfall, temperature, evapotranspiration (ET), runoff and other water supply indicators into a single number and gives a comprehensive picture for decision-making. Federal and State government agencies use such drought indices to assess and respond to drought. Among various drought indices, the Palmer Drought Severity Index (PDSI) (Palmer 1965), Crop Moisture Index (CMI) (Palmer 1968), Surface Water Supply Index (SWSI) (Shafer and Dezman 1982), and Standardized Precipitation Index (SPI) (McKee et al 1993) are used extensively for water resources management, agricultural drought monitoring and forecasting. Each of these drought indices are explained briefly in the following section.

Palmer Drought Severity Index (PDSI)

One of the most widely used drought indices is the Palmer Drought Severity Index (PDSI) (Palmer 1965). PDSI is primarily a meteorological drought index formulated to evaluate prolonged periods of both abnormally wet and abnormally dry weather conditions. PDSI has gained the widest acceptance because the index is based on a simple lumped parameter water balance model. The input data needed for PDSI are precipitation, temperature, and average available water content of the soil for the entire climatic zone. From these inputs, using a simple lumped parameter water balance model, various water balance components including evapotranspiration, soil recharge, runoff, and moisture loss from the surface layer are calculated. Using coefficients

established from 30-year historical weather data and the current water balance components, a Climatically Appropriate For Existing Conditions (CAFEC) precipitation is computed. Then the precipitation deficit is computed as the difference between the actual precipitation and the CAFEC precipitation. From this precipitation deficit, PDSI is calculated based on empirical relationships. More details on PDSI computations are presented in Palmer (1965), Alley (1984) and Akinremi and McGinn (1996).

Crop Moisture Index (CMI)

The PDSI developed by Palmer (1965) is a useful indicator for monitoring long-term drought conditions resulting from precipitation deficit. However, agricultural crops are highly susceptible to short-term moisture deficits during critical periods of crop growth. Further, there is a time lag between the occurrence of precipitation deficit and the agricultural drought due to the buffering effect caused by soil moisture reserve available for crop growth. Hence, Palmer (1968) developed the Crop Moisture Index (CMI) as an index for short-term agricultural drought from procedures within the calculation of the PDSI. PDSI is calculated from precipitation deficits for monitoring long-term drought conditions, whereas CMI is calculated from evapotranspiration deficits for monitoring short-term agricultural drought conditions that affect crop growth. More details on the computation of CMI are presented in Palmer (1968).

Standardized Precipitation Index (SPI)

During the past decade, another meteorological drought index that has gained wide acceptance is the Standardized Precipitation Index (SPI). SPI is primarily a meteorological drought index based on the precipitation amount in a 3, 6, 9, 12, 24 or 48 month period. In calculating the SPI, the observed rainfall values during 3, 6, 9, 12, 24 or 48 month period are first fitted to a Gamma distribution. The Gamma distribution is then transformed to a Gaussian distribution (standard normal distribution with mean zero and variance of one), which gives the value of the SPI for the time scale used. More details on the computation of SPI are presented in McKee et al. (1993).

Surface Water Supply Index (SWSI)

The SWSI was primarily developed as a hydrological drought index with an intention to replace PDSI for areas where local precipitation is not the sole or primary source of water. For many water resources applications, such as urban and industrial water supplies, irrigation, navigation, and power generation, the water supply is primarily available in rivers and reservoirs. The SWSI is calculated based on monthly non-exceedance probability from available historical records of reservoir storage, stream flow, snow pack, and precipitation. More details on the computation of SWSI are presented in Shafer and Dezman (1982).

Limitations of Existing Drought Indices for Monitoring Agricultural Drought

PDSI and CMI

The U.S. Department of Agriculture (USDA) primarily uses PDSI and CMI to determine the magnitude of drought and when it is necessary to grant emergency drought assistance to farmers and ranchers. Despite the widespread acceptance of PDSI and CMI, Alley (1984) has observed several limitations, which are outlined in this section.

- In PDSI, potential evapotranspiration (ET) is calculated using Thornthwaite's method. Thornthwaite's equation for estimating ET is based on an empirical relationship between evapotranspiration and temperature (Thornthwaite 1948). Jensen et al. (1990) evaluated and ranked different methods of estimating ET under various climatic conditions and concluded that the poorest performing method overall was the Thornthwaite equation. Palmer (1965) also suggested replacing Thornthwaite's equation with a more appropriate method. Thus, a physically-based method like the FAO Penman-Monteith equation (Allen et al 1998) must be used for estimating ET.
- The water balance model used by Palmer (1965) is a two-layer lumped parameter model. Palmer assumed an average water holding capacity of the top two soil layers for the entire region in a climatic division (7000 to 100,000 km^2). However, in reality, soil properties vary widely on a much smaller scale. This often makes it difficult to spatially delineate the areas affected by drought.

Further, PDSI and CMI do not account for the effect of land use/land cover on the water balance.

- Palmer (1965) assumed runoff occurs when the top two soil layers become completely saturated. In reality, runoff depends on soil type, land use, and management practices. However, Palmer (1965) does not account for these factors while estimating runoff.

SPI

Unlike PDSI, SPI takes into account the stochastic nature of the drought and is therefore a good measure of meteorological drought. However, SPI does not account for the effect of soil, land use characteristic, crop growth, and temperature anomalies that are critical for agricultural drought monitoring. Also, the useable precipitation ultimately available for crop growth depends on the available soil moisture at the root zone rather than total rainfall itself. Hence, a drought index based on soil moisture conditions would be a better indicator of agricultural drought.

SWSI

The purpose of SWSI is primarily to monitor the abnormalities in surface water supply sources as influenced by precipitation, stream flow, reservoir storage, and snow pack. Hence it is a good measure to monitor the impact of hydrologic drought on urban and industrial water supplies, irrigation and hydroelectric power generation. According to 1997 estimates of the Economic Research Service (2000) of the USDA, only about

11.6% of total cropland in the U.S. is on irrigated land, whereas the vast majority of cropland is dry land agriculture, which depends on precipitation as the only source of water. There is a time lag before precipitation deficiencies are detected in surface and subsurface water sources. As a result, the hydrological drought is out of phase from meteorological and agricultural droughts. Because of this phase difference, SWSI is not a suitable indicator for agricultural drought.

Problem Statement

Most of the existing drought indices were solely based on precipitation and/or temperature since long-term records of these meteorological variables are readily available for most parts of the world. However, the amount of available soil moisture at the root zone is a more critical factor for crop growth than the actual amount of precipitation deficit or excess. The soil moisture deficit in the root zone during various stages of the crop growth cycle has a profound impact on the crop yield. For example, a 10% water deficit during the tasseling, pollination stage of corn could reduce the yield by as much as 25% (Hane and Pumphrey 1984). Hence, the development of a reliable drought index for agriculture requires proper consideration of vegetation type, crop growth and root development, soil properties, antecedent soil moisture condition, evapotranspiration, and temperature. The drought indices PDSI and CMI, both currently used for agricultural drought monitoring, do not give proper consideration to the aforementioned variables. Further the indices are based on a lumped parameter model that assumes a uniform soil property, precipitation and temperature for the entire

climatic division encompassing several thousand square kilometers and reported on a monthly time scale. Thus, they fail to capture any localized short-term soil moisture anomalies for weeks during critical stages of crop growth, which can have a significant impact on the crop yield. Hence, proper consideration of the spatial variability of soil and land use properties, as well as of crop growth and root development, will certainly improve our ability to monitor drought (i.e., moisture deficit) on a much more precise scale. Due to advancements in Geographical Information Systems (GIS), GIS-based distributed parameter hydrologic models, and remote–sensing, a more effective drought assessment system can be developed at a higher spatial and temporal resolution.

Dissertation Objectives

The objectives of this dissertation research are:

1. To develop a long-term record of soil moisture and evapotranspiration for different soil and land use types, using a comprehensive hydrologic and crop growth model Soil and Water Assessment Tool (SWAT), GIS and historical weather data for Texas,
2. To develop drought indices based on soil moisture and evapotranspiration deficits and evaluate the performance of the indices for monitoring agricultural drought, and
3. To study the effect of spatially distributed rainfall from NEXt generation weather RADar (NEXRAD) rainfall data in the estimation of the drought indices.

Significance of the Research

In the U.S., agriculture cropland accounts for 17% of the total land use but it is responsible for 85% of consumptive water use (Goklany 2002). Due to such high dependence on water and soil moisture reserves, agriculture is often the first sector to be affected by drought. Texas is the second leading agriculture-producing state in the U.S., with 22.5% of land in agriculture cropland. Texas is plagued by at least one serious drought every decade (Riggo et al. 1987). The dust bowl days of the 1930's, the mammoth drought during the 1950's that lasted seven years and the droughts during the 80's and the 90's had a devastating impact on the Texas agriculture and livestock industry. These emphasize the vulnerability of the agricultural sector to drought and the need for more research to understand and develop tools that would help in planning to mitigate the impacts of drought.

The proposed dissertation research will provide a new foundation for GIS-based approaches for assessing, monitoring and managing drought through the development of a spatially distributed drought index at a much finer spatial ($16km^2$) and temporal (weekly) resolution. The consideration of spatial variability of parameters like soil type and land use creates a better approximation of the hydrologic system and will improve our ability to monitor drought (i.e., moisture deficit) at a much better spatial resolution. The increased spatial and temporal resolution will give the farming community, water managers and policy makers a better tool for assessing, forecasting and managing agricultural drought on a much more precise scale.

CHAPTER II

MODELING LONG-TERM SOIL MOISTURE USING SWAT IN TEXAS RIVER BASINS FOR DROUGHT ANALYSIS

Synopsis

Soil moisture is an important hydrologic variable that controls various land surface processes. In spite of its importance to agriculture and drought monitoring, soil moisture information is not widely available on a regional scale. However, long-term soil moisture information is essential for agricultural drought monitoring and crop yield prediction. The hydrologic model Soil and Water Assessment Tool (SWAT) was used to develop a long-term record of soil water from historical weather data at a fine spatial ($16km^2$) and temporal (weekly) resolution. The model was calibrated and validated using stream flow data. However, stream flow accounts for only a small fraction of the hydrologic water balance. Due to the lack of measured evapotranspiration or soil moisture data, the simulated soil water was evaluated in terms of vegetation response, using 16 years of Normalized Difference Vegetation Index (NDVI) derived from satellite data. The simulated soil water was well-correlated with NDVI ($r \sim 0.6$) for agriculture and pasture land use types, during the active growing season April-September, indicating that the model performed well in simulating the soil water. The simulated soil moisture data can be used in subsequent studies for agricultural drought monitoring.

Introduction

Soil moisture is an important hydrologic variable that controls various land surface processes. The term "soil moisture" generally refers to the temporary storage of precipitation in the top one to two meters of soil horizon. Although only a small percentage of total precipitation is stored in the soil after accounting for evapotranspiration (ET), surface runoff and deep percolation, soil moisture reserve is critical for sustaining agriculture, pasture and forestlands. It holds more importance especially for non-irrigated agriculture because, according to 2002 county estimates of cropland in Texas, non-irrigated crop acreage of major crops like corn, wheat, cotton and sorghum far exceed the irrigated acreage (TASS 2003). Given the fact that precipitation is a random event, soil moisture reserve is essential for regulating the water supply for crops between precipitation events. Soil moisture is an integrated measure of several state variables of climate and physical properties of land use and soil. Hence, it is a good measure for scheduling various agricultural operations, crop monitoring, yield forecasting, and drought monitoring.

In spite of its importance to agriculture and drought monitoring, soil moisture information is not widely available on a regional scale. This is partly because soil moisture is highly variable both spatially and temporally and is therefore difficult to measure on a large scale. The spatial and temporal variability of soil moisture is due to heterogeneity in soil properties, land cover, topography, and non-uniform distribution of precipitation and ET.

On a local scale, soil moisture is measured using various instruments, such as tensiometers, TDR probes (TDR – Time Domain Reflectometry), neutron probes, gypsum blocks, and capacitance sensors (Zazueta and Xin 1994). The field measurements are often widely spaced and the averages of these point measurements seldom yield soil moisture information on a watershed scale or regional scale due to the heterogeneity involved.

In this regard, microwave remote sensing is emerging as a better alternative for getting a reliable estimate of soil moisture on a regional scale. With the current microwave technology, it is possible to estimate the soil moisture accurately only at the top 5cm of the soil (Engman 1991). However, the root systems of most agricultural crops extract soil moisture from 20 to 50cm at the initial growth stages and extend deeper as the growth progresses (Verigo and Razumova 1966). Further, the vegetative characteristics, soil texture and surface roughness strongly influence the microwave signals and introduce uncertainty in the soil moisture estimates (Jackson et al. 1996).

Field scale data and remotely sensed soil moisture data are available for only a few locations and are lacking for large areas and for multiyear periods (Huang et al. 1996). However, long-term soil moisture information is essential for agricultural drought monitoring and crop yield prediction. Keyantash and Dracup (2002) also noted the lack of a national soil moisture monitoring network in spite of its usefulness for agricultural drought monitoring.

Long-term Soil Moisture Modeling

A possible alternative for obtaining long-term soil moisture information is to use historical weather data. Long-term weather data, such as precipitation and temperature, are widely available and can be used with spatially distributed hydrologic models to simulate soil moisture. Very few modeling studies conducted in the past were aimed at using hydrologic models for the purpose of monitoring soil moisture and drought.

Palmer (1965) used a simple two-layer lumped parameter water balance model to develop the Palmer Drought Severity Index (PDSI). The model is based on monthly time step and uses monthly precipitation and temperature as weather inputs and average water holding capacity for the entire climatic division (7000 to 100,000 km^2). From these inputs, a simple lumped parameter water balance model is used to calculate various water balance components including ET, soil recharge, runoff, and moisture loss from the surface layer. Then, using empirical relationships, the water balance components are converted into precipitation deficit from which the PDSI is calculated. Alley (1984) has highlighted the limitations of Palmer's approach, primarily concerning the water balance calculation and the use of the lumped parameter approach for modeling such a large area. Further, land use characteristics and crop growth, which significantly affect the hydrology of the watershed, are not considered in the model.

Akinremi and McGinn (1996) found that the water balance model used by Palmer (1965) did not account for snowmelt, which is significant in Canadian climatic conditions. In order to overcome this limitation, Akinremi and McGinn (1996) used the

modified Versatile Soil Moisture Budget (VB), developed by Akinremi et al. (1996). In the VB, the soil profile is divided into several zones and water is simultaneously withdrawn from different zones in relation to the ratio of potential ET and available soil moisture in each zone. Akinremi and McGinn (1996) found that VB coupled with Palmer's index simulated the soil moisture conditions better under snowmelt conditions in Canada.

Huang et al. (1996) developed a one-layer soil moisture model to derive a historical record of monthly soil moisture over the entire U.S. for applications of long-range temperature forecasts. The model uses monthly temperature and monthly precipitation as inputs, calculates surface runoff as a simple function of antecedent soil moisture and precipitation, and estimates ET using the Thornthwaite (1948) method. The model was calibrated using observed runoff data in Oklahoma, and the same parameters were applied for modeling the entire U.S. Eight-year average monthly soil moisture (1984-1991) measured at 16 stations in Illinois compared well with the average soil moisture predicted by the model at nine climate divisions.

In all of the aforementioned studies for determining soil moisture, the weather data is used at a coarse temporal (monthly) and spatial (several thousand km^2) resolution. However, precipitation has high spatial and temporal variability; hence, it is not realistic to assume a uniform distribution of precipitation over the entire climatic division. Further, physical properties of soil, land use and topography are highly heterogeneous and govern the hydrologic response on a local scale. Also, soil moisture

stress can develop rapidly over a short period of time, and moisture stress during critical stages of crop growth can significantly affect the crop yield. For example, a 10% water deficit during the tasseling, pollination stage of corn could reduce the yield as much as 25% (Hane and Pumphrey 1984).

There are other classes of models similar to the Simple Biosphere Model (SiB) (Sellers et al. 1986) that simulate land surface fluxes (radiation, heat, moisture) for use within the General Circulation Model (GCM), which handles large-scale climate change studies and climate forecasts over a long period of time. However, these models are developed for a different purpose – climate forecasting on a larger scale and are data intensive. They cannot be applied on a catchment scale due to the lack of model parameters and sub-hourly input data, primarily radiation.

A good compromise would be to select a hydrologic model that (1) takes into account the major land surface processes and climatic variables, (2) gives proper consideration to spatial variability of soil and land use properties, (3) models crop growth and root development, and (4) uses readily available data inputs. Such a model will certainly improve our ability to monitor soil moisture at a higher spatial and temporal resolution.

The objective of this paper is to develop long-term soil moisture information, at 4km × 4km spatial resolution and weekly temporal resolution, for selected watersheds in Texas, using a spatially distributed hydrologic model.

Hydrologic Model Selection

Many comprehensive spatially distributed hydrologic models have been developed in the past decade due to advances in hydrologic sciences, Geographical Information System (GIS), and remote-sensing. Among the many hydrologic models developed in the past decade, the Soil and Water Assessment Tool (SWAT), developed by Arnold et al. (1993), has been used extensively by researchers. This is because SWAT (1) uses readily available inputs for weather, soil, land, and topography, (2) allows considerable spatial detail for basin scale modeling, and (3) is capable of simulating crop growth and land management scenarios.

SWAT has been integrated with GRASS GIS (Srinivasan and Arnold 1994; Srinivasan et al. 1998b) and with ArcView GIS (Di Luzio et al. 2002b), and the hydrologic components of the model have been validated for numerous watersheds under varying hydrologic conditions (Arnold and Allen 1996; Arnold et al. 2000; Harmel et al. 2000; Saleh et al. 2000; Sophocleous and Perkins 2000; Spruill et al. 2000; Santhi et al. 2001; Srinivasan et al. 1998a; Srinivasan et al. 1998b).

Arnold and Allen (1996) compared multiple components of water budget including surface runoff, groundwater flow, groundwater ET, ET in the soil profile, groundwater recharge, and groundwater heights simulated by the SWAT model with measured data for three Illinois watersheds (122-246km^2). The predicted data compared well with the measured data for each component of the water budget and demonstrated that the interaction among different components of the model was realistic. Most

components of the water budget were within 5% of the measured data and nearly all were within 25%.

Srinivasan and Arnold (1994) used SWAT to design the Hydrologic Unit Model for the United States (HUMUS) to improve water resources management at the local and regional levels. About 2,150 eight-digit hydrologic unit areas were simulated and the uncalibrated runoff was compared with observed runoff from over 5,951 stream gauging stations unaffected by manmade structures like reservoirs and diversions for the period 1951-80. The model simulated runoff compared reasonably well with observed streamflow data, encompassing a wide variety of terrains and climatic zones, ranging from high runoff in the northeastern states to low runoff in the southwestern states and the rugged terrains of Appalachian Mountains. However, due to the lack of weather stations at high elevations, the model under-predicted runoff in mountainous terrain.

SWAT is recognized by the U.S. Environmental Protection Agency (EPA) and has been incorporated into the EPA's BASINS (Better Assessment Science Integrating Point and Non-point Sources) (Di Luzio et al. 2002a). [BASINS is a multipurpose environmental analysis software system developed by the EPA for performing watershed and water quality studies on various regional and local scales.]. In order to optimally calibrate the model parameters, especially for large-scale modeling, an auto-calibration routine has been added to SWAT (Eckhardt and Arnold 2001; Van Griensven and Bauwens 2001). Hence, SWAT will be used in this study to simulate historical soil

moisture available at the root zone, using readily available soil, topography, land use, and weather data.

Methodology

Soil and Water Assessment Tool (SWAT)

SWAT is a physically based basin-scale continuous time distributed parameter hydrologic model that uses spatially distributed data on soil, land use, Digital Elevation Model (DEM), and weather data for hydrologic modeling and operates on a daily time step. Major model components include weather, hydrology, soil temperature, plant growth, nutrients, pesticides, and land management. A complete description of the SWAT model components (Version 2000) is found in Arnold et al. (1998) and Neitsch et al. (2002). A brief description of the SWAT hydrologic component is given here.

For spatially explicit parameterization, SWAT subdivides watersheds into sub-basins based on topography, which are further subdivided into hydrologic response units (HRU) based on unique soil and land use characteristics. Four storage volumes represent the water balance in each HRU in the watershed: snow, soil profile (0-2m), shallow aquifer (2-20m), and deep aquifer (> 20m). The soil profile can be subdivided into multiple layers. Soil water processes include surface runoff, infiltration, evaporation, plant water uptake, inter (lateral) flow, and percolation to shallow and deep aquifers.

SWAT can simulate surface runoff using either the modified SCS curve number

(CN) method (USDA Soil Conservation Service 1972) or the Green and Ampt infiltration model based on infiltration excess approach (Green and Ampt 1911) depending on the availability of daily or hourly precipitation data, respectively. The SCS curve number method was used in this study with daily precipitation data. Based on the soil hydrologic group, vegetation type and land management practice, initial CN values are assigned from the SCS hydrology handbook (USDA Soil Conservation Service 1972). SWAT updates the CN values daily based on changes in soil moisture.

The excess water available after accounting for initial abstractions and surface runoff, using SCS curve number method, infiltrates into the soil. A storage routing technique is used to simulate the flow through each soil layer. SWAT directly simulates saturated flow only and assumes that water is uniformly distributed within a given layer. Unsaturated flow between layers is indirectly modeled using depth distribution functions for plant water uptake and soil water evaporation. Downward flow occurs when the soil water in the layer exceeds field capacity and the layer below is not saturated. The rate of downward flow is governed by the saturated hydraulic conductivity. Lateral flow in the soil profile is simulated using a kinematic storage routing technique that is based on slope, slope length and saturated conductivity. Upward flow from a lower layer to the upper layer is regulated by the soil water to field capacity ratios of the two layers. Percolation from the bottom of the root zone is recharged to the shallow aquifer.

SWAT has three options for estimating potential ET – Hargreaves (Hargreaves and Samani 1985), Priestley-Taylor (Priestley and Taylor 1972), and Penman-Monteith

(Monteith 1965). The Penman-Monteith method was used in this study. SWAT computes evaporation from soils and plants separately as described in Ritchie (1972). Soil water evaporation is estimated as an exponential function of soil depth and water content based on potential ET and a soil cover index based on above ground biomass. Plant water evaporation is simulated as a linear function of potential ET, leaf area index (LAI), root depth (from crop growth model), and soil water content.

The crop growth model used in SWAT is a simplification of the EPIC crop model (Williams et al. 1984). A single model is used for simulating both annual and perennial plants. Phenological crop growth from planting is based on daily-accumulated heat units above a specified optimal base temperature for each crop, and the crop biomass is accumulated each day based on the intercepted solar radiation until harvest. The canopy cover, or LAI, and the root development are simulated as a function of heat units and crop biomass.

Study Area

Six watersheds located in major river basins across Texas were selected for this study (Fig.2.1 and 2.2). These watersheds were selected to simulate hydrology under diverse vegetation, topography, soil, and climatic conditions. The watershed characteristics and the land use distribution of each watershed are given in Table 2.1 and Table 2.2 respectively. The land use distribution, sub-basins and United States Geological Survey (USGS) streamgage locations for six watersheds are shown in Figures 2.3 to 2.8.

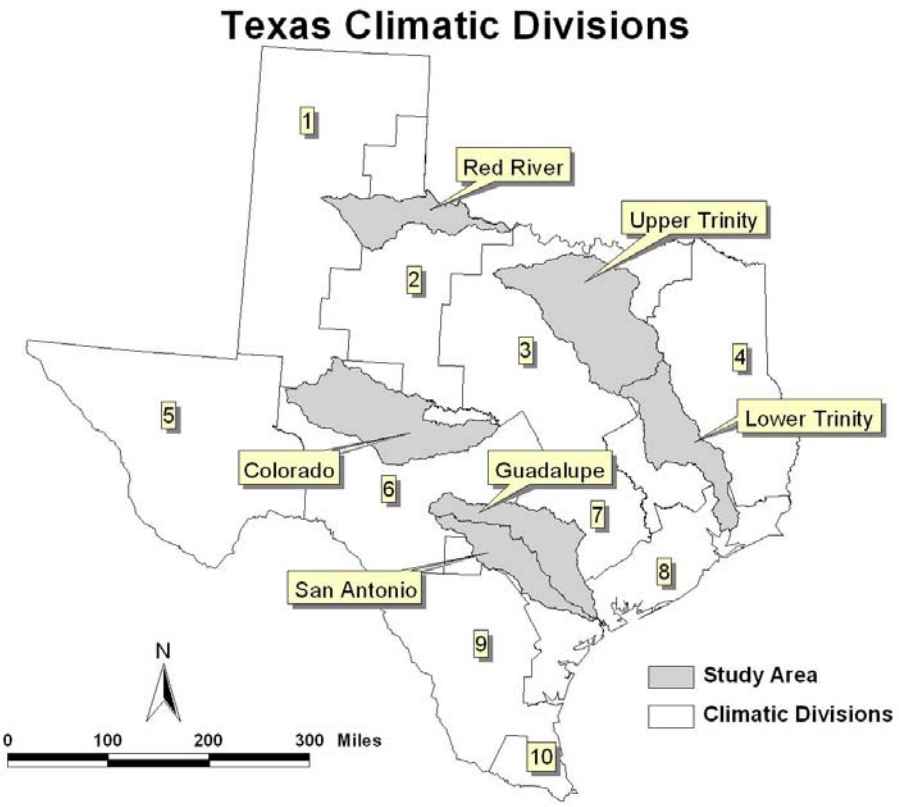

Figure 2.1 Texas climatic divisions and locations of six watersheds.

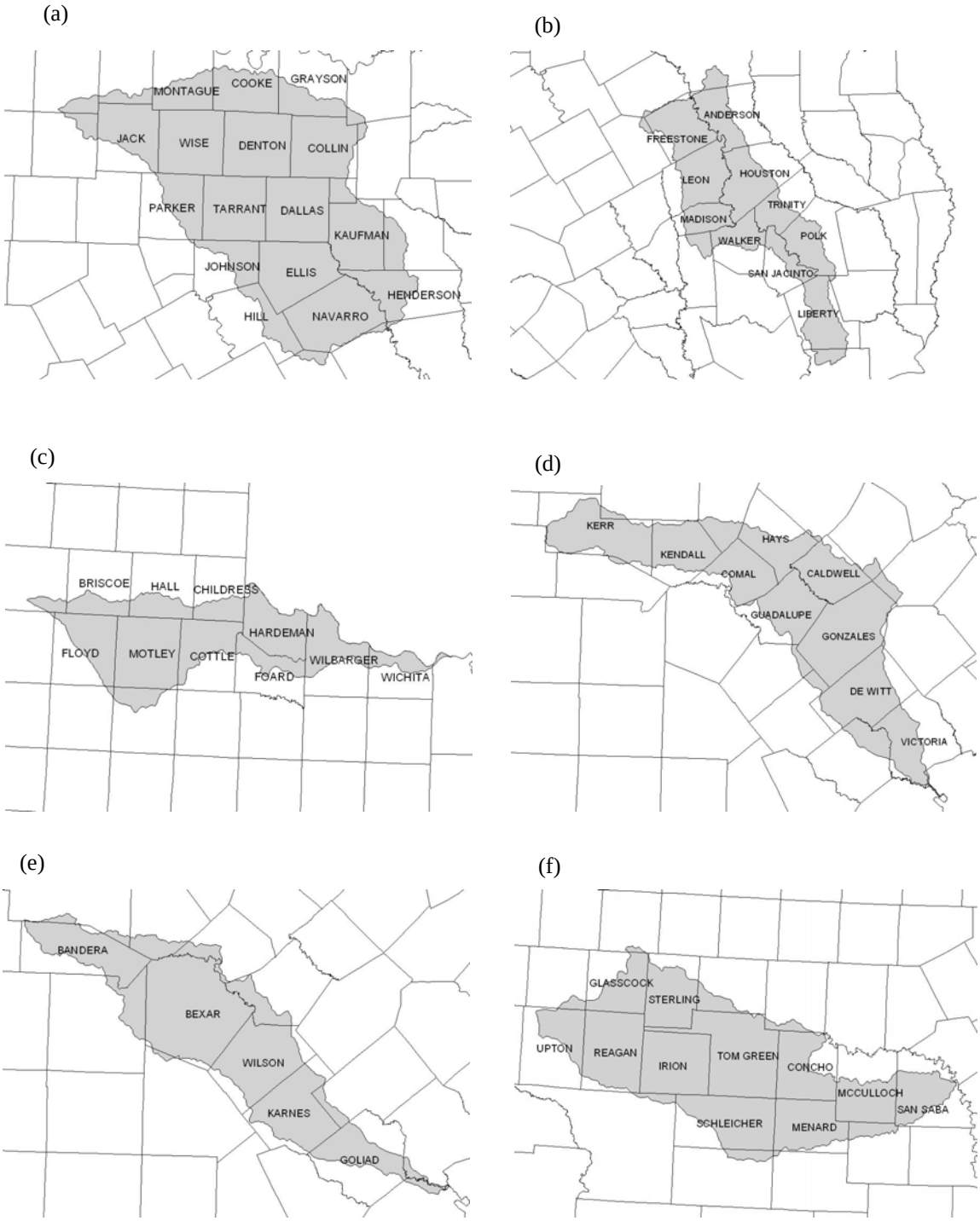

Figure 2.2 Counties located in six watersheds. a) Upper Trinity b) Lower Trinity c) Red River d) Guadalupe River e) San Antonio River f) Colorado River.

Table 2.1 Watershed characteristics.

Watershed	USGS 6-digit Hydrologic Cataloging Unit No.	Area (km^2)	Number of 4km×4km sub-basins	Elevation* (m)	Mean Annual Precipitation** (mm)
Upper Trinity	120301	29664	1854	78 - 408	729 - 1084
Lower Trinity	120302	15200	950	0 - 180	978 - 1368
Red River	111301	11632	727	295 - 1064	488 - 748
Guadalupe	121002	14736	921	6 - 728	712 - 990
San Antonio	121003	10320	645	7 - 688	693 - 976
Colorado	120901	25656	1541	400 - 886	365 - 708

* USGS 7.5-minute DEM (USGS 1993)
**NRCS PRISM annual precipitation data (Daly et al. 1994)

Table 2.2 Land use distribution in watersheds obtained from USGS National Land Cover Data.

Watershed	Land use (%)						
	Agriculture	Urban	Forest	Pasture	Rangeland	Wetland	Water
Upper Trinity	5.1	8.8	1.6	79.9	0	0.4	4.2
Lower Trinity	1.5	0.8	34.2	54.2	0	6.2	3.1
Red River	49.9	0.1	0	34	16	0	0
Guadalupe	1.8	1.1	30.4	59.1	6.2	1.1	0.3
San Antonio	4.3	8.5	32.9	47	6.4	0.6	0.3
Colorado	10.3	0.5	1.1	4.9	82.9	0	0.3

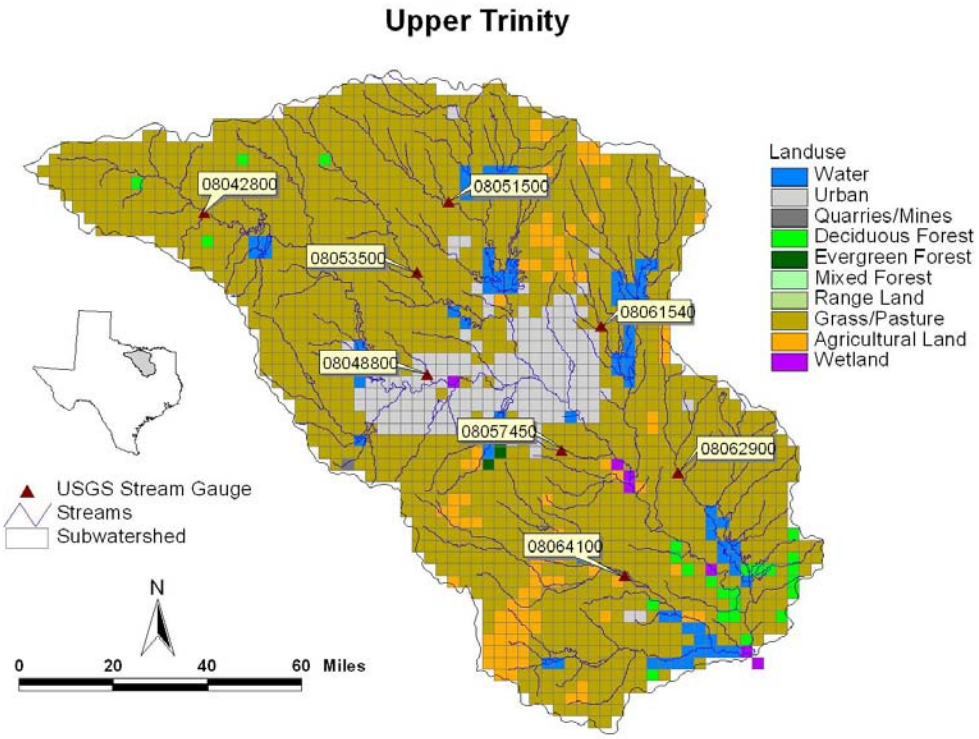

Figure 2.3 Sub-basins, NLCD land use data based on dominant land use within each sub-basin, and USGS stations in Upper Trinity watershed.

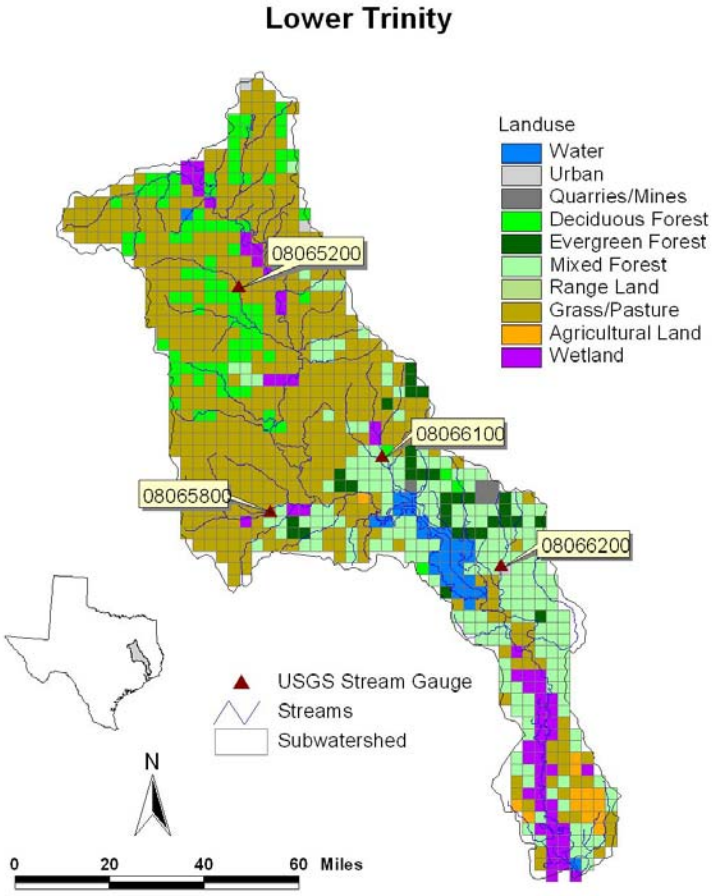

Figure 2.4 Sub-basins, NLCD land use data based on dominant land use within each sub-basin, and USGS stations in Lower Trinity watershed.

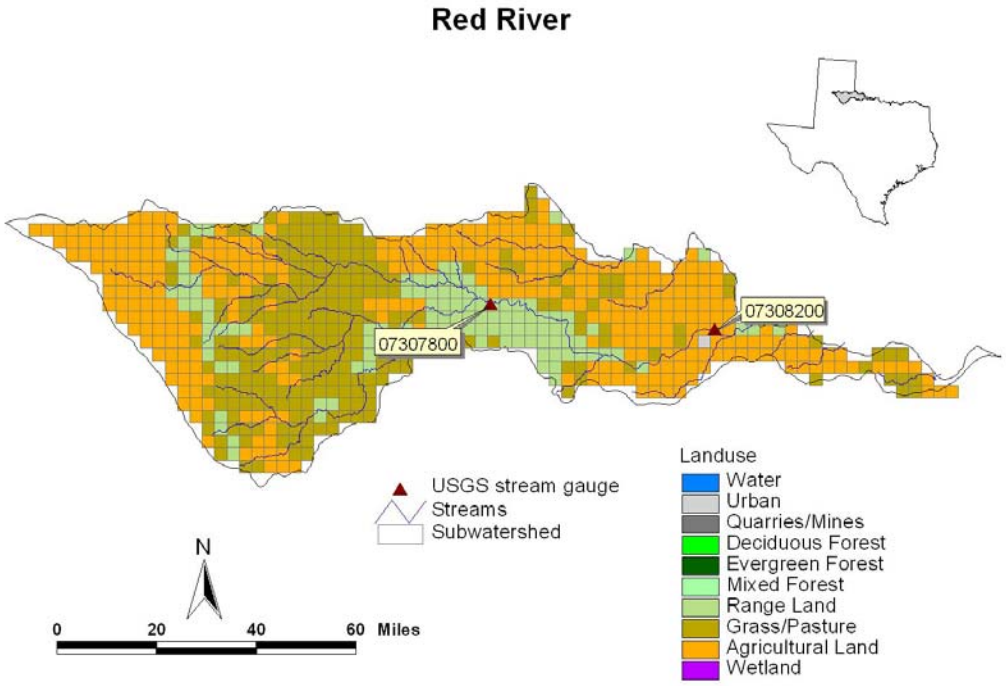

Figure 2.5 Sub-basins, NLCD land use data based on dominant land use within each sub-basin, and USGS stations in Red River watershed.

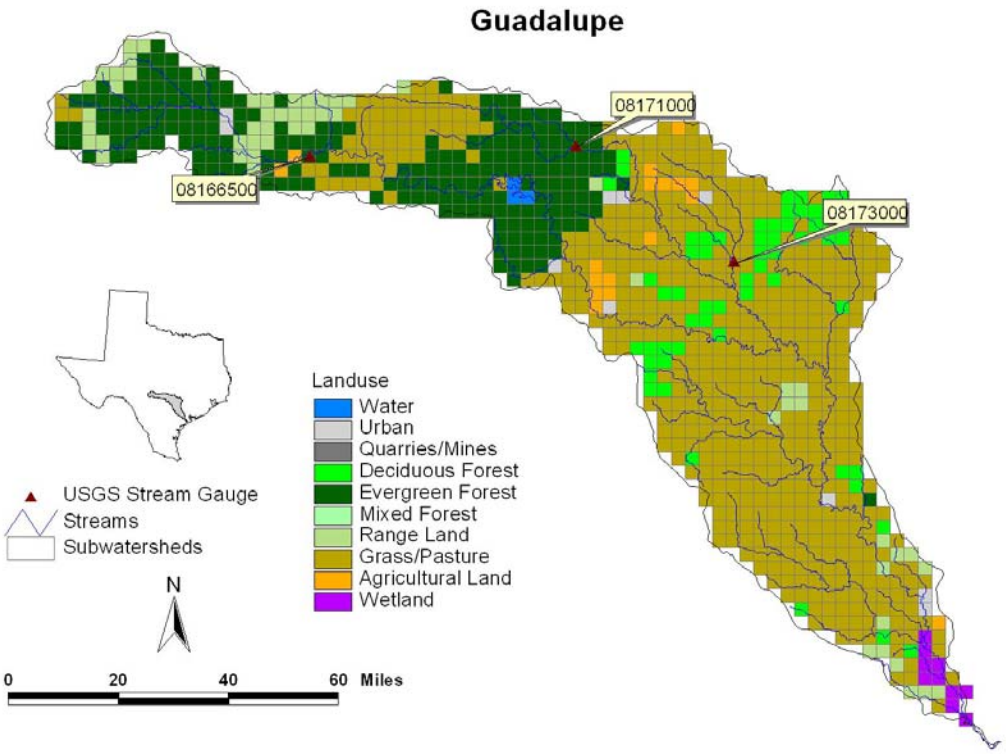

Figure 2.6 Sub-basins, NLCD land use data based on dominant land use within each sub-basin, and USGS stations in Guadalupe River watershed.

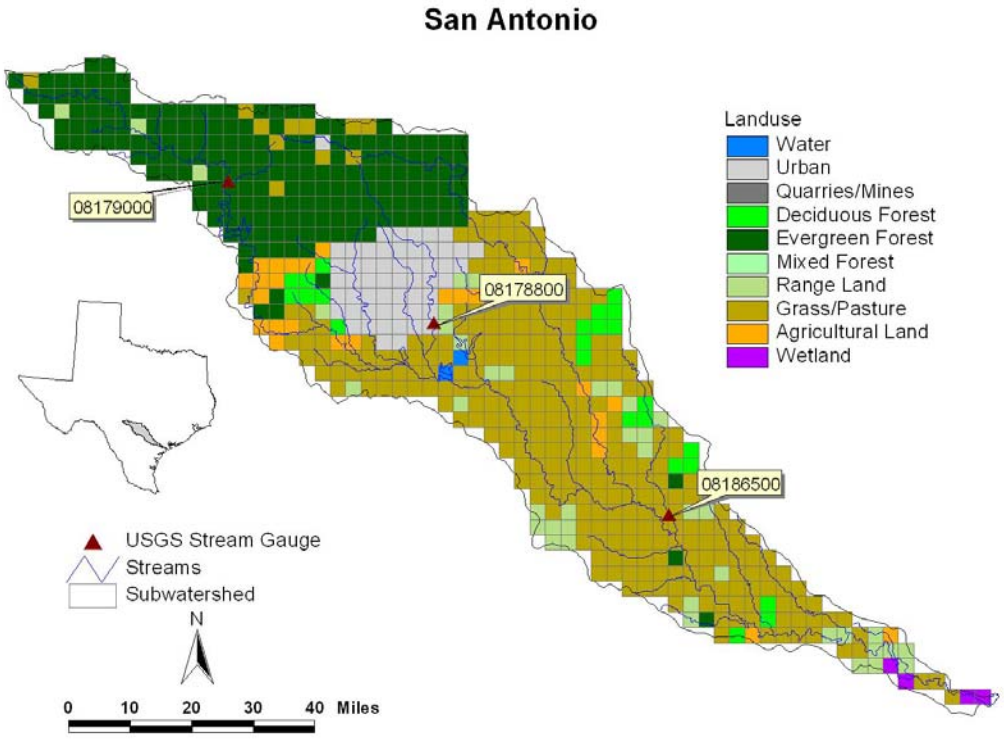

Figure 2.7 Sub-basins, NLCD land use data based on dominant land use within each sub-basin, and USGS stations in San Antonio River watershed.

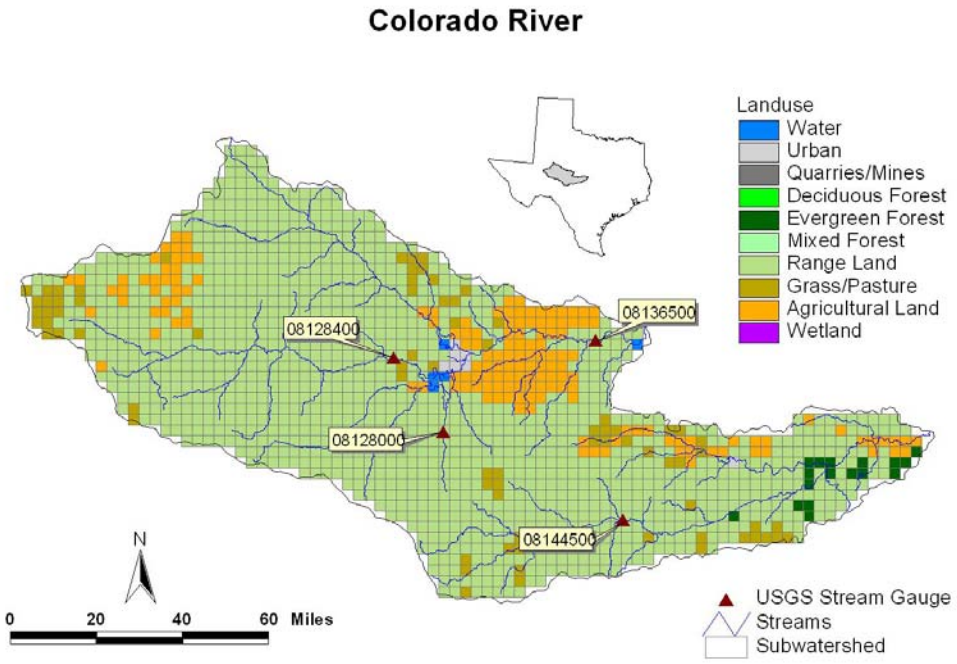

Figure 2.8 Sub-basins, NLCD land use data based on dominant land use within each sub-basin, and USGS stations in Colorado River watershed.

Pasture is the dominant land use in all of the watersheds except in the Red River and Colorado watersheds. In the Red River and Colorado watersheds, agriculture and rangeland are the respective dominant land uses. A significant portion of the Guadalupe and San Antonio watersheds are forestlands. The elevation difference between the upstream and downstream ends of all the watersheds is greater than 400m, except for the Lower Trinity which is 180m. Mean annual precipitation varies considerably among different watersheds and within each watershed (Table 2.1), which represent a wide spectrum of precipitation regimes in Texas.

Model Inputs

Weather inputs needed by SWAT are precipitation, maximum and minimum air temperatures, wind velocity, relative humidity, and solar radiation. Except daily air temperature and precipitation, daily values of weather parameters were generated from average monthly values using the weather generator built within SWAT. For this study, daily precipitation measured at 903 weather stations, and maximum and minimum air temperatures measured at 492 weather stations across Texas were obtained from the National Climatic Data Center (NCDC) (Fig.2.9 and 2.10). The data were obtained for the past 102 years (1901-2002) for the purpose of simulating a historical record of soil moisture for the watersheds. Missing precipitation and temperature records of individual stations were filled from the nearest stations where data was available.

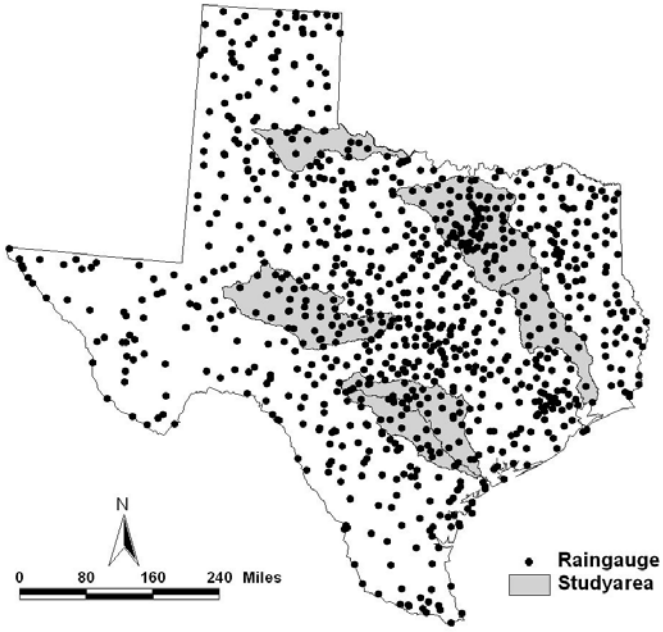

Figure 2.9 NCDC weather stations that measure daily precipitation.

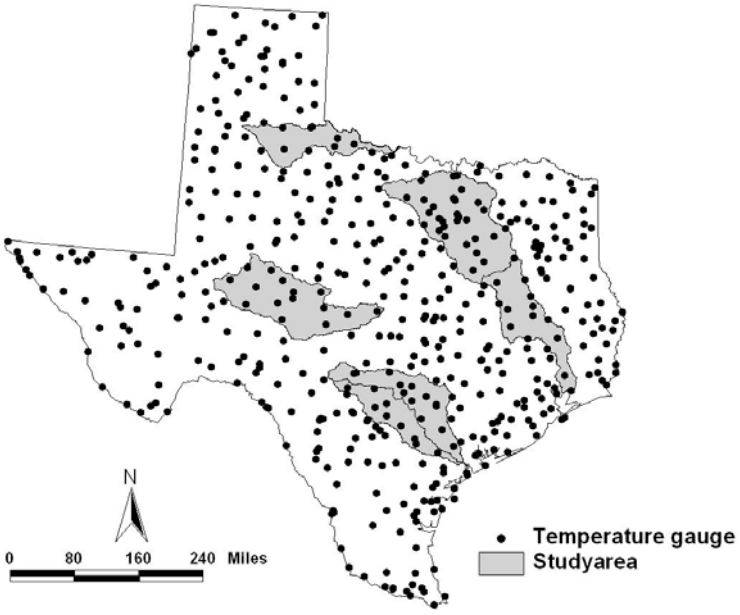

Figure 2.10 NCDC weather stations that measure daily maximum and minimum temperatures.

The USDA-NRCS State Soil Geographic Database STATSGO (USDA Soil Conservation Service 1992) soil association map (1:250,000 scale) and datasets were used for obtaining soil attributes. The physical soil properties needed by SWAT are texture, bulk density, available water capacity, saturated hydraulic conductivity, and soil albedo for up to ten soil layers. The land use/land cover data is the 1992 National Land Cover Data (NLCD) at 30m resolution, obtained from USGS (Vogelmann et al. 2001). The elevation data is the 7.5-minute Digital Elevation Model (DEM) obtained at 30m resolution from USGS (USGS 1993).

Model Setup

For this study, a spatial resolution of 4km × 4km was chosen to capture adequate spatial variability over a large watershed and for future integration studies with NEXRAD radar precipitation that has a similar spatial resolution. The ArcView interface for the model (Di Luzio et al. 2002b) was used to extract model parameters from the GIS layers with minor modifications to delineate sub-basins at 4km × 4km resolution. Each watershed was divided into several sub-basins (grids) at 4km × 4km resolution, using a DEM resampled to the same resolution (e.g. Upper Trinity was divided into 1854 sub-basins, each 4km × 4km (Fig.2.3)). Topographic parameters and stream channel parameters were estimated from the DEM. A dominant soil and land use type within each sub-basin was used to develop soil and plant inputs to the model. Initial CN II values were assigned based on the soil hydrologic group and vegetation type (USDA Soil Conservation Service 1972). Based on the land use assigned for each grid, plant growth parameters like maximum leaf area index, maximum rooting depth,

maximum canopy height, optimum and base temperatures, were obtained from a crop database within SWAT. Corn was assumed to be the crop grown in all agricultural land. The planting and harvest dates of crops and active growing period of perennials were scheduled using a heat unit scheduling algorithm (Arnold et al. 1998). The weather data for each sub-basin was assigned from the closest weather station. In order to simulate the natural hydrology and long-term soil moisture balance, all the crops in the watershed were assumed to be rainfed and hence irrigation was not considered in this study.

Calibration and Validation Procedure

Stream flow measured at 24 USGS streamgages, located in six watersheds, was used for calibrating and validating the model. Only those streamgages that are not affected by reservoirs, diversions or return flows were selected for model calibration and validation (Fig.2.3 to 2.8). Five years of measured stream flow data was used for model calibration. The calibration period for each USGS station was selected after careful analysis of the stream flow time series. The five contiguous years of stream flow that had fair distribution of high and low flows were selected for model calibration. This was done to obtain optimal parameters that improve the model simulation in both wet and dry years.

The model was calibrated using VAO5A Harwell subroutine library (1974), a non-linear auto calibration algorithm. VAO5A uses a non-linear estimation technique known as the Gauss-Marquardt-Levenberg method to estimate optimal model parameters. The objective function is to minimize the mean squared error in the

measured versus simulated stream flow. The strength of this method lies in the fact that it can generally estimate parameters using fewer model runs than other estimation methods (Demarée 1982). The model parameters selected for auto calibration using the VAO5A algorithm are listed in Table 2.3. These model parameters were selected because of the sensitivity of surface runoff to them, reported in several studies (Arnold et al. 2000; Lenhart et al. 2002; Santhi et al. 2001; Texas Agricultural Experiment Station 2000). In order to prevent the algorithm from choosing extreme parameter values, the model parameters were allowed to change only within reasonable limits (Table 2.3).

After optimal calibration of parameters was achieved, the model was validated at each of the 24 USGS calibration stations using ten years to thirty years of observed stream flow data based on the data availability. As the objective of this study was to develop the soil moisture data on a weekly time step, the measured and simulated stream flow was also averaged over a weekly period for statistical comparison. The coefficient of determination (R^2) and the coefficient of efficiency (E) (Nash and Sutcliffe 1970) were the statistics used to evaluate the calibration and validation results. The R^2 and E are calculated as follows:

$$R^2 = \left(\frac{\sum_{i=1}^{N} (O_i - \dddot{O})(P_i - \dddot{P})}{\sqrt{\sum_{i=1}^{N} (O_i - \dddot{O})^2} \sqrt{\sum_{i=1}^{N} (P_i - \dddot{P})^2}} \right)^2 \qquad (2.1)$$

Table 2.3 Parameters used in model calibration

SWAT parameter name	Description	Calibration range
CN2	Moisture condition II curve number	± 20%
SOL_AWC	Available water capacity	± 20%
SOL_K	Saturated hydraulic conductivity	± 20%
ESCO	Soil evaporation compensation coefficient	0.10 to 0.95
CANMX*	Maximum canopy storage	0 to 20mm
GW_REVAP	Groundwater revap coefficient	0.05 to 0.40
RCHRG_DP	Deep aquifer percolation coefficient	0.05 to 0.95
GWQMN	Threshold water level in shallow aquifer for base flow	0 to 100mm
REVAPMN	Threshold water level in shallow aquifer for revap or percolation to deep aquifer	0 to 100mm
CH_K(2)	Effective hydraulic conductivity of main channel	0 to 50mm/hr

* Maximum canopy storage (CANMX) is calibrated only for forest and heavy brush infested rangeland. For other land cover types CANMX is 0mm.

$$E = 1.0 - \frac{\sum_{i=1}^{N}(O_i - P_i)^2}{\sum_{i=1}^{N}(O_i - \ddot{O})^2} \qquad (2.2)$$

where:

O_i - observed stream flow at time i,

P_i - predicted stream flow at time i,

$\ddot{O}$ - mean of the observed stream flow,

$\ddot{P}$ - mean of the predicted stream flow, and

N - number of observed/simulated values.

The value of R^2 ranges from 0 to 1, with higher values indicating better agreement. The value of E ranges from $-\infty$ to 1, with E values greater than zero indicating that the model is a good predictor. R^2 evaluates only linear relationships between variables, thus is insensitive to additive and proportional differences between model simulations and observations. However, E is sensitive to differences in the means and variances of observed and simulated data and hence is a better measure to evaluate model simulations.

Vegetation Index

Stream flow is often the only component of the water balance that is regionally observed and hence, widely used for calibrating hydrologic models. However, in the current study, soil water is the hydrologic component of interest and it would be ideal to use soil moisture and/or ET for calibration if the measured data were available at the study area in a natural hydrologic setting (without irrigation). Due to a lack of measured

soil moisture and ET data, a pseudo indicator of soil moisture condition, the Normalized Difference Vegetation Index (NDVI), can be used to analyze the model's predicted soil moisture.

NDVI is a vegetation index obtained from red and infrared reflectance measured by satellite. It is an indicator of photosynthetic activity, greenness and health of vegetation (Defries et al. 1995). Among various stress factors that affects vegetation, water stress is an import factor that affects photosynthetic activity and greenness of the vegetation. Farrar and Nicholson (1994) found that NDVI and soil moisture are well correlated in the concurrent month of the growing season. Hence, NDVI can be a useful indicator to analyze the simulated soil moisture during the active growing season of the crop and to determine the usefulness of soil moisture for drought monitoring. Ten-day NDVI composite data measured by NOAA-AVHRR satellite from 1982 to 1998 at a spatial resolution of 8km × 8km was used for this study. The satellite data was resampled to 4km × 4km to match the sub-basin resolution used in this study and was linearly interpolated between two ten-day composites to get weekly NDVI data. The weekly NDVI data was correlated with weekly simulated soil moisture to evaluate the hydrologic model predictions.

Results and Discussion

Calibration and Validation of Stream Flow

The model was calibrated using the non-linear auto calibration algorithm, VAO5A (Harwell subroutine library 1974), and selected model parameters were

changed within reasonable limits as indicated in Table 2.3. The model was calibrated using five years of measured stream flow data and validated using a long record of measured stream flow data whenever available. Measured stream flow data from 24 USGS streamgage stations with combined station years of about 125 and 490 years of stream flow data was used for model calibration and validation, respectively. The distribution of Curve Number (CN2) and the Available Water Capacity (AWC) after calibration for all the watersheds are given in Figures 2.11 and 2.12 respectively. The curve numbers for different land use were within reasonable range, as is suggested by the SCS hydrology handbook (USDA Soil Conservation Service 1972). As expected, agricultural lands were located in soils with high water holding capacity when compared to other land use types.

Weekly stream flow statistics during the calibration and validation periods at the 24 USGS streamgages in six watersheds are given in Tables 2.4 through 2.9. In general, the simulated stream flow compared well with the measured stream flow, with R^2 values greater than 0.7 and E values greater than 0.65 for most of the streamgages. The difference between simulated and measured stream flow can be a result of (1) a change in land use over a period of time, (2) errors in measured rainfall and/or stream flow data, (3) sparse distribution of raingage across the watershed, (4) point source discharges from industries and other sources, (5) pumping for irrigation and water diversion directly from a river, and (6) springs and aquifer outcrops that discharge directly into a river, not accounted in modeling.

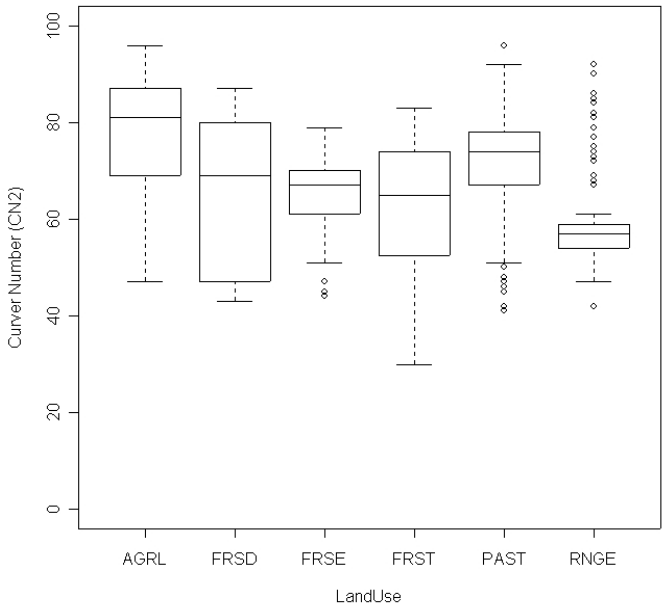

Figure 2.11 Distribution of curve number according to land use at six watersheds after calibration.

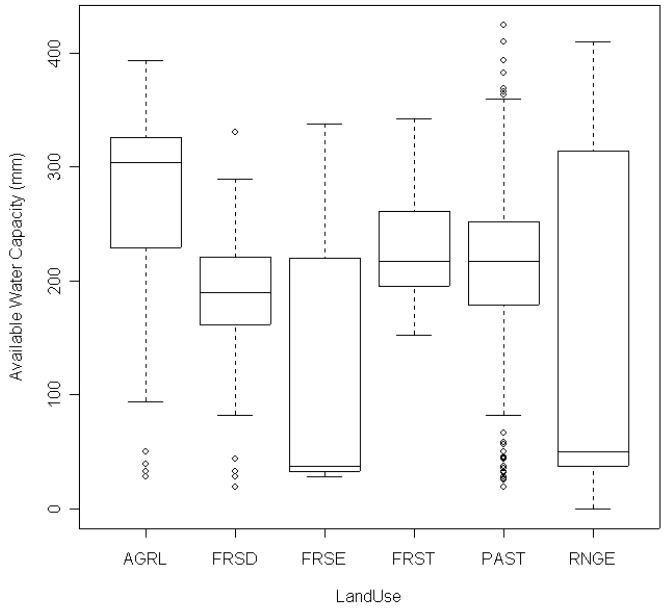

Figure 2.12 Distribution of available water capacity according to land use at six watersheds after calibration. [Agriculture (AGRL), Pasture (PAST), Rangeland (RNGE), Evergreen Forest (FRSE), Deciduous Forest (FRSD), Mixed Forest (FRST)]

Table 2.4 Calibration and validation statistics at USGS streamgages in Upper Trinity.

USGS Gage No.	Calibration				Validation			
	Years	No. of Years	R^2	E	Years	No. of Years	R^2	E
08042800	1980 to 1985	6	0.91	0.90	1962 to 1997	36	0.83	0.81
08048800	1962 to 1967	6	0.72	0.66	1962 to 1972	11	0.70	0.59
08051500	1986 to 1990	5	0.90	0.87	1962 to 1997	36	0.80	0.80
08053500	1986 to 1990	5	0.82	0.80	1962 to 1997	36	0.70	0.68
08057450	1970 to 1974	5	0.70	0.68	1970 to 1978	9	0.68	0.67
08061540	1980 to 1985	6	0.80	0.77	1969 to 1997	29	0.70	0.69
08062900	1977 to 1982	6	0.73	0.69	1963 to 1986	24	0.71	0.68
08064100	1988 to 1993	6	0.76	0.74	1984 to 1997	14	0.70	0.66

Table 2.5 Calibration and validation statistics at USGS streamgages in Lower Trinity.

USGS Gage No.	Calibration				Validation			
	Years	No. of Years	R^2	E	Years	No. of Years	R^2	E
08065200	1967 to 1972	6	0.54	0.54	1963 to 1997	35	0.63	0.63
08065800	1979 to 1984	6	0.83	0.80	1968 to 1997	30	0.75	0.70
08066100	1976 to 1981	6	0.68	0.68	1975 to 1984	10	0.67	0.66
08066200	1989 to 1994	6	0.70	0.68	1975 to 1995	21	0.64	0.62

Table 2.6 Calibration and validation statistics at USGS streamgages in Red River.

USGS Gage No.	Calibration				Validation			
	Years	No. of Years	R^2	E	Years	No. of Years	R^2	E
07307800	1978 to 1981	4	0.56	0.52	1975 to 1992	18	0.65	0.55
07308200	1976 to 1981	6	0.85	0.85	1962 to 1982	21	0.67	0.60

Table 2.7 Calibration and validation statistics at USGS streamgages in Guadalupe River.

USGS Gage No.	Calibration				Validation			
	Years	No. of Years	R^2	E	Years	No. of Years	R^2	E
08167000	1986 to 1990	5	0.82	0.75	1962 to 1992	31	0.68	0.66
08171000	1985 to 1990	6	0.87	0.85	1962 to 1992	31	0.78	0.76
08173000	1985 to 1990	6	0.90	0.90	1962 to 1992	31	0.76	0.73

Table 2.8 Calibration and validation statistics at USGS streamgages in San Antonio River.

USGS Gage No.	Calibration				Validation			
	Years	No. of Years	R^2	E	Years	No. of Years	R^2	E
08178800	1972 to 1977	6	0.87	0.85	1965 to 1978	14	0.81	0.80
08179000	1972 to 1977	6	0.66	0.57	1965 to 1977	12	0.70	0.68
08186500	1972 to 1976	5	0.67	0.55	1965 to 1978	14	0.82	0.67

Table 2.9 Calibration and validation statistics at USGS streamgages in Colorado River.

USGS Gage No.	Calibration				Validation			
	Years	No. of Years	R^2	E	Years	No. of Years	R^2	E
08128000	1938	1	0.92	0.92	1959	1	1.00	0.97
08128400	1974	1	0.99	0.99	1986	1	0.98	0.85
08136500	1956 to 1961	6	0.87	0.78	1940 to 1961	22	0.78	0.74
08144500	1935 to 1938	4	0.91	0.88	1974 to 1975	2	0.92	0.90

Analysis of time series plots showed that most of the differences between the observed and measured rainfall/stream flow data occurred due to non-availability of a raingage at the watershed or the precipitation events not measured by a raingage nearest to the watershed. Few runoff peaks observed in each of the 24 USGS streamgages either did not match with the measured precipitation data to the same intensity or the precipitation event was not at all captured by the raingage at or near the watershed. These missed precipitation events resulted in reduced R^2 and E statistics at a few USGS streamgages. This was very much the case of USGS gages 08065200 and 07307800, located in the Lower Trinity and Red River watersheds, which had the low coefficient of efficiency (E) values 0.54 and 0.52, respectively, during the calibration period. In the case of USGS gage 08065200, there was no weather station or raingage within the drainage area. The time series plots of measured stream flow at USGS gage 08065200, SWAT simulated stream flow and measured precipitation data at the nearest raingage are shown in Figure 2.13. SWAT simulated stream flow matched closely with the available precipitation data, whereas some of the peak stream flow events observed at the USGS station does not correspond well with the nearest raingage data used in the model. In this study, the precipitation data was used as such from the nearest raingage to the sub-basin and spatial interpolation of raingage data was not attempted. Using spatially distributed rainfall from RADAR could improve the model results. Nevertheless, the general time series pattern of stream flow at the watershed was well-simulated by the model.

The hydrology of the Colorado River watershed is different from other watersheds modeled in this study. The Colorado River watershed has a semi-arid

climate and is located above the recharge zone of Edwards-Trinity Plateau aquifer. This watershed has exposed bedrock at the land surface, fractures and sinkholes, a characteristic of Karst aquifer formation. Analysis of stream flow data for this watershed showed that flash runoff occurs during rainfall events and disappears (Fig. 2.14). During peak rainfall events, runoff occurs in a flash and disappears without persistence. Most of the precipitation enters through fractures and sinkholes and there is very little runoff during normal precipitation events. The unique hydrology of the Colorado River watershed coupled with sparse distribution of raingages made the model calibration and validation complex. Hence, for the Colorado River watershed to reduce surface runoff, the curve number was reduced up to 40% from the recommended value with all other calibration parameters within the range as noted in Table 2.3. Further, short periods of stream flow record, which matched the available precipitation data, were selected for model calibration and validation.

The downstream portion of the Colorado River watershed is dominated by agriculture. The USGS streamgage (08136500) measurements located in this portion of the watershed were affected by a reservoir upstream. Hence, the USGS recorded reservoir release upstream of the watershed, which was routed through the main channel of the watershed along with the surface runoff simulated from measured precipitation data. It was difficult to select a period where the contribution to stream flow was from surface runoff alone because there was considerable release from the reservoir during the rainfall events as well. Hence, a period of record that had a good contribution of surface runoff from precipitation as well as release from the reservoir was selected for model

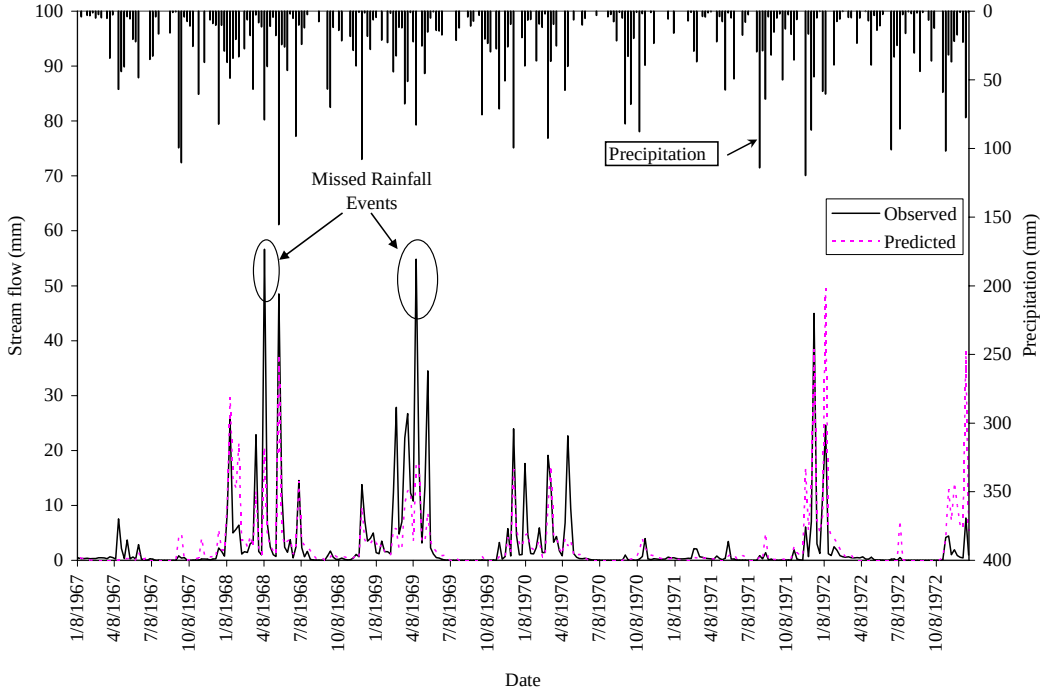

Figure 2.13 Weekly measured and simulated stream flows at USGS gage 08065200 and weekly cumulative rainfall.

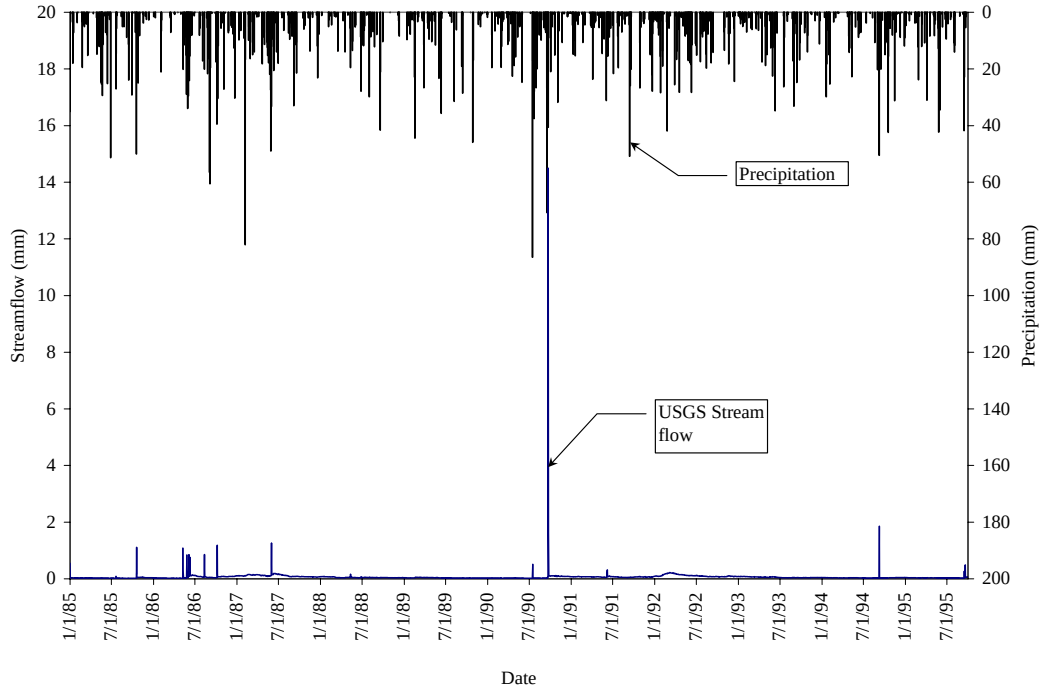

Figure 2.14 Measured stream flow at USGS gage 08128000 and measured rainfall.

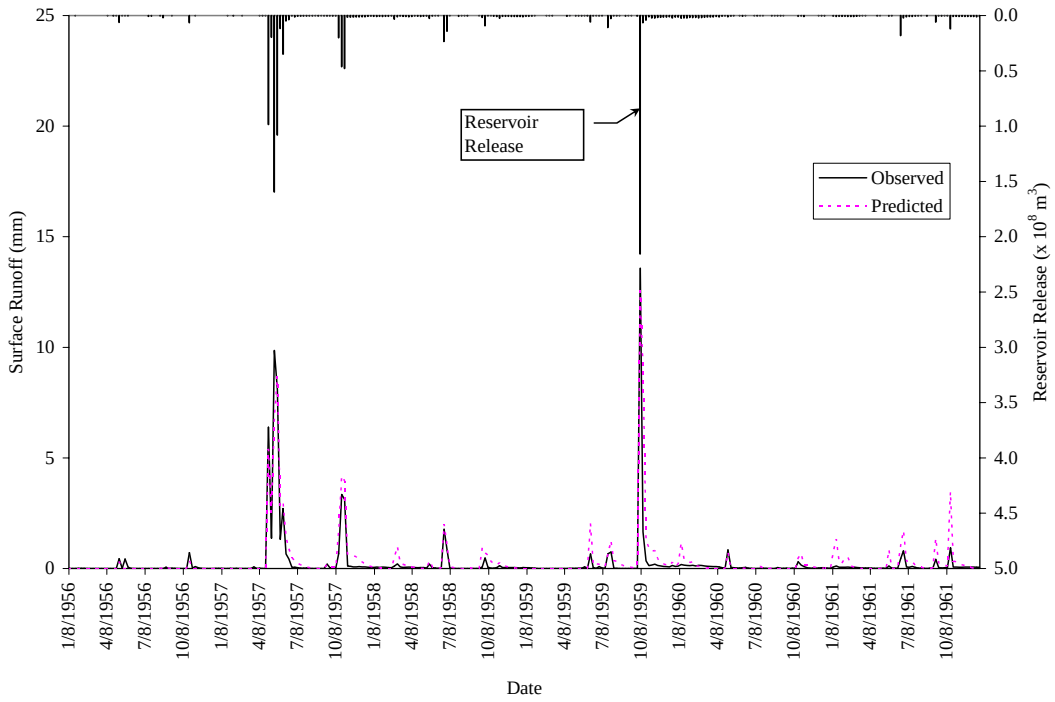

Figure 2.15 Weekly measured and simulated stream flows at USGS gage 08136500 and weekly cumulative reservoir release from upstream.

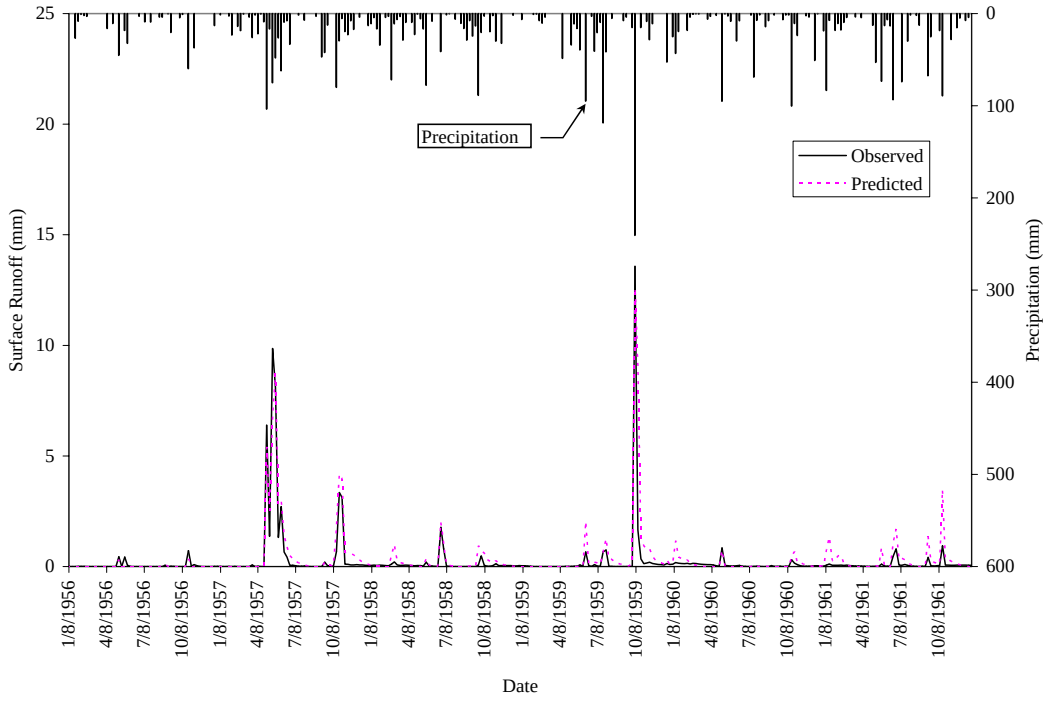

Figure 2.16 Weekly measured and simulated stream flows at USGS gage 08136500 and weekly cumulative rainfall.

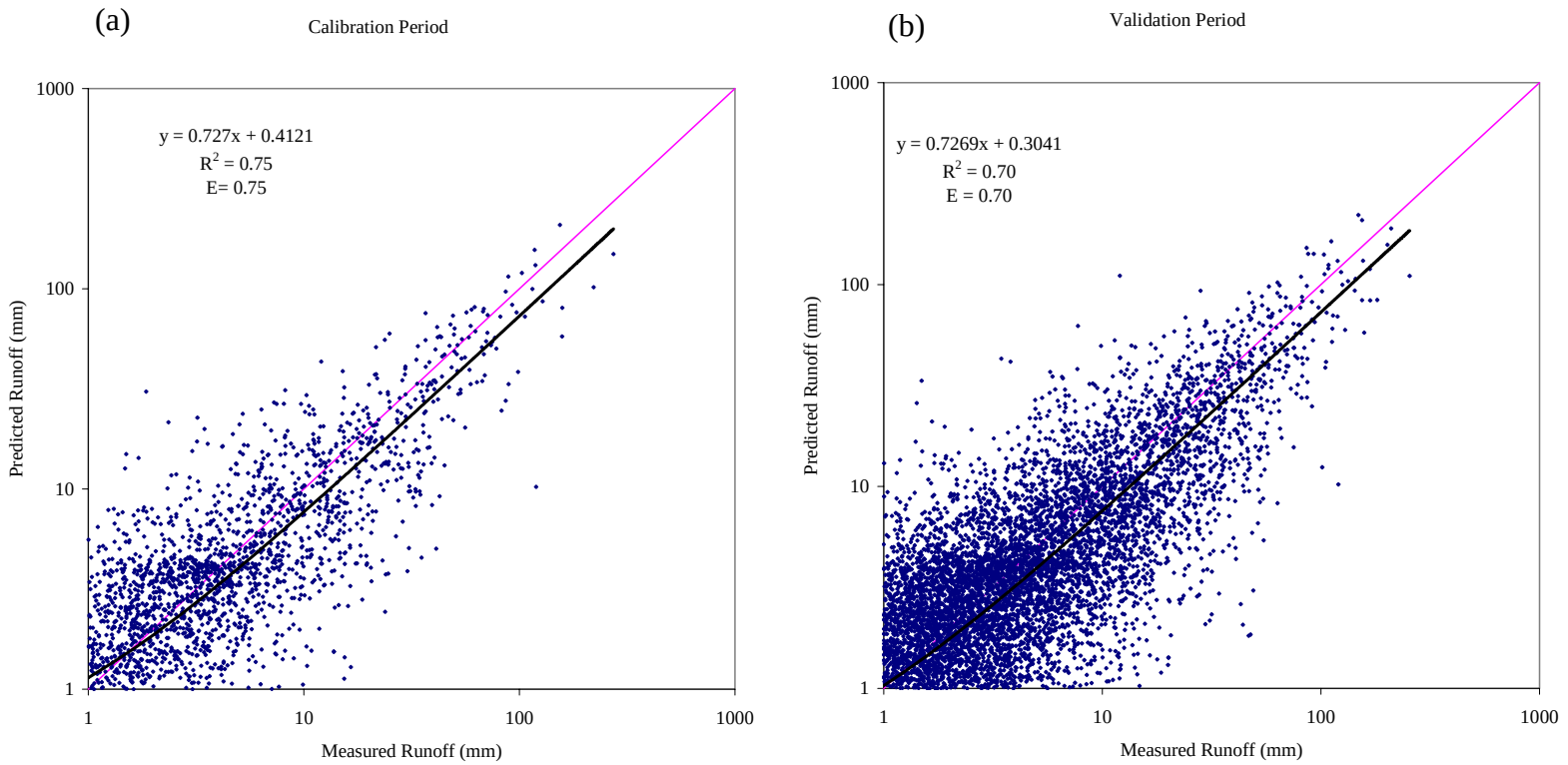

Figure 2.17 Weekly measured and predicted stream flows (log-log scale) at all 24 USGS streamgages. (a) Calibration period (b) Validation period

calibration (Figures 2.15 and 2.16). The model simulations compared well with the measured stream flow during the calibration and validation period with both R^2 and E statistics close to 0.75.

The log-log scatter plots of measured and simulated stream flows at all 24 USGS streamgages during the calibration and validation period is shown in Figures 2.17. The slope of the regression line during the calibration and validation period is close to 0.70 and indicates that SWAT under-predicts runoff, the reasons of which are explained above. The overall R^2 and E values for the calibration period was 0.75 and the validation period was 0.70. Overall, the model was well–calibrated, and the simulated stream flow compared well with the observed stream flow under varying land use, hydrologic and climatic conditions.

Evapotranspiration

Analysis of the simulation results at each watershed showed that actual growing season ET (March through October) was about 45%-90% of growing season precipitation (P) and varied with land use and the climatic zone of each watershed (Fig.2.18). Upper Trinity and Lower Trinity had low ET/P ratios compared to other watersheds due to a high amount of precipitation in these watersheds. Red River had the highest ET/P ratio, with over 90% of precipitation returning as ET for all the land use classes in the watershed. Irrespective of the watershed, agriculture and pastureland had the highest ET/P ratio, with 70 – 90% of precipitation returning to the atmosphere as ET. This was because agriculture and pastureland were mainly located in soils with high

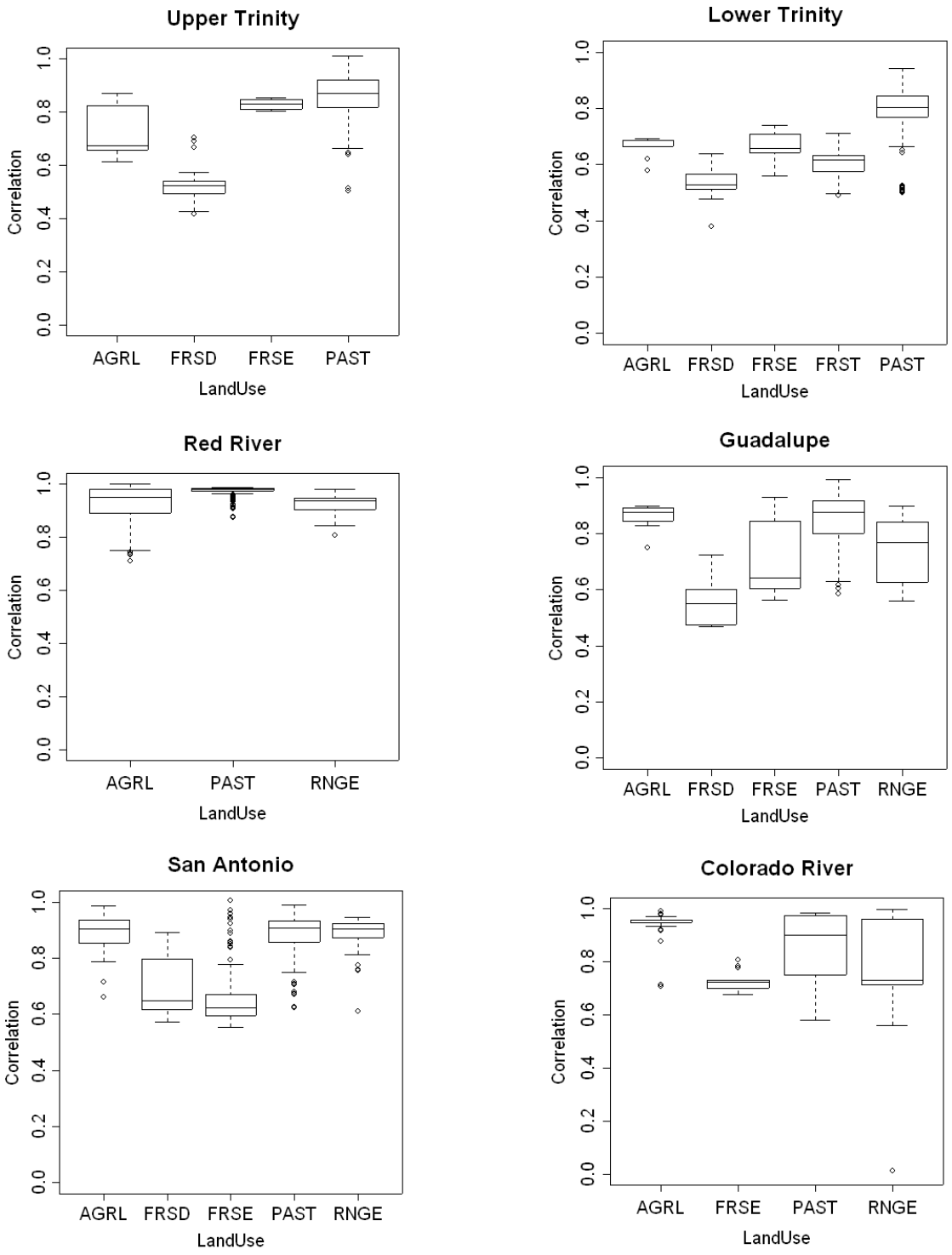

Figure 2.18 Ratio of growing season ET to growing season precipitation at the six watersheds. [Agriculture (AGRL), Pasture (PAST), Rangeland (RNGE), Evergreen Forest (FRSE), Deciduous Forest (FRSD), Mixed Forest (FRST)]

available water capacity (Fig. 2.12). Thus, more water was stored from precipitation and was available for ET when compared to soils of low water holding capacity. Dugas et al. (1999) measured ET by the Bowen ratio/energy balance method for Bermuda grass, Native Prairie and sorghum at Blackland Research Center in Temple, TX, which has an average annual precipitation of about 880mm. The measured ET reported by Dugas et al. (1999) during the growing season (March through October of 1993 and 1994) accounted for about 75 – 90% of the growing season precipitation. This matches well with the model results and indicates that the model was able to simulate the growing season ET of pasture and agriculture land within reasonable limits.

Analysis of Simulated Soil Water Using NDVI

Stream flow was the only water balance component that was widely available for the model calibration and validation. The ability of the model to simulate soil water could not be evaluated quantitatively due to a lack of measured data. Hence, simulated soil water was analyzed using NDVI measured by NOAA-AVHRR satellite. The weekly NDVI was compared with simulated average weekly soil water for each sub-basin during the active phase of the growing season (April to September) from 1982 to 1998 (except 1994). A lag analysis was performed with the current week's NDVI and the simulated soil water in the concurrent week and past four weeks. The lag analysis showed that NDVI lags behind simulated soil water by at least one week for most of the sub-basins. This was expected because it takes some time for the plants to respond to the water stress in the root zone. However, the lag between NDVI and soil water was

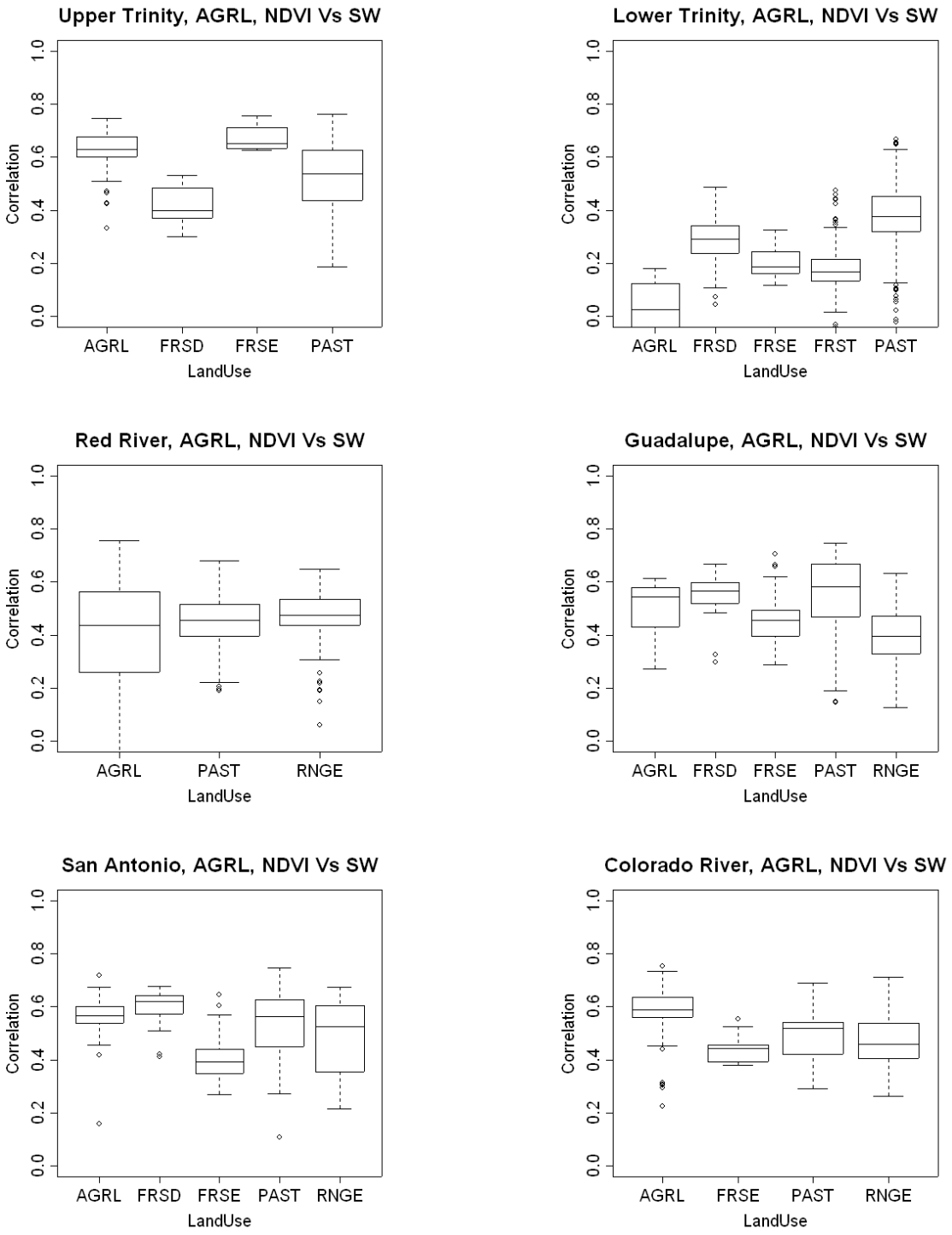

Figure 2.19 Correlations of weekly NDVI and simulated soil water during active growing period (April-September) of 1982-1998 for all sub-basins within each watershed.

not a constant and varied from year to year for the same land use and sub basin. This could be due to the difference in the onset of seasonal precipitation from year to year and the quantity of precipitation. Nevertheless, for most of the sub-basins, the correlation between NDVI and soil water at zero lag was only slightly less than the maximum correlation obtained at a certain lag. The distribution of maximum correlation obtained from lag analysis between NDVI and soil water among sub-basins with same land use within a watershed is given as a box plot in Figure 2.19. Except for the Lower Trinity watershed, in general, there is a good correlation between NDVI and simulated soil water for agriculture and pasture land cover types ($r \sim 0.6$).

The correlations of NDVI and soil water for agricultural sub-basins for each year at six watersheds are plotted in Figure 2.20. The correlations were as high as 0.8 during some years, yet low in other years. In general, Upper Trinity had better correlation between NDVI and soil water than other watersheds. This is because there is less irrigation activity in this watershed and the crop growth depends mostly on soil water replenished by rainfall. In contrast, a large portion of agricultural lands in the Red River and Colorado River watersheds are under irrigation. Some agricultural lands in Red River grow winter wheat that has a different growing season than corn. It is a common agricultural practice to grow corn and wheat during alternate years in the same agricultural field. Hence, there was a wide distribution of correlation in the Red River watershed when compared to other watersheds. The lower correlation between NDVI and soil water for agricultural lands during certain years could be due to several reasons. For example, in Upper Trinity, the lower correlations during 1989 and 1992 were

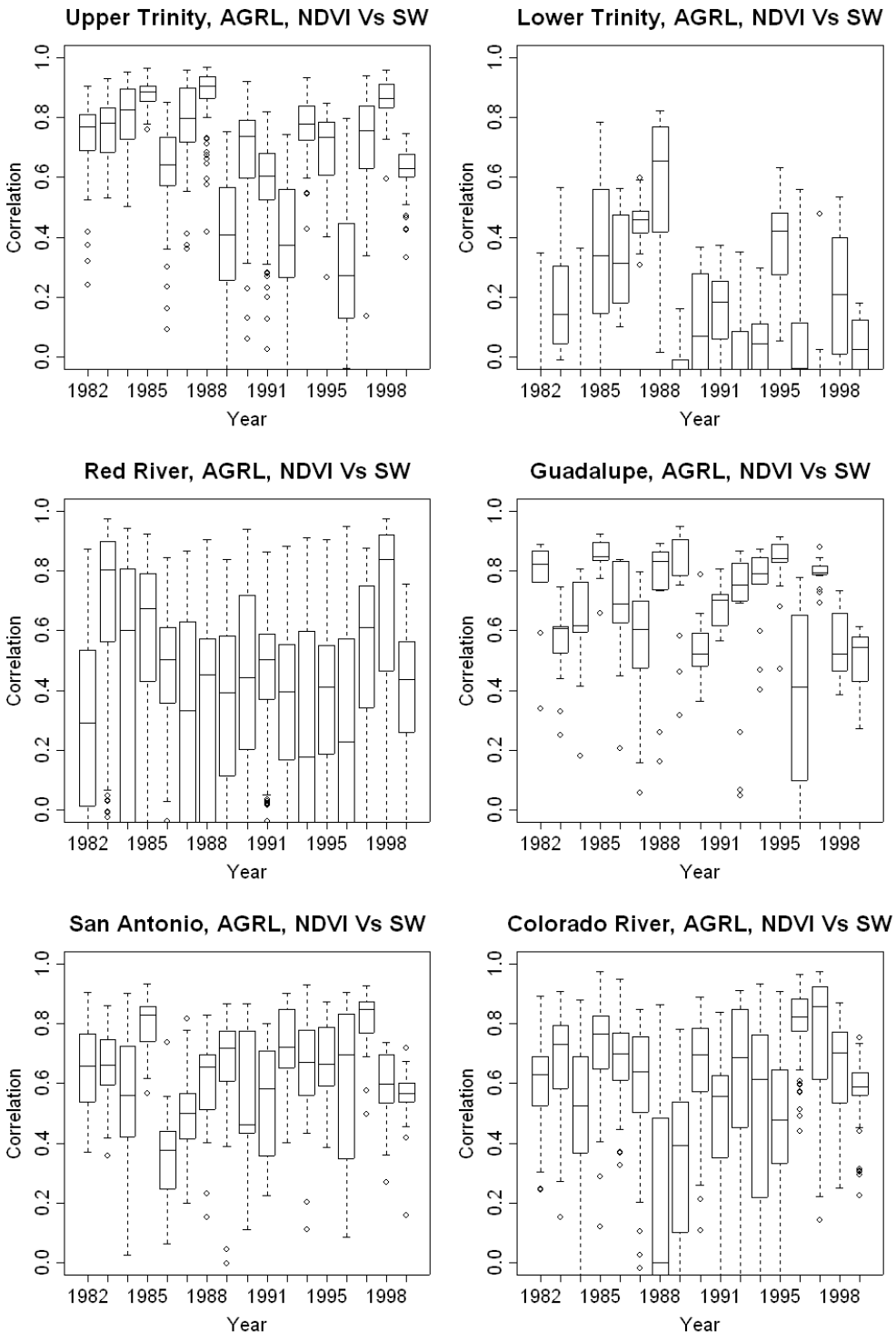

Figure 2.20 Correlations of weekly NDVI and simulated soil water during active growing period (April-September) for agriculture land use within each watershed.

because of high precipitation during those years for which the NDVI response was much different than other years. Similarly during 1996, much less precipitation was received during the growing season. Hence, the NDVI was much less, indicating no crop growth during that year. This was the same case for a lower correlation at the Guadalupe River watershed during 1996, and at the Colorado watershed during 1988 and 1989. In Lower Trinity, there were only few agricultural lands and were scattered adjacent to the wetlands close to Gulf of Mexico. These agricultural lands predominantly grow rice. Further, among the six study areas, Lower Trinity is located in a high rainfall zone. Because of the high annual rainfall, the NDVI did not fluctuate much with changes in soil water. Thus, the correlation between NDVI and SW was low at Lower Trinity.

The correlations of NDVI and soil water for pasture sub-basins for each year at six watersheds are plotted in Figure 2.21. In general, pasture had a wider spread of correlation distribution across sub-basins than agriculture. This could be because pasture is cut and grazed all summer during the growing season. Cutting and grazing of pasture could change the NDVI values sensed by satellite due to lesser leaf area. Hence, the NDVI fluxes were not purely due to natural soil moisture fluctuations alone. The correlation was generally less at Lower Trinity, except during few years. Analysis of precipitation data showed that the correlation between NDVI and soil water was markedly high at Lower Trinity during dry years of 1985 and 1988. This could be because Lower Trinity is wet during most parts of the year, with an annual precipitation of more than 1000mm, and has a lesser evaporative fraction for all land use types when compared to other watersheds (Fig.2.19). Hence, the fluctuations in soil moisture during

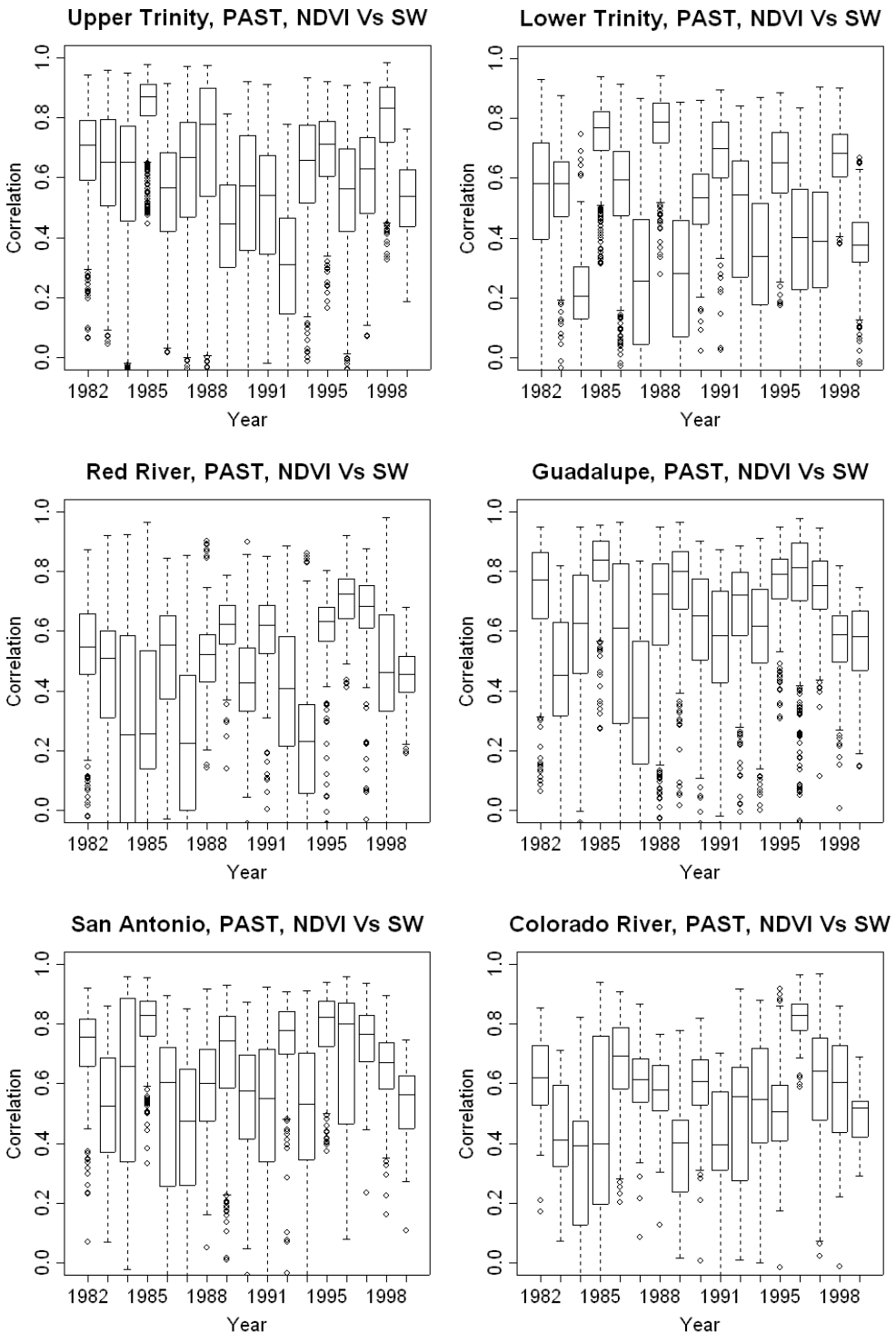

Figure 2.21 Correlations of NDVI and simulated soil water during active growing period (April-September) for pasture land use within each watershed.

normal or high precipitation years don't seem to affect the NDVI much, except during dry years when the available soil moisture becomes less at the root zone.

The NDVI response to soil water was relatively well for agriculture and pasturelands because they have shallow root systems that can extract water only from the root zone. In contrast, brush species in rangeland and trees of forestland have well-developed root systems that can extract soil water beyond the root zone from deep layers of the aquifer. Hence, it was difficult to explain the NDVI response for these land use types purely in terms of simulated soil water alone. A lagged correlation analysis was conducted with current NDVI and cumulative precipitation of the past four, eight and twelve weeks. However, the analysis (the results are not presented here) yielded similar or lesser correlations than that of soil water. Thus, with the current understanding of the processes, it was difficult to explain the NDVI responses of rangeland and forestland in terms of soil water or precipitation alone and needs further analysis.

Summary and Conclusions

The hydrologic model SWAT was used for developing a long-term soil moisture dataset at a spatial resolution of 4km × 4km and at a weekly temporal resolution. The hydrologic model was calibrated for stream flow using an auto-calibration algorithm and validated over multiple years. The overall R^2 and E values for the calibration period was 0.75 and the validation period was 0.70 on weekly stream flow. Most of the differences between the measured and simulated stream flow occurred due to a lack of raingage network in the watershed. This could be overcome by using spatially distributed

RADAR rainfall data. Overall, the model was well–calibrated, and the simulated stream flow compared well with the observed stream flow under varying land use, hydrologic and climatic conditions.

Due to a lack of measured evapotranspiration or soil moisture data, simulated soil moisture was analyzed using 16 years of NDVI data. Analysis showed that the simulated soil moisture was well-correlated with NDVI for agriculture and pasture land use types ($r \sim 0.6$). The correlations were as high as 0.8 during certain years, indicating that the model performed well in simulating the soil moisture. There was a lag of at least one week between the simulated soil moisture and NDVI because it takes some time for the plant to respond to the water stress in the root zone. In high precipitation zones like Lower Trinity, NDVI was well-correlated only during the dry years because NDVI doesn't fluctuate much during normal or wet years due to high available soil moisture. Further analysis is needed to explain the NDVI response of forest and rangeland in terms of soil water or precipitation due to the well-developed root system that can extract water beyond the root zone.

The current study showed that NDVI could be used as a good indicator to evaluate the hydrologic model in terms of soil water prediction when measured soil moisture data are not available. Further, as NDVI respond well to the soil water, it demonstrates that soil water can be a good indicator of crop stress and onset of agricultural drought conditions. The simulated soil moisture data can be used in subsequent studies to develop a drought indicator for agricultural drought monitoring.

CHAPTER III

DEVELOPMENT OF A SOIL MOISTURE INDEX FOR AGRICULTURAL DROUGHT MONITORING

Synopsis

Drought is one of the major natural hazards that bring about billions of dollars in loss to the farming community around the world each year. Drought is most often caused by a departure of precipitation from the normal amount, and agriculture is often the first sector to be affected by the onset of drought due to its dependence on water resources and soil moisture reserves during various stages of crop growth. Currently used drought indices like the Palmer Drought Severity Index (PDSI) and Standardized Precipitation Index (SPI) have coarse spatial (7000 to 100,000 km^2) and temporal resolution (monthly). Hence, the distributed hydrologic model SWAT was used to simulate evapotranspiration and soil moisture from daily weather data at a high spatial resolution (16km^2) using GIS. Using this simulated data the drought indices Evapotranspiration Deficit Index (ETDI) and Soil Moisture Deficit Index (SMDI) were developed based on weekly evapotranspiration deficit and soil moisture deficit, respectively. SMDI was computed at four different levels, using soil water available in the entire soil profile, then soil water available at the top two feet, four feet, and six feet. This was done because the potential of the crop to extract water from depths varies during different stages of the crop growth and also by crop type. ETDI and SMDI-2 had

less auto-correlation lag, indicating that they could be used as good indicators of short-term drought. The developed drought indices showed high spatial variability (Standard deviation ~ 1.00) in the study watersheds, primarily due to high spatial variability of precipitation. The wheat and sorghum crop yields were highly correlated ($r > 0.75$) with the ETDI and SMDI's during the weeks of critical crop growth stages, indicating that the developed drought indices can be used for agricultural drought monitoring.

Introduction

Drought is one of the major natural hazards that bring about billions of dollars in loss to the farming community around the world every year. According to the U.S. Federal Emergency Management Agency (FEMA), droughts occur almost every year across a portion of the nation, and the United States loses $6-8 billion annually on average due to drought (FEMA 1995). During the 1998 drought, Texas alone lost a staggering $5.8 billion (Chenault and Parson 1998), which is about 39% of the $15 billion annual agriculture revenue of the state (Sharp 1996). In spite of the economic and the social impact caused by drought, it is the least understood of all natural hazards due to the complex nature and varying effects of droughts on different economic and social sectors (Wilhite 2000).

Departure of precipitation from the normal is the major cause for drought. However, this departure from the normal does not affect the entire community at the same time. A simple departure from the normal precipitation creates a "meteorological drought". If this departure continues for few weeks and then the soil moisture depletes,

crop growth is affected and an “agricultural drought” begins. If the departure sustains over a period of several months to a year, then the flow in the rivers and streams will reduce as will the storage in the reservoirs. This affects the water supply to cities, generation of hydro electric power and navigation, and thus, it creates “hydrologic drought”. If the drought sustains for more than a year and affects the society and the regional economy, then it creates “socioeconomic drought” (Wilhite and Glantz 1985). Hence, there is a time lag before the drought effects are felt by the entire community. Due to this time lag, drought losses are not immediately detectable until after the damage has already occurred.

Agriculture is often the first sector to be affected by the onset of drought due to dependence on water resources and soil moisture reserves during various stages of crop growth. The droughts of the 1930’s, 1980’s and 1990’s emphasize the vulnerability of the agricultural sector to drought and the need for more research to understand and determine the impacts of agricultural drought. Understanding and developing tools to predict and monitor drought would help in planning to mitigate the impacts of drought.

Drought Indices

Federal and State government agencies use drought indices to assess and respond to drought. A drought index integrates various hydrological and meteorological parameters like rainfall, evapotranspiration (ET), runoff and other water supply indicators into a single number and gives a comprehensive picture for decision-making. The Palmer Drought Severity Index (PDSI) (Palmer 1965) and Crop Moisture Index

(CMI) (Palmer 1968) are extensively used for water resources management and agricultural drought monitoring and forecasting. The U.S. Department of Agriculture uses PDSI and CMI to determine the magnitude of drought and the proper time to grant emergency drought assistance to farmers.

PDSI and CMI are based on a simple lumped parameter water balance model that calculates precipitation deficit and ET deficit, respectively. The model assumes that parameters like land use/land cover, and soil properties are uniform over the entire climatic zone (7000 to 100,000 km^2). However, in reality, parameters like land use/land cover and soil properties vary widely. Several studies have highlighted the limitation of PDSI and CMI (Akinremi and McGinn 1996; Alley 1984; Guttman 1998). A brief description of several drought indices and their limitations are discussed in Chapter I. Hence, a better tool for agricultural drought monitoring is essential for the farming community and the decision-makers. Due to advancements in Geographical Information Systems (GIS) and GIS-based distributed parameter hydrologic models, a better drought assessment system can be developed.

Agricultural crops are sensitive to soil moisture. The soil moisture deficit in the root zone during various stages of the crop growth cycle will have a profound impact on the crop yield. The objective of this study is to develop a drought index for Texas, based on weekly soil moisture deficit, which is estimated using a comprehensive hydrologic model and GIS. The consideration of spatial variability of parameters like soil type and land use/land cover is a better approximation of the hydrologic system and will improve

our ability to monitor soil moisture deficit/drought at a much better spatial resolution ($16km^2$). At present, drought indices like PDSI or CMI are reported for the entire climatic zone at a spatial resolution ranging from 7000 km^2 to 100,000 km^2. The increased temporal resolution and spatial accuracy will give the farming community, water managers and policy makers a better tool for assessing, forecasting and managing agricultural drought on a much finer scale.

Methodology

Hydrologic Modeling

A spatially distributed hydrologic model is essential for developing the drought index. In this study, the hydrologic model Soil and Water Assessment Tool (SWAT) was used. SWAT is a comprehensive, distributed parameter hydrologic model developed by Arnold et al. (1993) to help water resource managers assess water supplies and sediment transport on watersheds based on various land use and management practices. SWAT uses spatially distributed data on soil properties, land use and Digital Elevation Model (DEM) for hydrologic modeling, and it operate on a daily time step. A brief description of SWAT hydrologic component is given in Chapter II. A complete description of the SWAT model components (Version 2000) is found in Arnold et al. (1998) and Neitsch et al. (2002).

In Chapter II, six watersheds were selected for modeling the hydrology and simulating long-term soil moisture data from historical weather data (1901-2002). Each watershed was divided into several sub-basins of 4km × 4km each. SWAT was

calibrated and validated using measured stream flow at 24 USGS stream gauging stations distributed across six watersheds in Texas. Measured stream flow data from 24 USGS streamgage stations with combined station years of about 125 and 490 years of stream flow data were used for model calibration and validation, respectively. The overall R^2 and Coefficient of efficiency (E) values for the calibration period was 0.75, and the validation period was 0.70. Due to a lack of measured soil moisture data, the simulated soil moisture data was analyzed using the Normalized Difference Vegetation Index (NDVI), measured from satellite during the active growing season (April to September) from 1983 to 1998. Analysis showed that the simulated soil moisture was well-correlated with NDVI for agriculture and pasture land use types ($r \sim 0.6$), indicating that the model performed well in simulating the soil moisture. The simulated soil moisture in Chapter II will be used in this study for developing the drought index.

Characteristics of Drought Index

Before elaborating on the development of the drought index, it is essential to discuss the characteristics of a drought index. They are:

1. The index must be able to reflect developing short-term dry conditions, thus responding to agricultural drought.

2. The index should not have any seasonality (i.e., the index should be able to indicate a drought irrespective of whether it is summer or winter).

3. The drought index should be spatially comparable, irrespective of climatic zones (humid or arid).

These characteristics were taken into account in the development of the two drought indices, the Soil Moisture Deficit Index (SMDI) and the Evapotranspiration Deficit Index (ETDI).

Soil Moisture Deficit Index (SMDI)

The daily model output of available soil water in the root zone was averaged over a seven-day period to get weekly soil water for each of the 52 weeks in a year for each sub-basin. The long-term soil moisture for each week in a year was obtained by taking the median of the available soil water for that week during a 70-year period (1911-1980). The median was chosen over the mean as a measure of "normal" available soil water because median is more stable and is not influenced by few outliers. The maximum and minimum soil water for each week was also obtained from the 70-year data. Using this long-term median, maximum and minimum soil water, weekly percentage soil moisture deficit or excess for 98 years (1901-1998) was calculated as:

$$SD_{i,j} = \frac{SW_{i,j} - MSW_j}{MSW_j - \min SW_j} \times 100 \qquad \text{if } SW_{i,j} \le MSW_j$$

$$SD_{i,j} = \frac{SW_{i,j} - MSW_j}{\max SW_j - MSW_j} \times 100 \qquad \text{if } SW_{i,j} > MSW_j \qquad (3.1)$$

where:

$SD_{i,j}$ = Soil water deficit (%),

$SW_{i,j}$ = Mean weekly soil water available in the soil profile (mm),

MSW_j = Long-term median available soil water in the soil profile (mm),

$max.SW_j$ = Long-term maximum available soil water in the soil profile (mm),

$min.SW_j$ = Long-term minimum available soil water in the soil profile (mm).

(where i = 1901 to 1998 and j = 1 to 52 weeks)

By using Equation 3.1 the seasonality inherent in soil water was removed. Hence, the deficit values can be compared across seasons. The SD values during a week range from -100 to +100 indicating very dry to very wet conditions. As the SD values for all the sub-basins were scaled between -100 and +100 they are also spatially comparable across different climatic zones (humid or arid).

The SD value during any week gives the dryness (wetness) during that week when compared to long-term historical data. Drought occurs only when the dryness continues for a prolonged period of time that can affect crop growth. As the limits of SD values were between -100 and +100, the worst drought can be represented by a straight line with the equation:

$$\sum_{t=1}^{j} Z_t = -100t - 100 \qquad (3.2)$$

where, t is the time in weeks. If this line defines the worst drought (i.e., -4 for the drought index to be comparable with PDSI), then SMDI for any given week can be calculated by:

$$SMDI_j = \frac{\sum_{t=1}^{j} SD_t}{(25t + 25)} \qquad (3.3)$$

Now we are faced with a complicated task of choosing the time period (weeks) over which the dryness values need to be accumulated to determine drought severity. In order to overcome this and take the time period into account indirectly, the drought index was calculated on an incremental basis as suggested by Palmer (1965):

$$SMDI_j = SMDI_{j-1} + \Delta SMDI_j \qquad (3.4)$$

In order to evaluate the contribution of each month to drought severity, we can set i = 1 and t = 1 in Equation 3.3 and we have:

$$SMDI_1 = \frac{SD_1}{50} \qquad (3.5)$$

Since this is the initial month:

$$SMDI_1 - SMDI_0 = \Delta SMDI_1 = \frac{SD_1}{50} \qquad (3.6)$$

A drought will not continue in the extreme category if subsequent months are normal or near normal. Therefore the rate at which SD must increase in order to maintain a constant value of SMDI depends on the value of SMDI to be maintained. For

this reason, an additional term must be added to Equation 3.6 for all months following an initial dry month:

$$\Delta SMDI_j = \frac{SD_j}{50} + cSMDI_{j-1} \qquad (3.7)$$

where: $\Delta SMDI_j = SMDI_j - SMDI_{j-1}$

Equation 3.7 can now be solved for c. By assuming SMDI is -4 during subsequent time steps, then SD_i should be -100:

$$\Delta SMDI_j = \frac{-100}{50} + c(-4.0)$$
$$0 = -2 - 4c$$
$$c = -0.5$$

Therefore, drought severity in any given week is given by:

$$SMDI_j = SMDI_{j-1} + \frac{SD_j}{50} - 0.5SMDI_{j-1} \qquad (3.8)$$
$$SMDI_j = 0.5SMDI_{j-1} + \frac{SD_j}{50}$$

SMDI during any week will range from -4 to +4 representing dry to wet conditions. SMDI was computed at four different levels, using soil water available in the entire soil profile, then soil water available at the top two feet, four feet, and six feet that are represented as SMDI, SMDI-2, SMDI-4, and SMDI-6, respectively. This was done because the potential of the crop to extract water from depths varies during different stages of crop growth and by crop type.

Evapotranspiration Deficit Index (ETDI)

ETDI was calculated using a procedure similar to the one explained above for SMDI, except that the water stress ratio given by Equation 3.9 was used instead of using ET alone. The daily model output of actual evapotranspiration and potential evapotranspiration were cumulated over a seven-day period to get weekly actual and potential evapotranspiration for each of the 52 weeks in a year for each sub-basin. Water stress ratio for the week is calculated as:

$$WS = \frac{PET - AET}{PET} \tag{3.9}$$

where:

WS = Weekly water stress ratio,

PET = Weekly potential evapotranspiration,

AET = Weekly actual evapotranspiration.

WS values range from 1 to 0, with 1 indicating no evapotranspiration and 0 indicating evapotranspiration occurring at the same rate as potential ET. The long-term water stress for each week in a year was obtained by taking the median of the water stress for that week during a 70-year period (1911-1980). The maximum and minimum water stress ratio for each week was also obtained from the 70-year data. From the long-term median, maximum and minimum water stress, percentage water stress anomaly during any week for 98 years (1901-1998) is calculated as:

$$WSA_{i,j} = \frac{MWS_j - WS_{i,j}}{MWS_j - \min WS_j} \times 100 \qquad \text{if } WS_{i,j} \leq MWS_j$$

$$WSA_{i,j} = \frac{MWS_j - WS_{i,j}}{\max WS_j - MWS_j} \times 100 \qquad \text{if } WS_{i,j} > MWS_j \qquad (3.10)$$

where:

WSA = Weekly water stress anomaly,

MWS_j = Long-term median water stress of week j,

$\max.WS_j$ = Long-term maximum water stress of week j,

$\min.WS_j$ = Long-term minimum water stress of week j,

WS = Weekly water stress ratio.

(where i = 1901 to 1998 and j = 1 to 52 weeks).

The water stress anomaly during any week ranges from -100 to +100 indicating very dry to very wet conditions with respect to evapotranspiration. Adopting a similar cumulating procedure of SMDI, drought severity due to evapotranspiration deficit is given by:

$$ETDI_j = 0.5ETDI_{j-1} + \frac{WSA_j}{50} \qquad (3.11)$$

Using Equations 3.8 and 3.11, Soil Moisture Deficit Index (SMDI) at two feet, four feet, six feet and Evapotranspiration Deficit Index (ETDI) were calculated for 98 years of simulated soil moisture and evapotranspiration data from 1901-1998.

Results and Discussion

Time-series Characteristics

An auto-correlation analysis was done to study the characteristics of the drought index based on soil and land use characteristics. The correlogram of simulated soil water available in the root zone for one of the sub-basins is shown in Fig.3.1a. From the correlogram, we observed that soil water available in the root zone was highly auto-correlated. This is because soil water in the current time step depends on the soil water available during previous time steps. The sinusoidal pattern of the correlogram indicates that soil water was also highly seasonal, fluctuating according to seasonal precipitation and evapotranspiration. Hence, the soil water was differenced with median long-term weekly soil water to remove the seasonality. The correlogram of SMDI (Fig.3.1b) derived from the differenced soil water showed that the seasonal differencing effectively removed the seasonality, which is ideal for drought monitoring, irrespective of season.

Incidentally, Equations 3.8 and 3.11, derived for calculating drought index from soil moisture and evapotranspiration deficits, respectively, are also analogous to the first order auto-correlation process with white noise represented by the SD and WSA terms (Dryness or wetness during the week compared to historical data). The auto-correlation lags (i.e., the lag at which the correlation is less than $\pm 2/\sqrt{N}$, where N is the number of

(a)

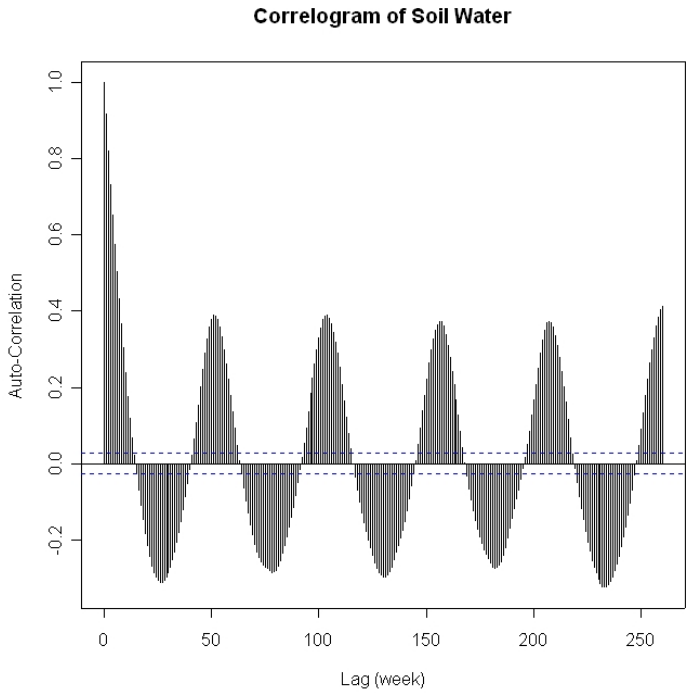

(b)

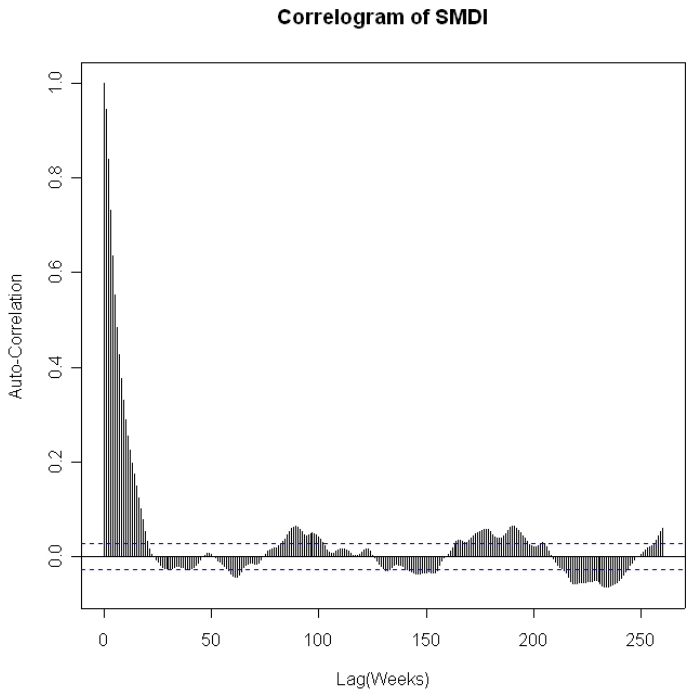

Figure 3.1. Correlogram of sub-basin 1454 in Upper Trinity watershed. (a) soil moisture (b) Soil Moisture Deficit Index (SMDI).

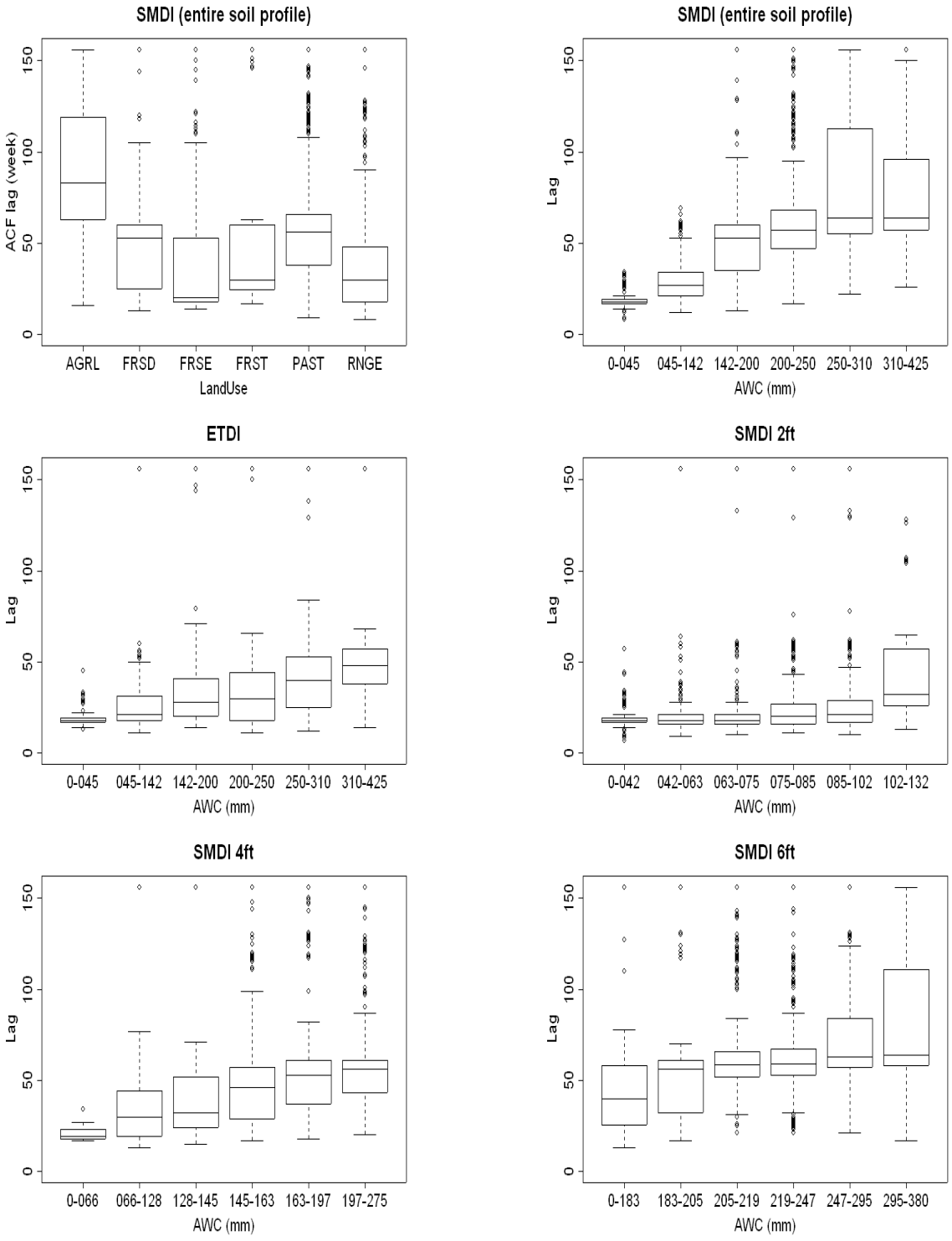

Figure 3.2. Auto-correlation lags of drought indices based on available water holding capacity of soil and land use.

data points) for individual sub-basins for different drought indices are shown in Fig.3.2. The auto-correlation lag seems to closely depend on the available water holding capacity of the soil with the lag increasing with water holding capacity. This was expected because if the water holding capacity of the soil is high, then the current soil water and evapotranspiration will be affected by events (precipitation and evapotranspiration) that happened in the distant past rather than for the soils with low water holding capacity. The lag also increases with depth due to increase in total available water holding capacity. Lag does not seem to depend much on the land use however, among different land use types, agricultural lands have the largest lag. This is because most of the agricultural lands are located on soils with high water holding capacity (Fig.2.12).

Among different drought indicators, SMDI-2ft had the lowest auto-correlation lag (approximately 3 months). This is because the top two feet of the soil profile very actively participate in the evapotranspiration of available soil water. Most of the pasture and agriculture crops have shallow root systems that primarily use the soil water available at the top two feet of the soil profile. For the same reason, the ETDI also have smaller auto-correlation lags when compared to SMDI, derived from an entire soil profile, which has a lag of approximately 1.5 years. Hence, ETDI and SMDI-2 could be useful indicators of short-term drought conditions, whereas SMDI derived from an entire soil profile could be a good indicator of long-term drought conditions.

Spatial Variability

A spatial variability analysis was done to study the effect of the spatially distributed model along with distributed model parameters on soils, land use and topography, and weather variables like precipitation and temperature on the drought index. Standard Deviation of the drought index, calculated during each time step, was used as a measure of spatial variability of the drought index. The standard deviation was calculated for the entire watershed during each week for 98 years from 1901-1998. The distribution of standard deviation for 52 weeks during the 98-year period for six watersheds is shown in figs.3.3 to 3.8. For all six watersheds, irrespective of the drought index, the standard deviation was above 1.0. Considering that the range of drought indices is from -4 to + 4, a standard deviation of 1.0 indicates that the spatial variability of the drought index is high.

The mean and standard deviation of weekly precipitation and potential ET for each watershed were also analyzed to determine the reason for spatial variability in the drought index. Analysis of 98 years of precipitation data showed that the precipitation distribution in a year was bimodal for all six watersheds, with high precipitation occurring during late spring and mid fall seasons. Precipitation was the highly variable component both spatially and temporally during different years for the same season. Potential ET also showed some spatial variability with high variability occurring during the summer season. The highest spatial variability in potential ET was in the Colorado

and Red River watersheds, where the standard deviation was up to 10mm during the summer season.

The spatial variability (standard deviation) of the drought indices, especially ETDI, during different seasons closely followed the variability in precipitation and potential evapotranspiration across seasons. In order to get a sense of how the standard deviation reflects the spatial distribution of drought indices, SMDI derived during 46th week of 1988 and 24th week of 1990 with standard deviations of 1.0 and 1.5, respectively, are shown in figs.3.9a and 3.9b. As the standard deviation increased, the spatial variability of the drought index also increased considerably.

The spatial standard deviation of ETDI increased from 0.75 during the spring season to as much as 1.5 at the end of the summer season (Figs.3.3 to 3.8). This was because evapotranspiration was high during summer, following a season of high precipitation during spring that recharged the available soil water to varying degrees of saturation depending on the spatial distribution of precipitation and soil properties. The precipitation amount also gradually reduced during summer. Actual evapotranspiration depends on the amount of water already in the soil profile, soil physical properties and land use characteristics. Hence, the spatial variability of ETDI increases during the summer season.

The spatial variability of SMDI for all soil depths was above 1.0 during most of the seasons for all the watersheds. Except for Lower Trinity, the spatial variability of

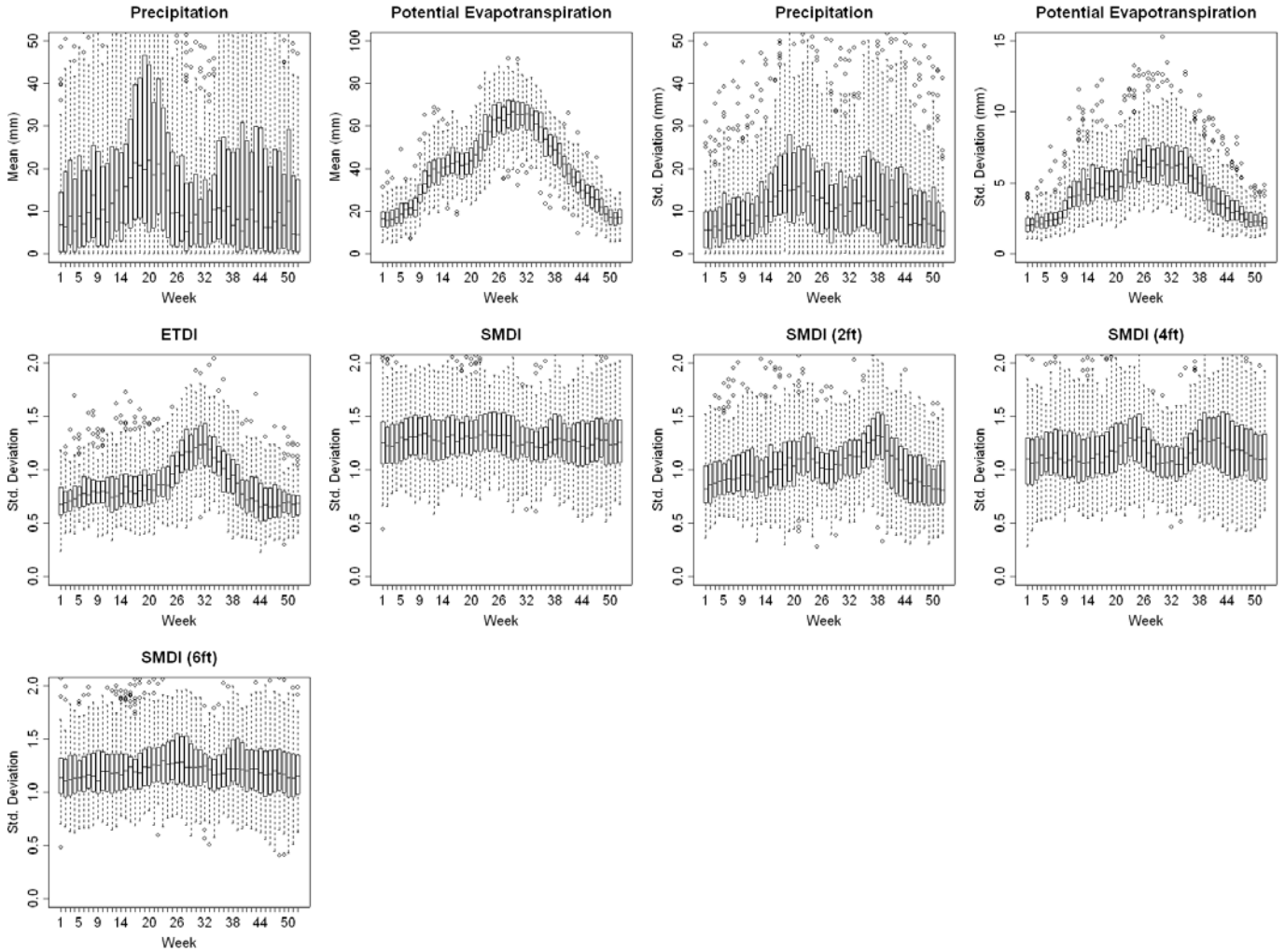

Figure 3.3. Distribution of spatial standard deviation of precipitation, evapotranspiration and drought indices for 98 years during each week in Upper Trinity.

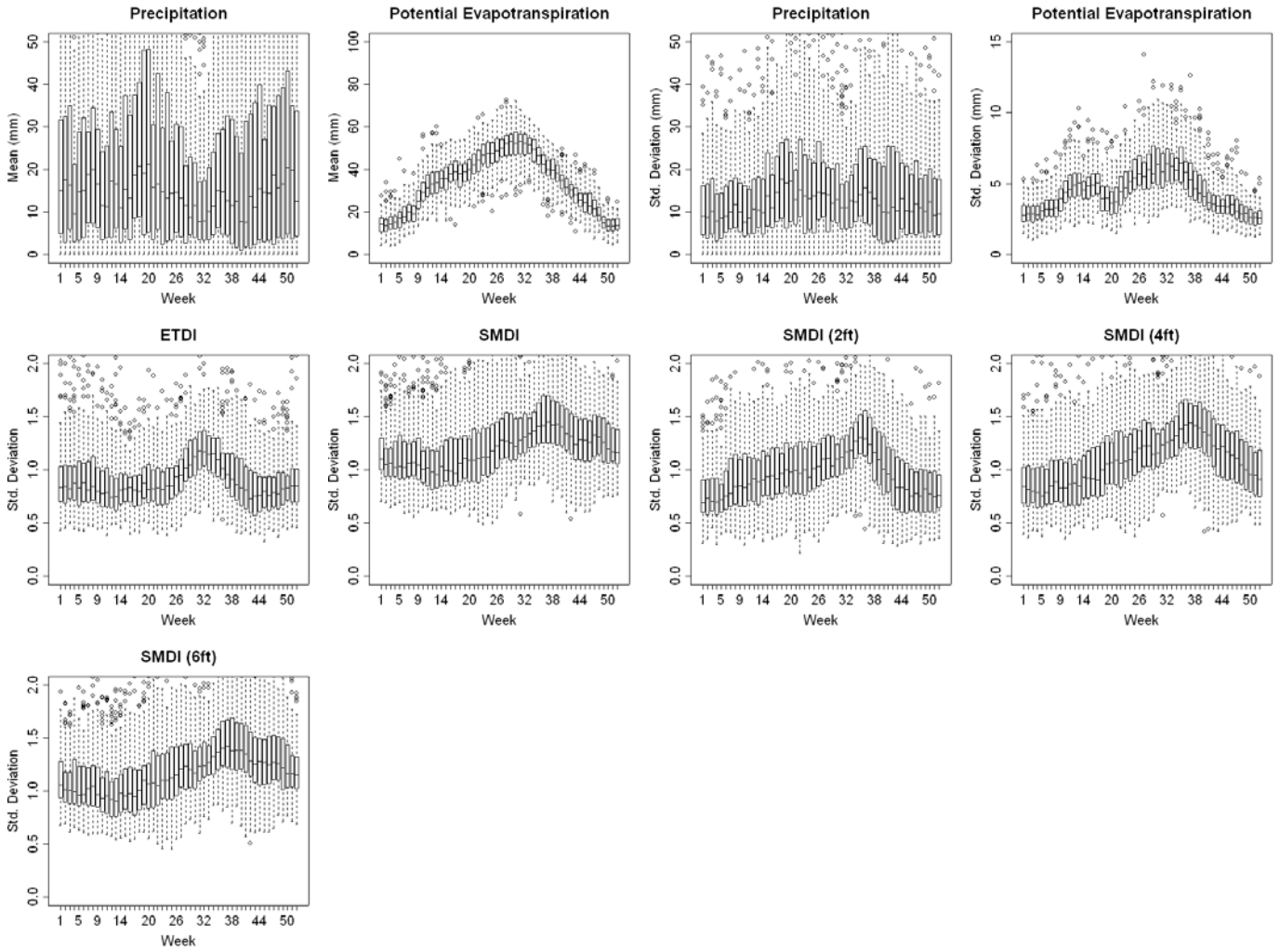

Figure 3.4. Distribution of spatial standard deviation of precipitation, evapotranspiration and drought indices for 98 years during each week in Lower Trinity.

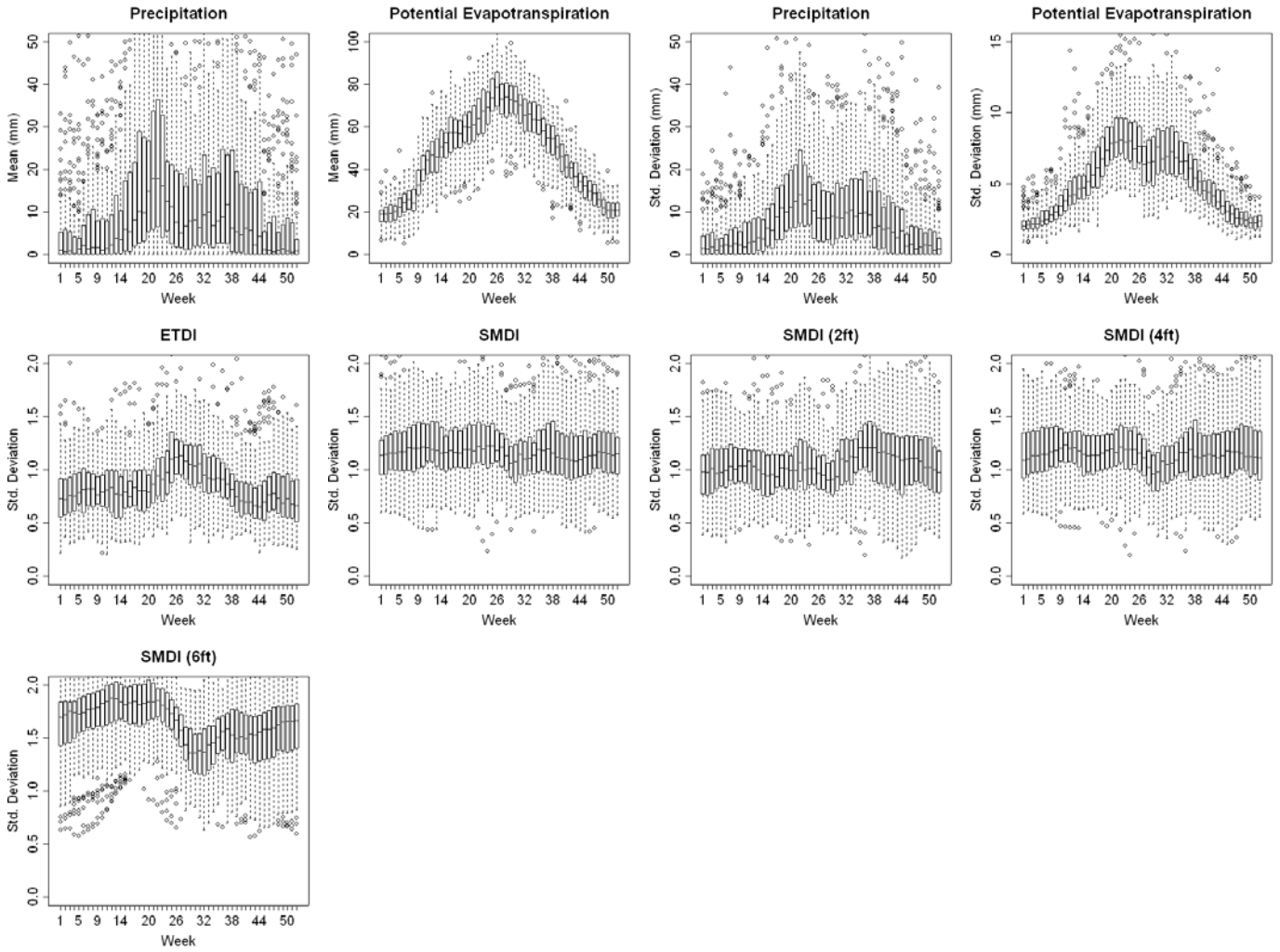

Figure 3.5. Distribution of spatial standard deviation of precipitation, evapotranspiration and drought indices for 98 years during each week in Red River.

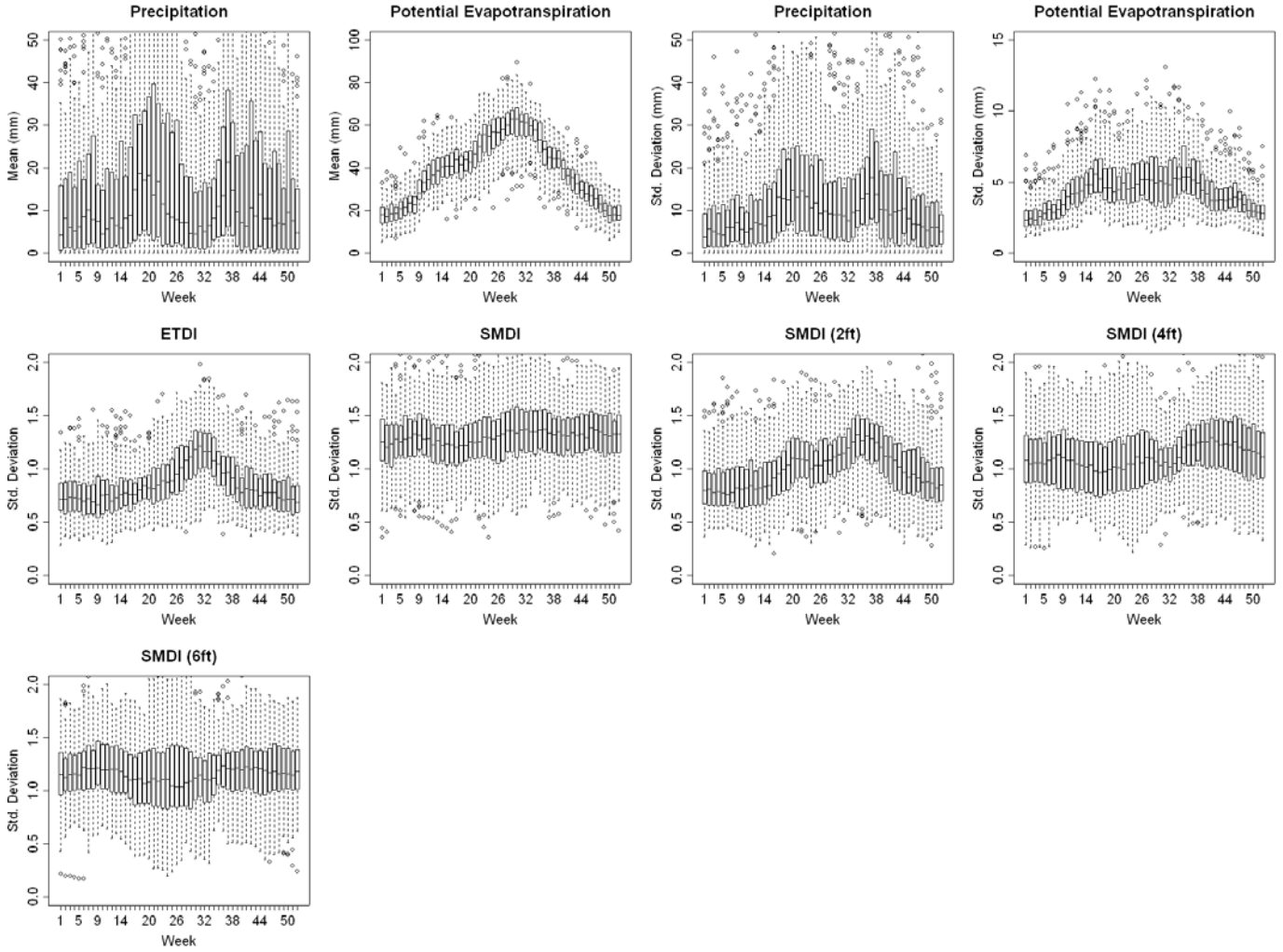

Figure 3.6. Distribution of spatial standard deviation of precipitation, evapotranspiration and drought indices for 98 years during each week in Guadalupe River.

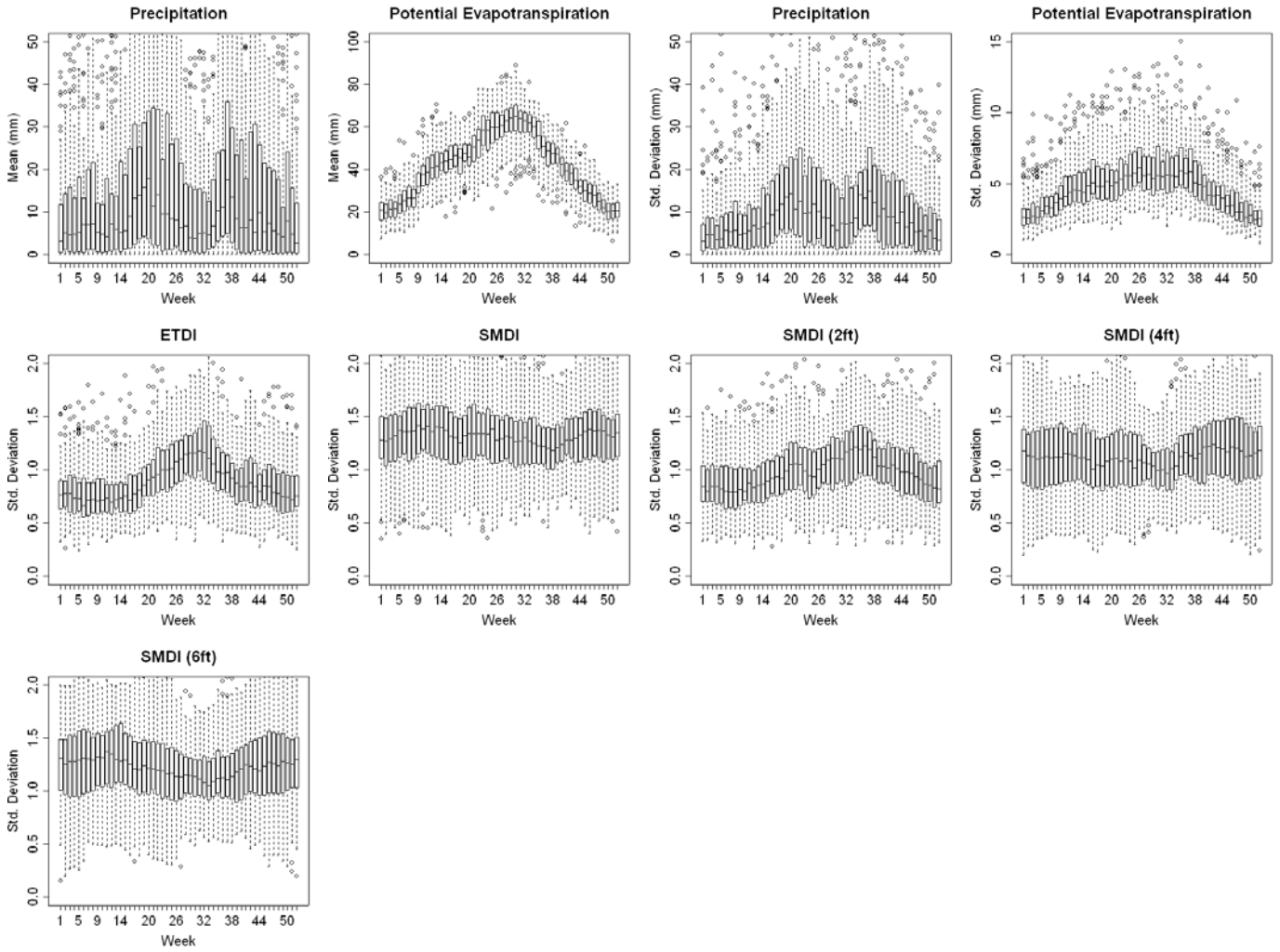

Figure 3.7. Distribution of spatial standard deviation of precipitation, evapotranspiration and drought indices for 98 years during each week in San Antonio River.

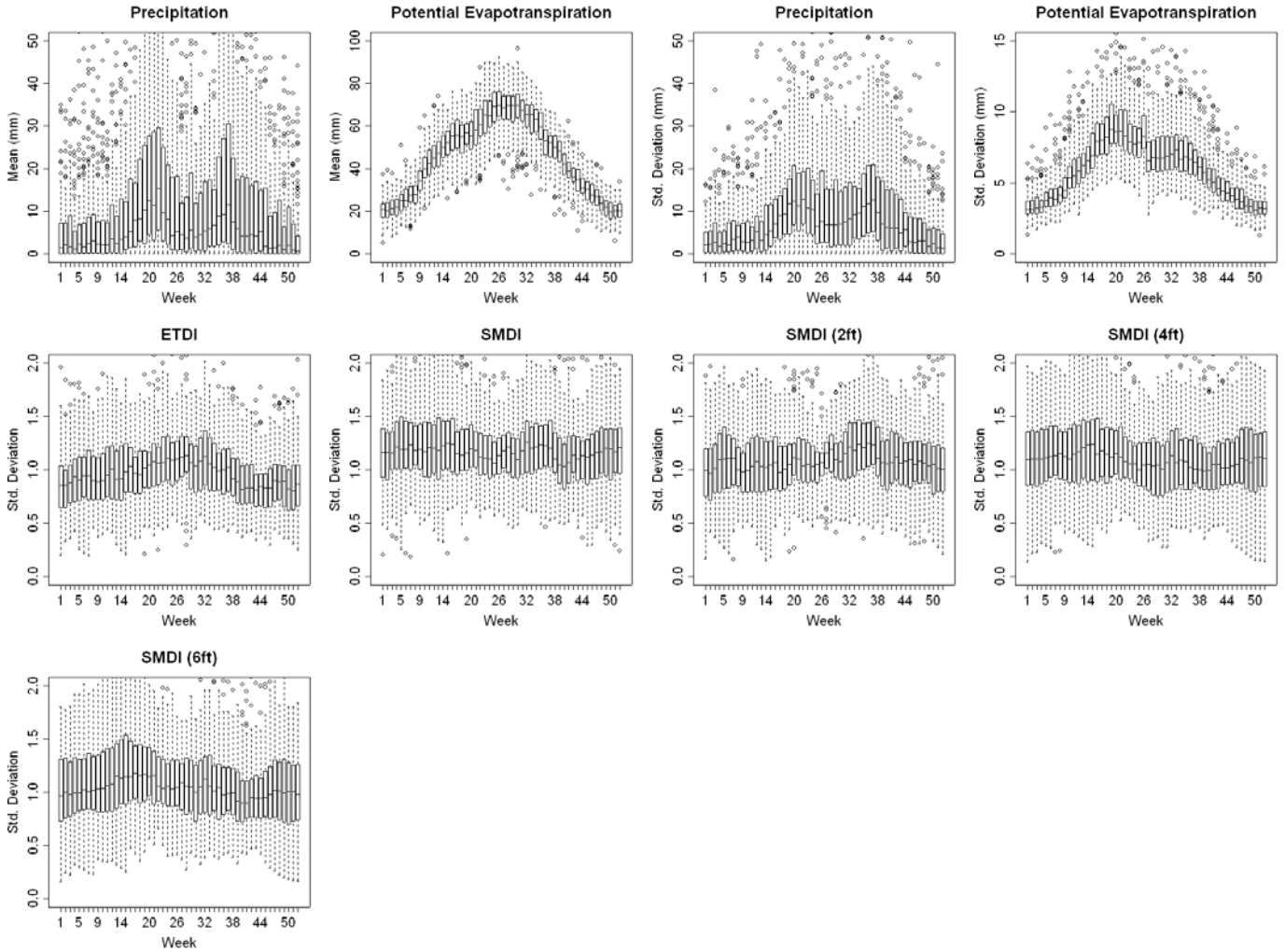

Figure 3.8. Distribution of spatial standard deviation of precipitation, evapotranspiration and drought indices for 98 years during each week in Colorado River.

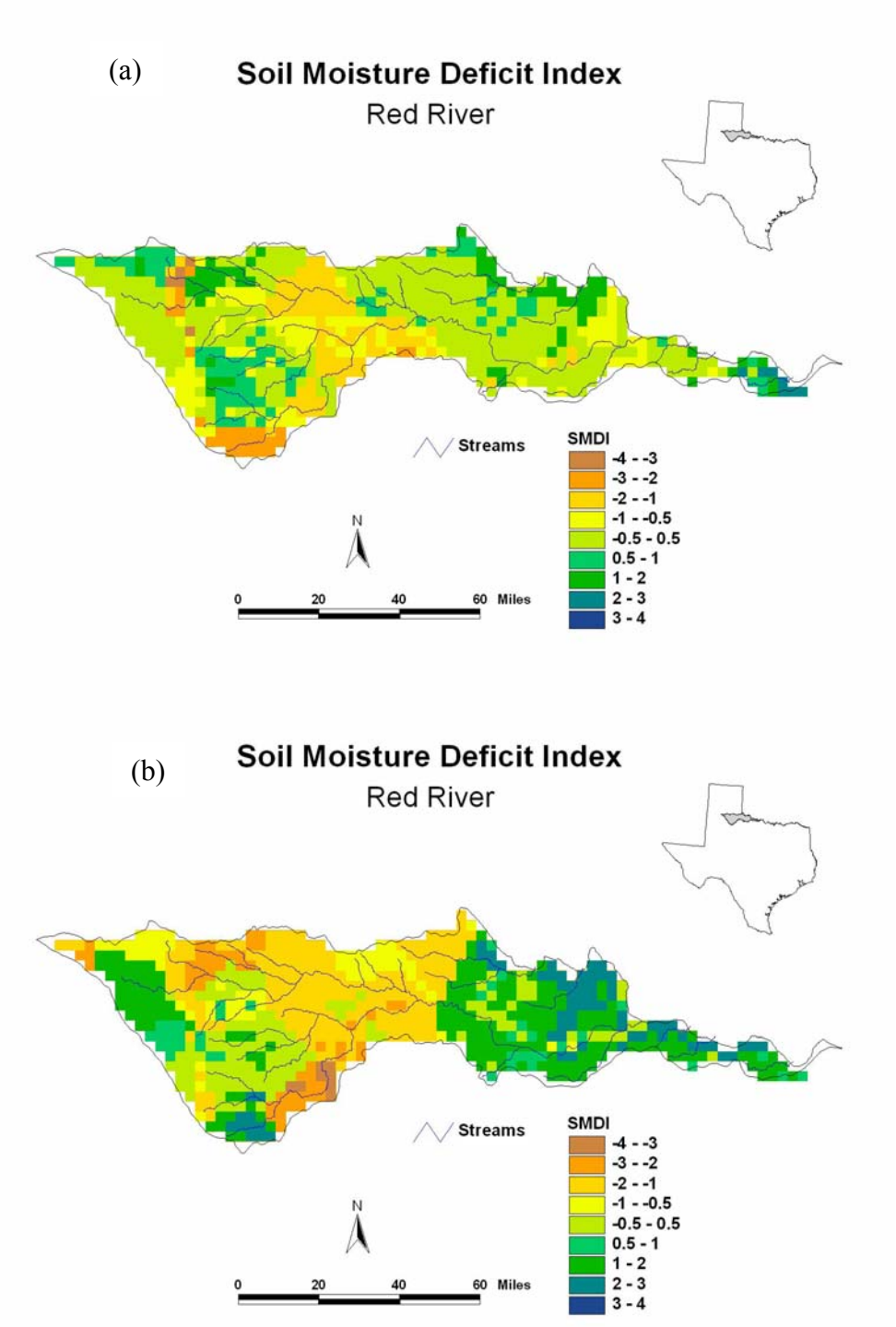

Figure 3.9. Spatial distribution of Soil Moisture Deficit Index (SMDI). a) 46th week of 1988 with standard deviation of 1.00 b) 24th week of 1990 with a standard deviation of 1.5.

SMDI during various seasons was similar in all the watersheds (Figs.3.3 to 3.8). The Lower Trinity watershed is located in a high precipitation zone with annual precipitation greater than 1000mm across most parts of the watershed and lower potential ET than all other watersheds. This high precipitation was enough to recharge the soil water to the highest level across the watershed, irrespective of soil characteristics. Thus, most of the spatial variability during various seasons closely follows the temperature cycle (evapotranspiration), lagged by few weeks with the characteristic sinusoidal response.

As evapotranspiration increased and precipitation decreased during the summer, soil water was depleted. Further, the spatial variability of actual evapotranspiration increased due to spatial variability in soil and land use characteristics. This increased the spatial variability of SMDI to as much as a standard deviation of 1.5. As precipitation increase again in winter, the soil water was recharged across the entire Lower Trinity watershed, thus reducing the spatial variability in SMDI.

The SMDI-6 for Red River had the highest standard deviation (~1.5) during most of the season and had a different seasonal pattern than other watersheds. This is because the Red River watershed covers a range of precipitation zones from 488mm in the west to 748mm in the east. The standard deviation of potential evapotranspiration was also the highest for Red River during the summer (~10mm) when compared to other watersheds. The standard deviation of SMDI-6 decreased during the summer because this part of the season was characterized by less precipitation (less spatial variability)

and high evapotranspiration (soils become mostly dry), and thus, the spatial variability of SMDI reduced during summer.

Comparison With Other Drought Indices

The drought indices developed in this study were compared with other drought indicators currently in use, such as the Palmer Drought Severity Index (PDSI) (Palmer 1965) and the Standardized Precipitation Index (SPI) (McKee et al. 1993). Brief descriptions of PDSI and SPI are given in Chapter I. PDSI and SPI are reported at the spatial scale of climatic divisions (Fig.2.1) and at a monthly temporal resolution. However, the drought indices developed in this study have a spatial resolution of 4km × 4km (Fig.3.9) and a weekly temporal resolution. Hence, the drought indices ETDI and SMDI need to be aggregated at spatial and temporal scales for comparison with PDSI and SPI.

Because ETDI and SMDI's were integrated measures of past weather conditions, instead of averaging the index temporally over the entire month, only the drought index calculated during the last week of every month was spatially averaged over the entire watershed for comparison with monthly PDSI and SPI. The spatially-averaged, monthly ETDI and SMDI's for 98 years (1901-1998) were compared with PDSI and SPI reported for climatic divisions in which major portions of each of the six study watersheds are located. The correlation (r) matrix of the drought indices developed in this study (ETDI and SMDI's) with PDSI and SPI's published for 1, 3, 6, 9, and 12 month precipitation amounts for six study watersheds are presented in Tables 3.1 to 3.6.

Table 3.1. Correlation matrix of drought indices - Upper Trinity.

	ETDI	SMDI	SMDI-2	SMDI-4	SMDI-6	PDSI	SPI-1	SPI-3	SPI-6	SPI-9	SPI-12
ETDI	1.00										
SMDI	0.80	1.00									
SMDI-2	**0.93**	0.85	1.00								
SMDI-4	0.82	0.98	0.90	1.00							
SMDI-6	0.73	0.98	0.78	0.96	1.00						
PDSI	0.58	**0.78**	0.59	0.73	**0.79**	1.00					
SPI-1	**0.75**	0.57	**0.74**	0.60	0.51	0.49	1.00				
SPI-3	0.69	**0.78**	0.73	**0.79**	0.76	0.73	0.62	1.00			
SPI-6	0.53	0.77	0.55	0.72	0.77	0.84	0.43	0.75	1.00		
SPI-9	0.43	0.70	0.44	0.63	0.72	**0.85**	0.35	0.61	0.85	1.00	
SPI-12	0.38	0.62	0.38	0.55	0.65	0.82	0.30	0.52	0.74	0.90	1.00

Table 3.2. Correlation matrix of drought indices - Lower Trinity.

	ETDI	SMDI	SMDI-2	SMDI-4	SMDI-6	PDSI	SPI-1	SPI-3	SPI-6	SPI-9	SPI-12
ETDI	1.00										
SMDI	0.81	1.00									
SMDI-2	**0.93**	0.84	1.00								
SMDI-4	0.88	0.97	0.93	1.00							
SMDI-6	0.82	0.99	0.85	0.97	1.00						
PDSI	0.53	0.72	0.53	0.64	0.72	1.00					
SPI-1	**0.71**	0.59	**0.72**	0.64	0.60	0.53	1.00				
SPI-3	0.61	**0.74**	0.61	**0.71**	**0.74**	0.76	0.61	1.00			
SPI-6	0.46	0.68	0.46	0.58	0.67	**0.84**	0.44	0.75	1.00		
SPI-9	0.39	0.63	0.39	0.51	0.62	**0.84**	0.36	0.61	0.85	1.00	
SPI-12	0.33	0.57	0.33	0.46	0.56	0.81	0.31	0.54	0.75	0.90	1.00

Table 3.3. Correlation matrix of drought indices - Red River.

	ETDI	SMDI	SMDI-2	SMDI-4	SMDI-6	PDSI	SPI-1	SPI-3	SPI-6	SPI-9	SPI-12
ETDI	1.00										
SMDI	0.79	1.00									
SMDI-2	**0.94**	0.86	1.00								
SMDI-4	0.83	0.99	0.91	1.00							
SMDI-6	0.73	0.99	0.81	0.97	1.00						
PDSI	0.58	0.65	0.58	0.64	0.63	1.00					
SPI-1	0.69	0.43	0.61	0.47	0.38	0.44	1.00				
SPI-3	**0.72**	0.64	**0.73**	**0.67**	0.59	0.65	0.60	1.00			
SPI-6	0.54	**0.66**	0.59	0.66	**0.64**	0.79	0.40	0.72	1.00		
SPI-9	0.47	0.64	0.50	0.62	0.63	**0.82**	0.35	0.59	0.83	1.00	
SPI-12	0.42	0.59	0.44	0.56	0.59	0.82	0.29	0.50	0.73	0.89	1.00

Table 3.4. Correlation matrix of drought indices - Guadalupe River.

	ETDI	SMDI	SMDI-2	SMDI-4	SMDI-6	PDSI	SPI-1	SPI-3	SPI-6	SPI-9	SPI-12
ETDI	1.00										
SMDI	0.80	1.00									
SMDI-2	**0.94**	0.86	1.00								
SMDI-4	0.82	0.98	0.89	1.00							
SMDI-6	0.72	0.97	0.78	0.96	1.00						
PDSI	0.55	**0.78**	0.56	0.73	**0.79**	1.00					
SPI-1	**0.75**	0.57	**0.71**	0.59	0.52	0.48	1.00				
SPI-3	0.68	0.77	0.70	**0.78**	0.76	0.73	0.63	1.00			
SPI-6	0.53	0.77	0.55	0.73	0.78	0.85	0.45	0.77	1.00		
SPI-9	0.44	0.72	0.45	0.66	0.75	**0.86**	0.37	0.63	0.87	1.00	
SPI-12	0.38	0.65	0.38	0.58	0.68	0.85	0.32	0.55	0.77	0.91	1.00

Table 3.5. Correlation matrix of drought indices - San Antonio River.

	ETDI	SMDI	SMDI-2	SMDI-4	SMDI-6	PDSI	SPI-1	SPI-3	SPI-6	SPI-9	SPI-12
ETDI	1.00										
SMDI	0.83	1.00									
SMDI-2	**0.96**	0.86	1.00								
SMDI-4	0.81	0.97	0.84	1.00							
SMDI-6	0.71	0.97	0.73	0.97	1.00						
PDSI	0.54	**0.75**	0.53	0.71	**0.78**	1.00					
SPI-1	**0.74**	0.60	**0.72**	0.58	0.51	0.48	1.00				
SPI-3	0.67	**0.75**	0.67	**0.75**	0.73	0.73	0.63	1.00			
SPI-6	0.52	0.74	0.53	0.72	0.77	0.85	0.45	0.77	1.00		
SPI-9	0.43	0.69	0.42	0.64	0.74	**0.86**	0.37	0.63	0.87	1.00	
SPI-12	0.36	0.62	0.35	0.56	0.67	0.85	0.32	0.55	0.77	0.91	1.00

Table 3.6. Correlation matrix of drought indices - Colorado River.

	ETDI	SMDI	SMDI-2	SMDI-4	SMDI-6	PDSI	SPI-1	SPI-3	SPI-6	SPI-9	SPI-12
ETDI	1.00										
SMDI	0.96	1.00									
SMDI-2	**0.98**	0.98	1.00								
SMDI-4	0.81	0.90	0.84	1.00							
SMDI-6	0.78	0.88	0.80	0.99	1.00						
PDSI	0.54	0.58	0.52	0.66	0.66	1.00					
SPI-1	**0.73**	**0.68**	**0.70**	0.52	0.50	0.48	1.00				
SPI-3	0.66	0.67	0.66	**0.68**	0.65	0.72	0.62	1.00			
SPI-6	0.52	0.58	0.52	**0.68**	**0.67**	0.85	0.45	0.76	1.00		
SPI-9	0.44	0.52	0.44	0.64	0.66	**0.87**	0.38	0.65	0.87	1.00	
SPI-12	0.38	0.46	0.37	0.58	0.61	0.83	0.32	0.55	0.77	0.91	1.00

ETDI and SMDI's were positively correlated with PDSI and SPI's ($r > 0.7$) for all the six watersheds. This suggests that the dry and wet period indicated by the ETDI and SMDI's were in general agreement with PDSI and SPI. However, the duration of the dryness or wetness and the intensity of drought measured by each index are different depending on the inherent characteristic of each drought index. The maximum correlations of ETDI and SMDI's to PDSI and SPI's for each watershed are indicated in bold font in Tables 3.1 to 3.6. By observing the correlation matrix, a trend evolves in correlation between the drought indices developed in this study and existing drought indices. The ETDI and SMDI-2 were well-correlated with SPI-1 ($r \sim 0.75$) for all the six watersheds. This was expected because ETDI and SMDI-2 had lesser auto-correlation lag (Fig.3.2) and thus depend on short-term weather conditions when compared to SPI's of higher duration or PDSI that are indicators of medium to long-term drought conditions. ETDI and SMDI-2 were also highly correlated with themselves ($r \sim 0.95$) because most of the active evapotranspiration takes place at the top two feet of soil profile and they both are complementary to each other.

SMDI derived from the entire soil profile and SMDI-6 were well-correlated with PDSI, SPI-3 and SPI-6. For Upper Trinity, Guadalupe and San Antonio River watersheds, SMDI and SMDI-6 had high correlation with PDSI ($r > 0.78$). For Lower Trinity watershed, SMDI and SMDI-6 had high correlation with SPI-3 ($r \sim 0.74$). For Colorado River, only 40% of the watershed had soils greater than 2ft deep. Hence, similar to SMDI-2, SMDI of Colorado River watershed had high correlation with SPI-1 ($r \sim 0.68$). However, for soils with depth greater than 6ft in Colorado River Watershed,

SMDI-6 was well correlated with SPI-6 (r ~ 0.67). Hence, SMDI and SMDI-6 are good measures of long-term drought conditions. For all the watersheds, SMDI-4 was well-correlated with SPI-3 (r ~ 0.7), suggesting that SMDI-4 could be a good intermediate measure between rapidly responding ETDI/SMDI-2 and slow evolving SMDI/SMDI-6.

For all the watersheds, PDSI was well-correlated with SPI-9 and SPI-12 (r~0.85), suggesting that PDSI is an indicator of long-term weather conditions. This was consistent with the observation made by Guttman (1998) that PDSI and SPI are in phase only at a period of about a year. The correlation of PDSI with SPI-9 and SPI-12 was greater than 0.84 for most of the watersheds, which was higher than the correlation of SPI's with ETDI and SMDI's that varied between 0.71 and 0.78, suggesting that precipitation is the dominant factor in PDSI. Precipitation was the dominant factor in ETDI and SMDI's as well; however, as the spatial variability analysis showed, the spatial variability in precipitation, ET, soil, and land use characteristics not accounted for by PDSI or SPI, were also critical in ETDI and SMDI for identifying localized drought conditions.

Correlation With Crop Yield

A correlation analysis was done with the drought indices and crop yield data to analyze if dryness during the critical period of crop growth affected the crop yield. Sorghum grown during summer (April – September) and wheat grown during winter (October – May) were selected for this analysis. The County crop yield data of sorghum and wheat during the past 26 years (1973 - 1998) were collected for various counties

from the National Agricultural Statistical Service (NASS). Only the crop yields obtained under non-irrigated conditions were used for correlation analysis. From the 26 years of crop yield data for both sorghum and wheat, six years with best yield and six years with worst yield (12 years total) were selected for correlation analysis in each County for sorghum and wheat. The six best and six worst yields were selected because there are other factors like soil fertility, pests, diseases, water logging, and frost, in addition to soil moisture stress that can affect crop yield. By selecting these high and low yield years, we assume that the yield was affected primarily due to moisture stress experienced during different stages of crop growth. With the drought indices at a spatial resolution of 4km × 4km, the weekly drought indices were spatially averaged across the County, only for sub-basins with agricultural land use, during each week for comparison with County crop yield data. The correlations of drought indices with sorghum yield during each week are given in Tables 3.7 to 3.15 and winter wheat yield correlations are given in Tables 3.16 to 3.24.

Sorghum: In major parts of Texas sorghum is planted during March-April and harvested in August-September. The critical growth stages of sorghum are tasseling, pollination and yield formation (June – July), during which a water stress at the root zone can have a significant impact on the crop yield (Hane and Pumphrey 1984). The correlation of weekly ETDI and SMDI's with the six best and six worst years of Sorghum yield also showed maximum correlation during the weeks in June and July (Tables 3.7a to 3.15a). For Floyd County, ETDI during the 29^{th} week (July) had the highest correlation with crop yield ($r \sim 0.93$). For Concho, Guadalupe, Wilson, and

Table 3.7. Correlation of drought indices with sorghum yield during the crop growing season – Floyd County.

a) ETDI and SMDI's.

Week	Month	ETDI	SMDI	SMDI-2	SMDI-4	SMDI-6
9	3	0.38	0.63	0.67	0.61	0.62
10	3	0.48	0.64	0.70	0.62	0.63
11	3	0.56	0.65	0.71	0.62	0.63
12	3	0.50	0.71	0.77	0.67	0.68
13	3	0.15	0.71	0.71	0.66	0.68
14	4	0.17	0.72	0.69	0.66	0.68
15	4	0.40	0.75	0.72	0.68	0.71
16	4	0.66	**0.79**	**0.83**	0.75	0.75
17	4	0.41	**0.79**	0.81	**0.78**	**0.76**
18	5	0.10	0.78	0.72	0.77	0.74
19	5	-0.12	0.74	0.46	0.73	0.71
20	5	-0.16	0.66	0.20	0.63	0.65
21	5	0.30	0.71	0.26	0.67	0.70
22	6	0.35	0.72	0.27	0.64	0.69
23	6	0.46	**0.79**	0.34	0.67	0.75
24	6	0.36	0.74	0.22	0.60	0.72
25	6	0.47	0.72	0.24	0.59	0.70
26	6	0.59	0.71	0.35	0.59	0.69
27	7	0.71	0.70	0.37	0.58	0.69
28	7	0.88	0.74	0.45	0.65	0.71
29	7	**0.93**	0.76	0.55	0.69	0.73
30	7	0.91	0.75	0.52	0.69	0.72
31	8	0.79	0.67	0.34	0.58	0.65
32	8	0.64	0.55	0.15	0.42	0.52
33	8	0.52	0.52	0.06	0.36	0.49
34	8	0.22	0.49	0.02	0.30	0.46
35	9	0.45	0.52	0.18	0.37	0.50
36	9	0.53	0.57	0.36	0.44	0.55
37	9	0.32	0.54	0.36	0.42	0.53
38	9	-0.05	0.39	0.14	0.26	0.39
39	9	-0.19	0.22	-0.02	0.08	0.21

b) PDSI and SPI's.

Month	PDSI	SPI-1	SPI-3	SPI-6	SPI-9
3	0.53	-0.29	0.04	0.36	0.55
4	0.65	0.23	0.43	0.44	**0.67**
5	0.54	0.15	0.31	0.32	0.65
6	0.64	**0.50**	0.52	0.49	0.54
7	**0.72**	0.43	0.45	0.56	0.57
8	0.70	0.34	**0.57**	**0.59**	0.64
9	0.53	-0.26	0.19	0.48	0.54

Table 3.8. Correlation of drought indices with sorghum yield during the crop growing season – Tom Green County.

a) ETDI and SMDI's.

Week	Month	ETDI	SMDI	SMDI-2	SMDI-4	SMDI-6
9	3	0.49	0.78	0.60	0.80	0.78
10	3	0.58	0.79	0.66	0.82	0.79
11	3	0.56	0.80	0.65	0.83	0.80
12	3	0.49	0.80	0.61	0.82	0.80
13	3	0.57	0.81	0.65	0.83	0.81
14	4	0.56	0.81	0.64	0.83	0.81
15	4	0.54	0.82	0.65	0.84	0.82
16	4	0.68	0.85	0.71	0.87	0.85
17	4	0.74	0.85	0.74	0.87	0.85
18	5	0.73	0.86	0.75	0.88	0.86
19	5	0.69	0.86	0.75	0.88	0.86
20	5	0.72	**0.88**	0.79	0.89	**0.88**
21	5	0.78	**0.88**	**0.81**	**0.90**	**0.88**
22	6	**0.82**	0.87	0.80	0.89	0.87
23	6	0.79	0.81	0.61	0.83	0.81
24	6	0.70	0.74	0.49	0.76	0.74
25	6	0.75	0.72	0.56	0.74	0.72
26	6	0.76	0.74	0.68	0.77	0.74
27	7	0.77	0.76	0.70	0.79	0.76
28	7	0.74	0.77	0.63	0.81	0.77
29	7	0.74	0.78	0.73	0.86	0.79
30	7	0.73	0.79	0.70	0.83	0.80
31	8	0.32	0.68	0.22	0.66	0.69
32	8	-0.09	0.39	-0.16	0.25	0.37
33	8	-0.30	0.13	-0.33	-0.04	0.10
34	8	-0.43	-0.06	-0.42	-0.23	-0.09
35	9	-0.40	-0.10	-0.42	-0.24	-0.13
36	9	-0.33	-0.08	-0.39	-0.21	-0.11
37	9	-0.20	-0.08	-0.34	-0.18	-0.11
38	9	-0.14	-0.06	-0.26	-0.14	-0.08
39	9	-0.32	-0.14	-0.32	-0.22	-0.16

b) PDSI and SPI's.

Month	PDSI	SPI-1	SPI-3	SPI-6	SPI-9
3	0.64	0.32	0.41	0.62	0.73
4	0.68	0.68	0.63	0.55	0.77
5	0.70	0.46	0.75	0.74	**0.85**
6	**0.72**	**0.66**	**0.78**	**0.76**	0.83
7	0.71	0.04	0.63	0.74	0.69
8	0.10	-0.53	-0.01	0.47	0.52
9	-0.08	-0.29	-0.60	0.19	0.29

Table 3.9. Correlation of drought indices with sorghum yield during the crop growing season – Concho County.

a) ETDI and SMDI's.

Week	Month	ETDI	SMDI	SMDI-2	SMDI-4	SMDI-6
9	3	0.53	0.72	0.68	0.72	0.73
10	3	0.48	0.70	0.68	0.71	0.72
11	3	0.46	0.68	0.64	0.68	0.70
12	3	0.47	0.69	0.63	0.70	0.71
13	3	0.54	0.71	0.64	0.71	0.73
14	4	0.52	0.72	0.63	0.72	0.73
15	4	0.48	0.71	0.62	0.71	0.72
16	4	0.48	0.68	0.60	0.68	0.69
17	4	0.55	0.67	0.61	0.68	0.68
18	5	0.38	0.63	0.56	0.63	0.63
19	5	0.32	0.59	0.46	0.60	0.60
20	5	0.41	0.57	0.47	0.59	0.59
21	5	0.60	0.64	0.59	0.67	0.66
22	6	0.55	0.61	0.51	0.64	0.63
23	6	0.44	0.50	0.32	0.53	0.53
24	6	0.44	0.52	0.34	0.51	0.53
25	6	0.50	0.55	0.44	0.55	0.55
26	6	0.64	0.65	0.59	0.66	0.63
27	7	**0.73**	0.72	**0.73**	0.75	0.65
28	7	0.68	0.72	0.70	0.77	0.65
29	7	0.65	**0.76**	0.73	**0.81**	**0.75**
30	7	0.67	0.75	0.67	0.77	0.74
31	8	0.28	0.61	0.35	0.58	0.65
32	8	-0.15	0.41	-0.07	0.27	0.45
33	8	-0.31	0.22	-0.29	-0.01	0.18
34	8	-0.44	0.04	-0.44	-0.23	-0.06
35	9	-0.40	-0.05	-0.43	-0.24	-0.14
36	9	-0.31	-0.13	-0.43	-0.28	-0.18
37	9	-0.19	-0.18	-0.38	-0.30	-0.21
38	9	-0.18	-0.18	-0.27	-0.25	-0.18
39	9	-0.22	-0.19	-0.25	-0.25	-0.19

b) PDSI and SPI's.

Month	PDSI	SPI-1	SPI-3	SPI-6	SPI-9
3	0.62	0.14	0.37	0.68	0.66
4	0.54	0.47	0.47	0.54	0.69
5	0.57	0.40	0.54	**0.68**	0.76
6	**0.64**	**0.64**	**0.66**	**0.68**	**0.81**
7	0.62	0.12	0.53	0.65	0.67
8	0.10	-0.53	-0.09	0.28	0.43
9	-0.10	-0.17	-0.48	0.08	0.17

Table 3.10. Correlation of drought indices with sorghum yield during the crop growing season – Guadalupe County.

a) ETDI and SMDI's.

Week	Month	ETDI	SMDI	SMDI-2	SMDI-4	SMDI-6
9	3	0.38	-0.02	0.35	0.29	0.07
10	3	0.31	-0.01	0.34	0.31	0.08
11	3	0.38	0.00	0.35	0.33	0.09
12	3	0.39	-0.01	0.35	0.32	0.08
13	3	0.22	-0.05	0.26	0.30	0.05
14	4	0.38	0.03	0.44	0.46	0.15
15	4	0.47	0.11	0.54	0.58	0.24
16	4	0.55	0.16	0.55	0.64	0.30
17	4	0.40	0.24	0.57	0.65	0.38
18	5	0.15	0.27	0.51	0.66	0.41
19	5	-0.01	0.23	0.42	0.56	0.34
20	5	0.09	0.20	0.37	0.49	0.30
21	5	0.36	0.25	0.49	0.52	0.35
22	6	0.54	0.34	0.64	0.61	0.45
23	6	0.74	0.45	**0.74**	0.67	0.54
24	6	0.63	0.48	0.72	0.67	0.57
25	6	0.68	0.52	0.70	0.68	0.60
26	6	0.77	**0.58**	0.73	**0.70**	**0.64**
27	7	**0.78**	0.53	0.59	0.63	0.59
28	7	0.71	0.44	0.17	0.47	0.49
29	7	0.35	0.27	-0.22	0.20	0.31
30	7	-0.09	0.14	-0.49	-0.02	0.18
31	8	-0.22	0.09	-0.52	-0.08	0.13
32	8	-0.30	0.11	-0.53	-0.08	0.15
33	8	-0.48	0.11	-0.52	-0.08	0.17
34	8	-0.65	0.06	-0.67	-0.20	0.12
35	9	-0.62	-0.01	-0.68	-0.26	0.05
36	9	-0.54	-0.04	-0.53	-0.19	0.01
37	9	-0.57	-0.07	-0.51	-0.24	-0.03
38	9	-0.53	-0.09	-0.48	-0.29	-0.05
39	9	-0.37	-0.07	-0.40	-0.25	-0.02

b) PDSI and SPI's.

Month	PDSI	SPI-1	SPI-3	SPI-6	SPI-9
3	0.33	0.58	0.33	0.36	0.23
4	0.65	0.25	0.52	0.52	0.34
5	0.62	0.40	**0.57**	0.57	0.45
6	**0.65**	0.49	0.50	**0.59**	**0.68**
7	0.56	-0.39	0.31	0.48	0.48
8	0.34	-0.28	-0.11	0.41	0.50
9	0.31	-0.03	-0.45	0.25	0.40

Table 3.11. Correlation of drought indices with sorghum yield during the crop growing season – Wilson County.

a) ETDI and SMDI's.

Week	Month	ETDI	SMDI	SMDI-2	SMDI-4	SMDI-6
9	3	0.24	0.35	0.12	0.36	0.54
10	3	0.30	0.39	0.16	0.41	0.55
11	3	0.71	0.55	0.59	0.65	0.67
12	3	0.70	0.60	0.68	0.71	0.70
13	3	0.38	0.59	0.54	0.71	0.68
14	4	0.35	0.71	0.46	0.82	0.78
15	4	0.23	0.60	0.36	0.62	0.68
16	4	0.17	0.53	0.31	0.53	0.62
17	4	0.01	0.50	0.24	0.48	0.59
18	5	-0.13	0.46	0.15	0.45	0.54
19	5	-0.16	0.41	0.06	0.39	0.47
20	5	-0.11	0.39	0.06	0.37	0.40
21	5	0.15	0.42	0.19	0.41	0.42
22	6	0.40	0.47	0.37	0.49	0.48
23	6	0.51	0.53	0.46	0.55	0.54
24	6	0.54	0.57	0.53	0.57	0.60
25	6	0.72	0.68	**0.75**	0.71	0.72
26	6	0.73	**0.70**	0.66	**0.72**	**0.76**
27	7	**0.74**	0.68	0.50	0.66	0.74
28	7	0.51	0.63	0.22	0.55	0.70
29	7	0.08	0.49	-0.11	0.32	0.58
30	7	-0.46	0.37	-0.44	0.11	0.49
31	8	-0.65	0.28	-0.63	-0.03	0.43
32	8	-0.78	0.23	-0.80	-0.15	0.41
33	8	-0.76	0.16	-0.82	-0.26	0.35
34	8	-0.73	0.12	-0.83	-0.33	0.31
35	9	-0.66	0.12	-0.76	-0.32	0.32
36	9	-0.61	0.12	-0.66	-0.26	0.29
37	9	-0.61	0.10	-0.61	-0.24	0.26
38	9	-0.47	0.10	-0.53	-0.24	0.23
39	9	-0.32	0.12	-0.38	-0.24	0.23

b) PDSI and SPI's.

Month	PDSI	SPI-1	SPI-3	SPI-6	SPI-9
3	**0.74**	0.58	0.43	0.66	0.46
4	0.67	0.14	0.44	0.56	0.57
5	0.70	0.48	0.52	0.58	0.67
6	**0.73**	**0.60**	**0.61**	**0.63**	**0.79**
7	0.50	-0.57	0.39	0.47	0.53
8	0.41	-0.13	0.04	0.45	0.60
9	0.38	-0.20	-0.46	0.27	0.48

Table 3.12. Correlation of drought indices with sorghum yield during the crop growing season – Collin County.

a) ETDI and SMDI's.

Week	Month	ETDI	SMDI	SMDI-2	SMDI-4	SMDI-6
9	3	0.08	0.11	-0.17	-0.02	0.17
10	3	0.34	0.29	0.12	0.00	0.16
11	3	0.40	0.41	0.32	0.08	0.19
12	3	0.33	0.32	0.28	0.07	0.15
13	3	0.09	0.09	-0.01	-0.12	0.00
14	4	0.11	0.09	0.00	-0.09	-0.02
15	4	0.08	0.09	-0.01	-0.07	0.00
16	4	-0.14	-0.04	-0.17	-0.11	-0.01
17	4	0.22	0.18	0.11	0.20	0.16
18	5	0.19	0.28	0.18	0.44	0.32
19	5	0.06	0.22	0.05	0.36	0.36
20	5	0.08	0.27	0.07	0.51	0.48
21	5	0.19	0.28	0.05	0.49	0.51
22	6	0.10	0.19	0.05	0.27	0.39
23	6	0.20	0.30	0.25	0.38	0.44
24	6	0.37	0.35	0.30	0.40	0.46
25	6	0.43	0.33	0.21	0.34	0.44
26	6	0.20	0.26	0.12	0.17	0.33
27	7	0.30	0.28	0.19	0.14	0.31
28	7	0.46	0.45	0.43	0.15	0.31
29	7	0.65	0.63	0.65	0.42	0.42
30	7	**0.73**	**0.76**	**0.73**	**0.56**	**0.54**
31	8	0.49	0.66	0.50	0.40	0.43
32	8	0.55	0.65	0.56	0.43	0.46
33	8	0.44	0.57	0.48	0.31	0.42
34	8	0.34	0.50	0.39	0.22	0.32
35	9	0.26	0.45	0.34	0.19	0.30
36	9	0.44	0.54	0.46	0.29	0.38
37	9	0.42	0.55	0.46	0.32	0.40
38	9	0.41	0.55	0.44	0.34	0.40
39	9	0.14	0.47	0.31	0.24	0.33

b) PDSI and SPI's.

Month	PDSI	SPI-1	SPI-3	SPI-6	SPI-9
3	0.22	-0.02	0.06	0.35	0.20
4	0.24	0.15	0.21	0.31	0.30
5	0.35	-0.02	0.01	0.16	0.32
6	0.41	**0.52**	0.39	0.23	0.40
7	0.48	0.51	0.49	0.45	0.47
8	0.47	-0.02	**0.63**	0.36	0.37
9	**0.63**	-0.07	0.19	0.43	0.31

Table 3.13. Correlation of drought indices with sorghum yield during the crop growing season – Denton County.

a) ETDI and SMDI's.

Week	Month	ETDI	SMDI	SMDI-2	SMDI-4	SMDI-6
9	3	-0.01	0.03	-0.26	-0.06	0.07
10	3	0.04	0.10	-0.04	0.10	0.15
11	3	-0.04	0.07	-0.02	0.04	0.12
12	3	0.13	0.10	0.12	0.09	0.15
13	3	0.15	0.09	0.07	0.06	0.12
14	4	0.09	0.06	0.02	0.05	0.09
15	4	0.12	0.07	0.02	0.08	0.11
16	4	-0.20	-0.02	-0.19	-0.09	0.01
17	4	0.09	0.09	0.02	0.11	0.13
18	5	0.18	0.19	0.11	0.23	0.23
19	5	0.19	0.19	0.07	0.19	0.23
20	5	0.63	0.37	0.52	0.54	0.42
21	5	**0.75**	0.57	0.67	0.74	0.62
22	6	0.64	0.61	0.55	0.64	0.64
23	6	0.75	**0.67**	0.66	0.69	0.69
24	6	0.61	0.57	0.51	0.57	0.59
25	6	0.62	0.54	0.46	0.51	0.55
26	6	0.50	0.50	0.44	0.47	0.51
27	7	0.65	0.49	0.48	0.49	0.50
28	7	0.57	0.50	0.59	0.56	0.52
29	7	0.53	0.55	**0.69**	0.67	0.57
30	7	0.53	0.62	0.69	**0.78**	**0.66**
31	8	0.25	0.56	0.38	0.60	0.59
32	8	0.26	0.55	0.23	0.50	0.56
33	8	0.23	0.54	0.14	0.44	0.54
34	8	0.13	0.55	0.13	0.45	0.55
35	9	0.27	0.56	0.19	0.48	0.57
36	9	0.36	0.58	0.27	0.52	0.59
37	9	0.40	0.56	0.28	0.52	0.57
38	9	0.34	0.49	0.23	0.44	0.49
39	9	-0.01	0.45	0.03	0.35	0.44

b) PDSI and SPI's.

Month	PDSI	SPI-1	SPI-3	SPI-6	SPI-9
3	-0.19	-0.09	-0.16	-0.15	-0.24
4	-0.03	-0.17	-0.10	-0.17	-0.14
5	0.35	0.63	0.29	0.00	0.14
6	0.49	**0.64**	0.65	0.50	0.27
7	0.59	0.56	**0.82**	**0.63**	0.46
8	**0.63**	0.12	0.68	0.60	0.46
9	0.57	-0.03	0.29	0.60	**0.50**

Table 3.14. Correlation of drought indices with sorghum yield during the crop growing season – Ellis County.

a) ETDI and SMDI's.

Week	Month	ETDI	SMDI	SMDI-2	SMDI-4	SMDI-6
9	3	0.46	0.02	0.37	0.08	0.00
10	3	0.46	0.04	0.42	0.11	0.01
11	3	0.28	0.00	0.33	0.07	-0.02
12	3	0.22	-0.01	0.28	0.08	-0.03
13	3	-0.04	-0.07	0.20	0.05	-0.09
14	4	-0.41	-0.14	0.02	-0.01	-0.14
15	4	-0.58	-0.22	-0.29	-0.09	-0.22
16	4	-0.62	-0.34	-0.52	-0.23	-0.32
17	4	-0.51	-0.37	-0.52	-0.23	-0.34
18	5	-0.15	-0.27	-0.09	-0.05	-0.28
19	5	-0.02	-0.21	0.04	0.03	-0.22
20	5	0.15	-0.11	0.20	0.13	-0.11
21	5	0.39	0.05	0.44	0.30	0.03
22	6	0.33	0.11	0.48	0.39	0.09
23	6	**0.55**	0.22	0.54	0.51	0.20
24	6	0.54	0.28	0.57	0.55	0.25
25	6	0.49	0.34	**0.61**	**0.57**	0.32
26	6	0.40	0.34	0.50	0.53	0.33
27	7	0.36	0.31	0.41	0.46	0.31
28	7	0.27	0.24	0.24	0.38	0.23
29	7	0.23	0.21	0.13	0.30	0.20
30	7	0.36	0.30	0.20	0.36	0.27
31	8	0.30	0.24	0.15	0.25	0.20
32	8	0.26	0.17	0.12	0.19	0.13
33	8	0.05	0.08	0.05	0.10	0.06
34	8	0.17	0.18	0.15	0.19	0.17
35	9	0.07	0.16	0.13	0.19	0.16
36	9	0.03	0.06	0.05	0.09	0.07
37	9	0.04	-0.03	-0.03	0.00	-0.03
38	9	-0.04	-0.09	-0.12	-0.07	-0.09
39	9	-0.36	-0.22	-0.24	-0.20	-0.22

b) PDSI and SPI's.

Month	PDSI	SPI-1	SPI-3	SPI-6	SPI-9
3	0.10	-0.07	0.07	0.33	0.08
4	0.08	-0.38	-0.15	0.10	0.07
5	0.39	0.42	0.11	0.12	0.36
6	0.51	**0.56**	0.40	0.29	0.47
7	**0.59**	0.40	**0.62**	0.45	**0.54**
8	0.50	0.00	0.46	0.38	0.40
9	0.38	-0.27	-0.02	0.26	0.25

Table 3.15. Correlation of drought indices with sorghum yield during the crop growing season – Liberty County.

a) ETDI and SMDI's.

Week	Month	ETDI	SMDI	SMDI-2	SMDI-4	SMDI-6
9	3	0.04	-0.33	-0.07	-0.12	-0.34
10	3	0.13	-0.23	0.04	-0.01	-0.23
11	3	-0.05	-0.22	0.00	-0.02	-0.22
12	3	-0.20	-0.27	-0.09	-0.09	-0.28
13	3	-0.29	-0.33	-0.15	-0.14	-0.34
14	4	-0.14	-0.22	-0.05	-0.02	-0.21
15	4	-0.11	-0.25	-0.10	-0.10	-0.25
16	4	-0.26	-0.35	-0.21	-0.23	-0.35
17	4	-0.21	-0.38	-0.22	-0.23	-0.39
18	5	-0.21	-0.44	-0.23	-0.26	-0.44
19	5	-0.05	-0.38	-0.10	-0.12	-0.37
20	5	-0.01	-0.30	-0.06	-0.07	-0.28
21	5	0.05	-0.24	-0.06	-0.06	-0.22
22	6	0.16	-0.12	0.02	0.00	-0.11
23	6	0.22	-0.01	0.09	0.08	0.01
24	6	0.19	0.00	0.07	0.08	0.03
25	6	-0.10	-0.08	-0.09	-0.02	-0.06
26	6	-0.08	-0.07	-0.08	-0.01	-0.07
27	7	0.25	0.03	0.20	0.12	0.04
28	7	0.48	0.12	**0.53**	0.25	0.13
29	7	0.40	0.13	0.50	0.24	0.13
30	7	0.38	0.16	0.48	0.27	0.17
31	8	0.44	0.18	0.46	0.28	0.19
32	8	0.36	0.11	0.36	0.18	0.11
33	8	0.37	0.11	0.35	0.22	0.12
34	8	0.36	0.16	0.35	0.30	0.18
35	9	0.16	0.11	0.22	0.19	0.12
36	9	0.28	0.16	0.32	0.26	0.17
37	9	0.07	0.07	0.15	0.12	0.08
38	9	0.14	0.06	0.15	0.10	0.07
39	9	0.41	0.21	0.44	0.31	0.23

b) PDSI and SPI's.

Month	PDSI	SPI-1	SPI-3	SPI-6	SPI-9
3	-0.18	0.10	0.02	-0.04	0.04
4	-0.22	-0.05	-0.04	-0.14	0.12
5	-0.04	0.15	0.09	0.07	0.09
6	-0.01	-0.12	0.11	0.04	-0.01
7	0.30	0.16	0.16	0.10	-0.03
8	0.28	0.18	0.14	0.22	0.18
9	0.33	0.31	0.32	0.32	0.22

Collin counties high correlations of ETDI with crop yield was observed during the weeks in July. However, for Tom Green and Denton counties, high correlations of ETDI and crop yield were observed during the weeks of June. Because of differences in planting dates among various counties, this critical period of high correlation shifts between June and July. For Concho, Guadalupe, Wilson, Collin, and Denton counties, SMDI's were also highly correlated with sorghum yield during the weeks of July ($r \sim 0.70$). In Floyd County, the SMDI's were highly correlated with sorghum yield ($r > 0.75$) during the plant emergence and tillering phase as well (weeks 16 and 17). Tom Green County also showed high correlations of ETDI and SMDI's with sorghum yield ($r > 0.8$) during the plant emergence and tillering phase. Although not to the same extent, other counties also showed higher correlations during plant emergence phase. This indicates that an adequate amount of soil moisture is needed during the sorghum crop establishment stage, as well as the tasseling and pollination stage, to have a better crop stand and increased crop yield.

The correlation with sorghum yield was also done on the monthly drought indices PDSI and SPI's reported for the climatic division (Tables 3.7b to 3.15b). PDSI and SPI's also demonstrated a higher correlation with sorghum yield during the critical months of June and July. Among the SPI's, SPI-9 was highly correlated with sorghum yield (r: 0.67 to 0.85) indicating that soil moisture replenished with the past 9 months of precipitation was important for sorghum. SPI-9 had correlations greater than 0.8 for Tom Green and Concho counties that are located in the low precipitation zone. However, for Collin, Denton, and Ellis counties, which are located in the high

precipitation zone, SPI-3 had high correlation with sorghum yield (r: 0.62 to 0.82). This indicates that the past 3 month of precipitation was enough to replenish the soil moisture in these high precipitation counties. Although PDSI and SPI's also showed good correlations with sorghum yield, ETDI and SMDI's have shown higher correlations ($r > 0.75$) for most of the counties than PDSI and SPI's during the critical growth stages. Among the SMDI's, SMDI-2 consistently had higher correlations ($r > 0.7$) with sorghum yield for most of the counties. This indicates that soil moisture in the top two feet of the soil profile was important for sorghum during the critical stages of crop growth. Hence, ETDI and SMDI-2 could be useful indicators for monitoring soil moisture stress during critical growth stages of sorghum.

For Ellis County the correlation between yield and drought indices was good ($r \sim 0.6$) but not as high as in other counties. For Liberty County, the correlations between the yield and drought indices, ETDI and SMDI's, and PDSI and SPI's was poor ($r < 0.5$) during the critical growth stages. Liberty County has high annual precipitation (> 1000mm) when compared to other counties. Analysis of the yield data and the drought indices for Liberty County showed that except for 1998 which was a drought year, other years with low yield were not all necessarily drought years. Hence, the low yield in Liberty County cannot be attributed to moisture stress alone. The low sorghum yield could be due to other factors like soil fertility, pests, diseases, water logging, and frost. For Guadalupe and Wilson counties, ETDI and SMDI-2 showed high negative correlations ($r \sim 0.6$) toward the end of the growing season. These negative correlations do not have any physical significance as the crops would be harvested by that time.

Winter wheat: In Texas, wheat is planted from mid September – October and harvested from mid May – June. The critical growth stages of wheat are head emergence, flowering and grain filling (March – April), during which a water stress at the root zone can have a significant impact on the crop yield (Hane and Pumphrey 1984). For Floyd and Concho counties, ETDI and SMDI's showed high correlations ($r > 0.8$) with wheat yield during flowering and grain filling stages (March – April) (Tables 3.16a and 3.20a). For Floyd and Concho counties, even though the correlations between wheat yield and drought indices were the highest during the critical period, the correlations were generally high ($r \sim 0.7$) during most of the wheat growing season. Similarly, the correlations were generally high during most of growing season for Wilbarger and McCulloch counties. For Collin County, the correlation was high only during the weeks of January (plant establishment phase). For Childress and Hardeman counties, only ETDI and SMDI-2 showed correlations above 0.7 during the weeks of January and March respectively (plant establishment and tillering phase). In contrast to sorghum, where high correlations occurred mainly during the critical growth periods, the high correlations of drought indices with wheat yield were widely spread during the growing season. This indicates that a reasonable amount of soil moisture during most of the growing season will be favorable for wheat production.

Compared to the summer crop sorghum, PDSI and SPI's were well-correlated with winter wheat. Similar to ETDI and SMDI's, PDSI and SPI also showed markedly high correlations during plant establishment – tillering stage and flowering – grain filling stage. The correlations of PDSI and SPI's were greater than 0.8 for McCulloch County.

Table 3.16. Correlation of drought indices with wheat yield during the crop growing season – Floyd County.

a) ETDI and SMDI's.

Week	Month	ETDI	SMDI	SMDI-2	SMDI-4	SMDI-6
40	10	-0.06	0.51	0.10	0.46	0.52
41	10	-0.18	0.46	0.01	0.41	0.47
42	10	-0.27	0.46	-0.04	0.41	0.46
43	10	-0.14	0.56	0.00	0.49	0.56
44	11	0.00	0.62	0.06	0.55	0.63
45	11	0.04	0.66	0.12	0.59	0.67
46	11	0.19	0.69	0.21	0.63	0.70
47	11	0.44	0.72	0.38	0.70	0.74
48	12	0.60	0.75	0.55	0.76	0.77
49	12	0.74	0.77	0.61	0.78	0.79
50	12	0.72	0.78	0.67	0.79	0.79
51	12	0.71	0.77	0.64	0.78	0.77
52	12	0.69	0.76	0.61	0.77	0.77
1	1	0.72	0.76	0.61	0.77	0.77
2	1	0.71	0.77	0.65	0.78	0.77
3	1	0.72	0.79	0.68	0.79	0.78
4	1	0.73	0.79	0.71	0.79	0.78
5	2	0.56	0.77	0.68	0.77	0.77
6	2	0.62	0.77	0.66	0.76	0.77
7	2	0.62	0.75	0.64	0.75	0.76
8	2	0.57	0.74	0.66	0.74	0.75
9	3	0.57	0.74	0.67	0.75	0.76
10	3	0.61	0.77	0.71	0.76	0.79
11	3	0.59	0.81	0.75	0.79	0.83
12	3	0.58	0.82	0.74	0.81	0.84
13	3	0.59	0.81	0.69	0.80	0.84
14	4	0.70	0.82	0.70	0.81	0.84
15	4	0.74	0.83	0.74	0.83	0.86
16	4	**0.81**	0.85	**0.80**	0.86	0.89
17	4	0.71	0.89	0.80	**0.89**	0.92
18	5	0.45	**0.93**	0.72	0.88	**0.95**
19	5	0.20	0.91	0.49	0.83	0.92
20	5	-0.01	0.88	0.28	0.77	0.87
21	5	0.03	0.84	0.25	0.73	0.84

b) PDSI and SPI's.

Month	PDSI	SPI-1	SPI-3	SPI-6	SPI-9
10	0.51	-0.09	0.09	0.71	0.33
11	0.69	0.53	0.20	0.76	0.51
12	0.72	0.52	0.56	0.46	0.65
1	0.83	**0.77**	**0.80**	0.66	0.81
2	0.87	0.57	0.79	0.65	**0.85**
3	**0.88**	0.44	0.71	0.81	0.71
4	0.90	0.52	0.64	**0.84**	0.74
5	0.75	-0.25	0.34	0.61	0.58

Table 3.17. Correlation of drought indices with wheat yield during the crop growing season – Childress County.

a) ETDI and SMDI's.

Week	Month	ETDI	SMDI	SMDI-2	SMDI-4	SMDI-6
40	10	-0.61	-0.33	-0.39	-0.35	-0.35
41	10	-0.64	-0.38	-0.44	-0.40	-0.40
42	10	-0.70	-0.42	-0.48	-0.44	-0.44
43	10	-0.63	-0.44	-0.49	-0.46	-0.46
44	11	-0.46	-0.43	-0.46	-0.44	-0.45
45	11	-0.38	-0.41	-0.42	-0.43	-0.44
46	11	-0.12	-0.36	-0.33	-0.37	-0.37
47	11	0.22	-0.17	0.01	-0.17	-0.20
48	12	0.50	-0.01	0.32	0.01	-0.04
49	12	0.59	0.06	0.41	0.09	0.03
50	12	0.50	0.09	0.42	0.12	0.06
51	12	0.52	0.12	0.43	0.15	0.09
52	12	0.45	0.15	0.46	0.19	0.13
1	1	0.55	0.23	0.53	0.27	0.21
2	1	0.64	0.28	0.57	0.32	0.27
3	1	0.78	0.32	0.61	0.36	0.30
4	1	**0.79**	0.34	0.64	0.38	0.32
5	2	0.66	0.32	0.62	0.37	0.31
6	2	0.67	0.31	0.60	0.36	0.30
7	2	0.65	0.32	0.62	0.37	0.31
8	2	0.62	0.32	0.63	0.38	0.32
9	3	0.71	0.34	0.66	0.40	0.33
10	3	0.72	0.35	**0.70**	0.42	0.34
11	3	0.63	0.31	0.69	0.38	0.29
12	3	0.60	0.29	0.63	0.36	0.27
13	3	0.52	0.27	0.56	0.33	0.25
14	4	0.46	0.27	0.53	0.33	0.25
15	4	0.36	0.23	0.52	0.30	0.21
16	4	0.40	0.26	0.57	0.34	0.24
17	4	0.44	0.26	0.57	0.35	0.24
18	5	0.31	0.23	0.59	0.35	0.20
19	5	0.25	0.20	0.51	0.32	0.19
20	5	0.20	0.15	0.39	0.25	0.14
21	5	-0.05	0.09	0.27	0.16	0.07

b) PDSI and SPI's.

Month	PDSI	SPI-1	SPI-3	SPI-6	SPI-9
10	0.65	-0.31	-0.52	0.07	0.25
11	0.66	0.30	-0.33	0.11	0.12
12	0.63	0.38	0.30	-0.16	0.23
1	0.68	0.53	**0.56**	-0.06	0.27
2	0.67	0.43	0.54	0.08	0.30
3	**0.69**	0.43	0.55	0.54	0.10
4	0.65	0.26	0.47	**0.61**	0.16
5	0.59	-0.13	0.15	0.43	0.12

Table 3.18. Correlation of drought indices with wheat yield during the crop growing season – Hardeman County.

a) ETDI and SMDI's.

Week	Month	ETDI	SMDI	SMDI-2	SMDI-4	SMDI-6
40	10	-0.17	0.05	0.02	0.02	0.02
41	10	-0.17	0.01	-0.03	-0.02	-0.01
42	10	-0.25	-0.03	-0.08	-0.06	-0.03
43	10	-0.31	-0.06	-0.12	-0.09	-0.06
44	11	-0.28	-0.07	-0.05	-0.08	-0.05
45	11	-0.10	-0.05	0.04	-0.05	-0.03
46	11	0.02	-0.03	0.11	-0.02	-0.01
47	11	0.00	-0.02	0.11	-0.01	0.00
48	12	0.33	0.11	0.37	0.16	0.13
49	12	0.44	0.18	0.47	0.25	0.21
50	12	0.41	0.21	0.51	0.29	0.24
51	12	0.31	0.21	0.49	0.28	0.23
52	12	0.31	0.20	0.48	0.27	0.23
1	1	0.33	0.21	0.47	0.27	0.24
2	1	0.52	0.24	0.50	0.30	0.26
3	1	**0.63**	0.28	0.58	0.36	0.29
4	1	0.62	0.33	0.65	0.42	0.34
5	2	0.51	0.34	0.66	0.43	0.35
6	2	0.62	0.36	0.70	0.47	0.37
7	2	0.51	0.36	0.71	0.47	0.37
8	2	0.50	0.40	0.74	0.51	0.41
9	3	0.59	0.43	**0.77**	0.54	0.44
10	3	0.57	0.42	0.76	0.53	0.43
11	3	0.49	0.41	0.70	0.51	0.42
12	3	0.48	0.39	0.70	0.49	0.41
13	3	0.30	0.37	0.61	0.44	0.39
14	4	0.42	0.38	0.63	0.45	0.40
15	4	0.56	0.40	0.70	0.49	0.43
16	4	0.47	0.39	0.62	0.47	0.42
17	4	0.55	0.42	0.61	0.48	0.44
18	5	0.53	0.42	0.66	0.50	0.45
19	5	0.52	0.42	0.63	0.51	0.45
20	5	0.33	0.41	0.55	0.48	0.44
21	5	0.39	0.53	0.66	**0.64**	0.55

b) PDSI and SPI's.

Month	PDSI	SPI-1	SPI-3	SPI-6	SPI-9
10	0.54	-0.17	-0.36	0.03	0.00
11	0.57	0.38	-0.16	0.17	0.03
12	0.54	0.06	0.28	-0.13	0.10
1	0.67	**0.69**	0.61	0.07	0.29
2	0.67	0.40	0.71	0.28	0.44
3	0.65	0.14	**0.76**	0.80	0.30
4	**0.69**	0.39	0.42	**0.77**	0.37
5	**0.69**	0.04	0.43	0.65	0.41

Table 3.19. Correlation of drought indices with wheat yield during the crop growing season – Wilbarger County.

a) ETDI and SMDI's.

Week	Month	ETDI	SMDI	SMDI-2	SMDI-4	SMDI-6
40	10	-0.19	-0.03	-0.09	0.01	0.01
41	10	-0.06	-0.04	-0.13	0.00	0.01
42	10	-0.05	-0.04	-0.10	0.00	0.04
43	10	0.05	-0.01	-0.02	0.04	0.06
44	11	-0.11	-0.04	-0.08	-0.02	0.04
45	11	-0.20	-0.08	-0.14	-0.06	0.01
46	11	-0.08	-0.07	-0.09	-0.04	0.02
47	11	-0.17	-0.07	-0.08	-0.01	0.01
48	12	0.13	0.00	0.16	0.11	0.08
49	12	0.20	0.04	0.21	0.16	0.11
50	12	0.20	0.05	0.22	0.19	0.12
51	12	0.28	0.09	0.29	0.26	0.16
52	12	0.45	0.20	0.45	0.40	0.25
1	1	0.56	0.31	0.55	0.49	0.34
2	1	0.56	0.36	0.59	0.53	0.38
3	1	0.61	0.39	0.67	0.56	0.41
4	1	0.71	0.42	0.77	0.61	0.44
5	2	0.76	0.49	0.88	0.68	0.49
6	2	**0.84**	0.53	**0.91**	0.71	0.53
7	2	0.65	0.53	0.89	0.70	0.53
8	2	0.59	0.55	0.82	0.70	0.54
9	3	0.55	0.58	0.78	0.70	0.55
10	3	0.53	0.59	0.72	0.70	0.56
11	3	0.58	0.61	0.71	0.71	0.58
12	3	0.71	**0.62**	0.81	**0.72**	**0.59**
13	3	0.69	0.60	0.83	0.69	0.58
14	4	0.73	0.60	0.81	0.67	0.58
15	4	0.77	0.59	0.79	0.66	0.56
16	4	0.41	0.54	0.62	0.59	0.52
17	4	0.40	0.52	0.54	0.56	0.51
18	5	0.01	0.46	0.30	0.46	0.46
19	5	-0.20	0.44	0.06	0.39	0.43
20	5	-0.11	0.45	0.10	0.39	0.44
21	5	-0.11	0.48	0.12	0.42	0.46

b) PDSI and SPI's.

Month	PDSI	SPI-1	SPI-3	SPI-6	SPI-9
10	0.46	-0.02	-0.48	-0.01	-0.04
11	0.43	0.22	-0.23	-0.02	-0.08
12	0.53	0.55	0.36	-0.16	0.19
1	0.68	0.62	0.70	0.08	0.33
2	0.69	0.39	**0.73**	0.25	0.39
3	**0.71**	**0.67**	0.70	**0.68**	0.21
4	0.52	0.02	0.36	0.63	0.24
5	0.47	-0.20	0.08	0.50	0.21

Table 3.20. Correlation of drought indices with wheat yield during the crop growing season – Concho County.

a) ETDI and SMDI's.

Week	Month	ETDI	SMDI	SMDI-2	SMDI-4	SMDI-6
40	10	-0.04	0.42	0.04	0.29	0.47
41	10	-0.06	0.42	-0.01	0.27	0.47
42	10	-0.24	0.33	-0.13	0.15	0.41
43	10	-0.44	0.18	-0.34	-0.07	0.26
44	11	-0.20	0.25	-0.20	0.02	0.29
45	11	-0.06	0.33	-0.09	0.10	0.35
46	11	0.19	0.40	0.03	0.17	0.42
47	11	0.54	0.51	0.26	0.32	0.52
48	12	0.58	0.55	0.38	0.40	0.56
49	12	0.56	0.57	0.41	0.43	0.57
50	12	0.76	0.63	0.55	0.50	0.62
51	12	**0.80**	0.67	0.67	0.56	0.66
52	12	0.74	0.68	0.68	0.57	0.66
1	1	0.74	0.69	0.66	0.59	0.68
2	1	0.74	0.68	0.66	0.58	0.67
3	1	0.72	0.68	0.66	0.59	0.66
4	1	0.65	0.66	0.65	0.57	0.66
5	2	0.64	0.67	0.66	0.58	0.66
6	2	0.67	0.72	**0.71**	0.62	0.71
7	2	0.62	0.75	0.70	0.64	0.73
8	2	0.44	0.71	0.61	0.59	0.69
9	3	0.63	0.74	0.65	0.64	0.73
10	3	0.58	0.74	0.64	0.64	0.73
11	3	0.61	0.75	0.65	0.65	0.74
12	3	0.71	**0.80**	**0.71**	**0.70**	0.80
13	3	0.64	0.79	0.67	0.69	**0.81**
14	4	0.67	0.79	0.67	0.69	**0.81**
15	4	0.68	0.78	0.68	0.69	0.80
16	4	0.58	0.74	0.64	0.66	0.77
17	4	0.43	0.73	0.60	0.64	0.75
18	5	0.36	0.68	0.57	0.60	0.71
19	5	0.26	0.67	0.44	0.58	0.70
20	5	0.21	0.65	0.28	0.53	0.68
21	5	0.31	0.67	0.29	0.53	0.70

b) PDSI and SPI's.

Month	PDSI	SPI-1	SPI-3	SPI-6	SPI-9
10	0.16	-0.45	-0.05	0.09	0.05
11	0.52	0.55	-0.01	0.10	0.09
12	0.64	**0.76**	0.39	0.38	0.43
1	0.61	0.21	**0.79**	0.42	0.47
2	0.61	0.46	0.65	0.43	0.42
3	**0.66**	0.66	0.55	0.63	0.47
4	0.65	0.47	0.60	**0.78**	**0.53**
5	0.62	0.16	0.53	0.66	0.51

Table 3.21. Correlation of drought indices with wheat yield during the crop growing season – McCulloch County.

a) ETDI and SMDI's.

Week	Month	ETDI	SMDI	SMDI-2	SMDI-4	SMDI-6
40	10	0.09	0.42	0.07	0.27	0.44
41	10	0.14	0.42	0.08	0.30	0.44
42	10	0.00	0.36	0.06	0.23	0.38
43	10	-0.18	0.35	0.03	0.21	0.37
44	11	0.21	0.44	0.23	0.31	0.45
45	11	0.24	0.45	0.31	0.32	0.47
46	11	0.51	0.46	0.38	0.35	0.48
47	11	0.62	0.48	0.47	0.40	0.50
48	12	0.65	0.49	0.55	0.43	0.51
49	12	0.74	0.50	0.60	0.45	0.52
50	12	0.86	0.52	0.65	0.48	0.55
51	12	0.89	0.61	0.77	0.59	0.64
52	12	0.88	0.71	0.87	0.70	0.73
1	1	0.90	0.78	0.89	0.75	0.80
2	1	**0.94**	0.81	0.91	0.77	0.83
3	1	0.91	0.81	**0.92**	0.77	0.84
4	1	0.75	0.82	0.88	0.76	0.84
5	2	0.60	0.82	0.85	0.75	0.84
6	2	0.68	0.83	0.84	0.75	**0.85**
7	2	0.61	**0.84**	0.82	0.75	**0.85**
8	2	0.57	0.83	0.82	0.75	**0.85**
9	3	0.82	**0.84**	0.87	0.78	0.86
10	3	0.76	0.83	0.86	0.77	**0.85**
11	3	0.72	0.83	0.84	0.77	**0.85**
12	3	0.78	**0.84**	0.87	**0.79**	**0.85**
13	3	0.76	**0.84**	0.87	0.78	**0.85**
14	4	0.76	**0.84**	0.86	0.78	**0.85**
15	4	0.71	0.83	0.84	0.76	0.84
16	4	0.74	0.83	0.85	0.76	0.84
17	4	0.74	0.82	0.87	0.76	0.83
18	5	0.32	0.79	0.74	0.71	0.81
19	5	0.08	0.76	0.42	0.63	0.77
20	5	0.06	0.71	0.12	0.53	0.73
21	5	0.24	0.70	0.09	0.48	0.72

b) PDSI and SPI's.

Month	PDSI	SPI-1	SPI-3	SPI-6	SPI-9
10	0.27	-0.06	0.19	0.25	0.13
11	0.58	0.46	0.26	0.28	0.23
12	0.79	0.76	0.57	0.47	0.55
1	0.78	0.37	0.80	0.58	0.57
2	0.79	0.73	**0.81**	0.63	0.62
3	**0.84**	**0.82**	0.77	0.78	0.66
4	0.76	0.38	0.76	**0.88**	**0.70**
5	0.69	-0.09	0.38	0.69	0.61

Table 3.22. Correlation of drought indices with wheat yield during the crop growing season – Collin County.

a) ETDI and SMDI's.

Week	Month	ETDI	SMDI	SMDI-2	SMDI-4	SMDI-6
40	10	-0.27	-0.48	-0.36	-0.22	-0.22
41	10	-0.16	-0.50	-0.40	-0.20	-0.20
42	10	-0.17	-0.37	-0.26	-0.16	-0.17
43	10	-0.04	-0.17	-0.07	-0.07	-0.10
44	11	-0.19	-0.17	-0.12	-0.07	-0.11
45	11	-0.20	-0.19	-0.15	-0.04	-0.12
46	11	0.10	-0.04	0.07	0.13	0.01
47	11	0.14	0.05	0.16	0.19	0.09
48	12	0.13	0.08	0.16	0.17	0.11
49	12	0.29	0.18	0.27	0.21	0.16
50	12	0.25	0.23	0.28	0.20	0.17
51	12	0.52	0.39	0.49	0.38	0.31
52	12	0.61	0.52	0.62	0.55	0.45
1	1	0.64	0.54	0.64	0.58	0.50
2	1	**0.72**	**0.58**	**0.67**	**0.60**	**0.54**
3	1	0.66	0.57	**0.67**	0.59	**0.54**
4	1	0.67	0.45	0.54	0.48	0.44
5	2	0.27	0.06	0.00	0.11	0.19
6	2	0.08	-0.09	-0.12	0.01	0.05
7	2	0.16	-0.04	-0.03	0.21	0.14
8	2	0.19	0.09	0.12	0.30	0.24
9	3	0.21	0.13	0.14	0.28	0.27
10	3	0.22	0.17	0.16	0.28	0.29
11	3	0.20	0.26	0.22	0.28	0.29
12	3	0.39	0.35	0.38	0.37	0.39
13	3	0.14	0.22	0.20	0.24	0.32
14	4	0.11	0.20	0.18	0.19	0.28
15	4	-0.17	0.04	0.00	0.04	0.13
16	4	-0.26	-0.08	-0.14	-0.04	0.09
17	4	-0.35	-0.23	-0.29	-0.47	-0.20
18	5	-0.45	-0.28	-0.32	-0.36	-0.30
19	5	-0.51	-0.39	-0.46	-0.55	-0.48
20	5	-0.69	-0.52	-0.61	-0.58	-0.50
21	5	-0.63	-0.48	-0.56	-0.51	-0.42

b) PDSI and SPI's.

Month	PDSI	SPI-1	SPI-3	SPI-6	SPI-9
10	-0.18	-0.20	-0.29	-0.45	-0.12
11	0.06	0.14	-0.32	-0.44	-0.30
12	0.25	0.67	0.17	-0.06	-0.04
1	0.20	0.16	**0.55**	0.07	-0.06
2	0.18	0.06	0.42	0.03	-0.07
3	0.23	0.29	0.20	0.18	0.03
4	-0.24	-0.46	-0.08	0.31	-0.01
5	-0.38	-0.66	-0.56	-0.05	-0.26

Table 3.23. Correlation of drought indices with wheat yield during the crop growing season – Denton County.

a) ETDI and SMDI's.

Week	Month	ETDI	SMDI	SMDI-2	SMDI-4	SMDI-6
40	10	-0.32	-0.52	-0.32	-0.32	-0.53
41	10	-0.01	-0.38	-0.18	-0.21	-0.36
42	10	0.12	-0.24	-0.02	-0.08	-0.21
43	10	0.22	-0.13	0.09	0.06	-0.09
44	11	-0.07	-0.15	-0.06	0.01	-0.12
45	11	-0.16	-0.17	-0.14	0.00	-0.13
46	11	0.03	-0.13	-0.04	0.07	-0.08
47	11	0.37	-0.05	0.19	0.19	0.00
48	12	0.65	0.07	0.52	0.35	0.13
49	12	**0.66**	0.17	**0.63**	0.46	0.23
50	12	0.47	0.23	0.56	0.48	0.29
51	12	0.44	0.23	0.50	0.47	0.29
52	12	0.21	0.24	0.46	0.46	0.32
1	1	0.08	0.22	0.33	0.39	0.28
2	1	0.33	0.24	0.40	0.41	0.30
3	1	0.33	0.23	0.44	0.44	0.30
4	1	0.33	0.12	0.26	0.39	0.19
5	2	0.05	-0.13	-0.18	0.02	-0.09
6	2	-0.07	-0.21	-0.17	-0.03	-0.17
7	2	-0.02	-0.21	-0.13	0.01	-0.16
8	2	0.24	-0.11	0.08	0.16	-0.06
9	3	0.38	-0.02	0.23	0.28	0.05
10	3	0.37	0.09	0.33	0.37	0.17
11	3	0.30	0.17	0.37	0.42	0.26
12	3	0.49	0.33	0.49	0.48	0.39
13	3	0.01	0.32	0.25	0.39	0.36
14	4	-0.03	0.32	0.14	0.35	0.34
15	4	-0.33	0.20	-0.11	0.19	0.21
16	4	-0.49	0.09	-0.35	0.06	0.11
17	4	-0.27	0.18	-0.23	0.13	0.19
18	5	-0.04	0.28	0.03	0.22	0.29
19	5	-0.13	0.23	-0.05	0.17	0.24
20	5	-0.37	0.00	-0.22	-0.05	0.01
21	5	-0.33	0.10	-0.04	0.08	0.11

b) PDSI and SPI's.

Month	PDSI	SPI-1	SPI-3	SPI-6	SPI-9
10	-0.38	-0.09	-0.38	-0.56	-0.39
11	-0.19	0.47	-0.13	-0.54	-0.44
12	-0.07	0.45	0.19	-0.28	-0.34
1	-0.10	0.02	0.42	-0.10	-0.36
2	-0.06	0.13	0.21	0.00	-0.34
3	0.10	0.35	0.18	0.19	-0.16
4	-0.34	-0.53	-0.13	0.15	-0.20
5	-0.34	-0.36	-0.40	-0.18	-0.24

Table 3.24. Correlation of drought indices with wheat yield during the crop growing season – Ellis County.

a) ETDI and SMDI's.

Week	Month	ETDI	SMDI	SMDI-2	SMDI-4	SMDI-6
40	10	-0.64	-0.38	-0.54	-0.49	-0.38
41	10	0.11	-0.25	-0.34	-0.36	-0.27
42	10	0.28	-0.07	-0.07	-0.14	-0.10
43	10	0.42	0.05	0.09	-0.01	0.01
44	11	0.03	-0.02	-0.06	-0.08	-0.04
45	11	0.04	-0.01	-0.08	-0.08	-0.04
46	11	0.14	-0.01	0.00	-0.07	-0.04
47	11	-0.21	-0.14	-0.20	-0.20	-0.16
48	12	-0.05	-0.12	-0.19	-0.19	-0.15
49	12	0.26	-0.02	0.03	-0.09	-0.06
50	12	0.09	0.00	-0.02	-0.06	-0.03
51	12	0.30	0.06	0.19	0.00	0.03
52	12	0.20	0.08	0.23	0.03	0.04
1	1	0.04	0.04	0.08	-0.01	0.01
2	1	-0.02	-0.01	-0.01	-0.06	-0.04
3	1	-0.08	-0.09	-0.12	-0.12	-0.10
4	1	0.07	-0.10	-0.05	-0.12	-0.11
5	2	-0.23	-0.20	-0.31	-0.24	-0.20
6	2	-0.08	-0.20	-0.19	-0.26	-0.20
7	2	0.03	-0.17	-0.05	-0.23	-0.17
8	2	0.14	-0.12	0.16	-0.19	-0.13
9	3	0.21	-0.04	0.33	-0.11	-0.06
10	3	0.23	0.00	0.37	-0.09	-0.03
11	3	0.26	0.06	0.41	-0.04	0.03
12	3	0.31	0.09	0.39	-0.01	0.05
13	3	0.25	0.07	0.38	-0.04	0.04
14	4	0.06	-0.01	0.16	-0.12	-0.03
15	4	-0.29	-0.10	-0.08	-0.21	-0.11
16	4	-0.56	-0.27	-0.41	-0.37	-0.25
17	4	-0.44	-0.27	-0.34	-0.33	-0.26
18	5	-0.77	-0.38	-0.60	-0.48	-0.36
19	5	-0.67	-0.49	-0.61	-0.54	-0.46
20	5	-0.55	-0.48	-0.52	-0.50	-0.47
21	5	-0.46	-0.43	-0.40	-0.44	-0.43

b) PDSI and SPI's.

Month	PDSI	SPI-1	SPI-3	SPI-6	SPI-9
10	-0.01	0.17	-0.28	-0.05	0.19
11	0.14	0.02	-0.23	-0.31	0.07
12	0.24	0.43	0.31	-0.23	0.08
1	0.10	-0.11	0.20	-0.12	0.06
2	0.07	0.05	0.17	-0.09	-0.17
3	0.11	0.18	0.03	0.20	-0.20
4	-0.27	-0.47	-0.24	0.01	-0.22
5	-0.35	-0.37	-0.46	-0.20	-0.37

However, ETDI and SMDI's have shown higher correlations with wheat yield with $r > 0.9$ for Floyd, Wilbarger, and McCulloch counties. Hence, ETDI and SMDI could be useful indicators for monitoring soil moisture stress during critical stages of wheat crop.

For Denton County, the correlations of ETDI and SMDI-2 were high ($r \sim 0.63$) during the weeks of December, much earlier in the growing season than other counties. For Denton and Ellis counties, the correlations between yield and drought indices, ETDI and SMDI's, and PDSI and SPI's were poor ($r < 0.5$) during the critical periods of the growing season. Ellis counties the correlations between yield and drought indices ETDI and SMDI's as well as PDSI and SPI's were less ($r < 0.5$) during the critical growth stages. Denton and Ellis counties are located in the high precipitation zone (> 900mm). Analysis of the crop yield data showed that the low yield years were not all necessarily dry years. Similarly, few high yield years also had short periods of dryness. Hence, the low yield in Denton and Ellis counties cannot be attributed to moisture stress alone. The low wheat yield could be due to other factors like soil fertility, pests, diseases, water logging, and frost.

Summary and Conclusions

Weekly soil moisture and evapotranspiration simulated by the calibrated hydrologic model SWAT was used to develop a set of drought indices – SMDI and ETDI, respectively. The drought indices were derived from soil moisture deficit and evapotranspiration deficit and scaled between -4 to 4 for spatial comparison of drought index, irrespective of climatic conditions.

- The auto-correlation lag of the drought indices, ETDI and SMDI, were closely related to the available water holding capacity of the soil, with lag increasing as a result of increased water holding capacity.

- ETDI and SMDI-2 had the lowest auto-correlation lag because the top two feet of the soil profile very actively participate in the evapotranspiration of available soil water. Hence, ETDI and SMDI-2 could be good indicators of short-term agricultural droughts.

- The spatial variability of the developed drought indices was high with a standard deviation greater than 1.0 during most of weeks in a year.

- The high spatial variability in the drought indices was mainly due to high spatial variability in rainfall distribution.

- The spatial variability (standard deviation) of the drought indices especially ETDI during different seasons closely followed the variability in precipitation and potential evapotranspiration across seasons.

- ETDI and SMDI's were positively correlated with PDSI and SPI's for all six watersheds. This suggests that the dry and wet period indicated by the ETDI and SMDI's were in general agreement with PDSI and SPI.

- For all six watersheds ETDI and SMDI-2 were well-correlated with SPI-1 month ($r \sim 0.7$), indicating that ETDI and SMDI-2 are good indicators of short-term drought conditions suitable for agricultural drought monitoring.

- PDSI was highly correlated with SPI-9 and SPI-12 months ($r > 0.8$), suggesting that precipitation was the dominant factor in PDSI, and PDSI is an indicator of long-term weather conditions.

- The wheat and sorghum crop yields were highly correlated with the drought indices ($r > 0.75$) during the weeks of critical crop growth stages, indicating that ETDI and SMDI's can be used for agricultural drought monitoring.

- For high precipitation zones, the reduction in crop yield could not be attributed to moisture stress alone. The yield reduction could also be due to factors such as soil fertility, pests, diseases, water logging, and frost.

The fine spatial resolution of ETDI and SMDI's combined with high temporal resolution will help in developing a better understanding of agricultural drought and would help in monitoring and planning to mitigate the impacts of drought.

CHAPTER IV

HYDROLOGIC MODELING AND DROUGHT MONITORING USING HIGH-RESOLUTION SPATIALLY DISTRIBUTED (NEXRAD) RAINFALL DATA

Synopsis

Rainfall is a critical input for hydrologic modeling, soil moisture and drought monitoring. It is also a highly variable component in both space and time. Although a dense network of raingages are not widely available to adequately characterize the spatial and temporal variability of rainfall, point observations of rainfall measured at raingages are widely used for hydrologic modeling. The assumption of spatial homogeneity in rainfall could introduce uncertainty in the calibration and estimation of model parameters. Radar rainfall data quality has improved over the years and could thus be used to effectively measure rainfall at a much better spatial resolution (4km × 4km). Rainfall data obtained from the National Weather Service's NEXt generation RADar (NEXRAD) and raingage data were used to simulate the hydrology of the Colorado River watershed located in the Edward Plateau region of Texas. A local bias adjustment was done to improve the accuracy of NEXRAD rainfall (R^2:0.86) using raingage data. Streamflow simulated using bias-adjusted NEXRAD rainfall data compared well with observed streamflow and had higher model statistics (E ~ 0.8) than streamflow simulations using raingage data (E < 0). The temporal correlations of soil

water simulated using raingage and NEXRAD rainfall data showed that variations in soil water simulations increased with distance from the raingage. The spatial cross-correlations at zero lag between weekly simulated spatial soil water datasets simulated using raingage and NEXRAD rainfall data also dropped markedly (~ 0.4), especially during drought, due to differences in NEXRAD and raingage rainfall data and their spatial distributions. However, the spatial cross-correlation of the soil water data increased (~ 0.8) as the soil became saturated at the end of drought. NEXRAD rainfall data was useful in capturing the spatial variability of rainfall, especially the small rainfall events missed by raingages that introduce considerable variability during drought. Hence, NEXRAD rainfall data effectively improved the model simulations and estimation of drought indices.

Introduction

Hydrologic modeling has made significant progress during the past two decades with the evolution of Geographical Information System (GIS). Due to advances in GIS, spatial data on soils, land use and elevation have become widely available at fine resolution and hence, many spatially distributed hydrologic models have been developed. However, rainfall, which is a highly variable component in both space and time and a critical input for hydrologic modeling, often comes from few sparsely located raingages. Dense networks of raingages are available for only a few small watersheds. However, for large-scale hydrologic modeling, dense networks of raingages are not available to adequately characterize the spatial and temporal variability of rainfall. Yet,

point observations made by raingages are widely used for large-scale hydrologic modeling and rainfall is assumed to be uniformly distributed across the sub-basins based on Thiessen polygon or the nearest raingage.

By assuming a spatially homogeneous rainfall across the watershed or sub-basins, the model parameters are calibrated using observed streamflow data. Although streamflow is an effective integrator of watershed response in space and time, the space – time variability of rainfall plays a vital role in the runoff generation process (Goodrich et al. 1995). Faurès et al (1995) demonstrated that even for small watersheds less than 5 ha, an assumption of uniform rainfall distribution across the watershed from a single raingage could lead to large uncertainties in runoff estimation. As the model parameters are inherently related to the space and time scales at which they are calibrated, the spatial variability of rainfall could introduce significant uncertainty in the estimation of model parameters (Chaubey et al. 1999). Hence, accurate representation of rainfall variability in space and time is essential for hydrologic modeling.

Studies Using NEXRAD Rainfall

The limitations of raingage data in characterizing the space-time variability of rainfall could be effectively overcome by the use of radar data. The National Weather Service's NEXt Generation RADar (NEXRAD) is used for monitoring storm movement and as an early warning system about dangerous weather conditions. Although radar has been in use for over forty years, it was primarily used for weather predictions. Only during the past decade has its use in hydrologic applications been explored (Krajewski

and Smith 2002). The primary reason for slow adaptability of radar data by the hydrologic community is the bias in the radar rainfall estimates (Smith et al. 1996). The bias in the radar rainfall is mainly due to lack of radar calibration and inaccurate radar reflectivity-rainfall rate relationship (Seo et al. 1999). However, the accuracy of NEXRAD rainfall estimates has improved considerably with the development of improved radar data processing algorithms and bias adjustment procedures (Seo et al. 1999). Jayakrishnan (2001) compared five years of NEXRAD data with raingage data from 1995 to 1999 and found that the accuracy of NEXRAD rainfall estimates has improved considerably since 1998. The study found that during 1998-1999 more than 63% of raingages had a radar bias less than 20% compared to only 13% of raingages during 1995. Smith et al (1996) observed that NEXRAD has far superior capability for monitoring heavy rainfall than even the dense raingage networks in Tulsa, Oklahoma, United States. Several storm systems producing hourly rainfall exceeding 50mm observed by NEXRAD were completely missed by the raingage network (Smith et al. 1996). This illustrates the fundamental advantage of NEXRAD over a raingage network to characterize the spatial variability of rainfall.

Several studies have highlighted the improvements in simulated streamflow by using NEXRAD radar data. Johnson et al (1999) used the Sacramento Soil Moisture Accounting (SAC-SMA) model to simulate streamflow in three watersheds of sizes varying from 285 to 1646 km^2 located on the Oklahoma-Arkansas border. The storm hydrograph simulated using NEXRAD data compared better with observed data than the one simulated using raingage data.

Bedient et al (2000) used the HEC-1 flood hydrograph model to simulate three storm events in the Brays Bayou watershed in Houston, Texas. The peak streamflow values simulated using NEXRAD were within 8% of the observed streamflow. However, the peak streamflow simulated using raingage data underpredicted the peaks by as much as 50%.

The scope of the studies mentioned above is limited to short-term simulations of streamflow for flood forecasting using simple hydrologic models. However, studies on the use of NEXRAD data for continuous, long-term streamflow simulations over large watersheds are very limited. Jayakrishnan (2001) used the Soil and Water Assessment Tool (SWAT) to simulate continuous streamflow in three watersheds of sizes varying from 196 to 2227km^2 in Texas from 1995-1999. In addition to the bias corrections performed by the NWS on the NEXRAD data, Jayakrishnan (2001) found that local bias corrections using raingage data at the watersheds improved the overall model streamflow predictions. The modeled streamflow using local bias adjusted radar rainfall data produced reasonably good simulation results when compared to raingage data without any model parameter calibration. The better performance of bias adjusted radar data in streamflow predictions has great implications for ungaged watersheds where parameter calibration is not possible.

Significance of the Study

Most of the studies in the past investigated the significance of spatial variability of rainfall on the runoff process alone. However, studies on the significance of spatial

variability of rainfall on regional distribution of soil moisture are still lacking. Soil moisture is an important hydrologic variable that controls various land surface processes and it is an integrated measure of several state variables of climate such as precipitation and temperature and physical properties of land use and soil. Hence, it is a good measure for scheduling various agricultural operations, crop monitoring, yield forecasting, and drought monitoring. The soil moisture deficit in the root zone during various stages of the crop growth cycle will have a profound impact on the crop yield. In spite of its importance to agriculture and drought monitoring, spatial distribution of soil moisture is not widely available on a regional scale.

Hence, the objective of this research is to study the significance of spatially distributed NEXRAD rainfall data over raingage data for simulating streamflow and weekly soil moisture field over a large river basin. Further, the soil moisture data simulated using NEXRAD and raingage data will be analyzed in terms of whether the use of NEXRAD rainfall data provides distinct advantage over the raingage data in terms of agricultural drought monitoring.

Methodology

Site Description

The watershed selected for this study was the Colorado River basin located in the Edward Plateau region of Texas, United States (Figure 4.1), which has a semi-arid climate. The drainage area of the basin is 25,656 km^2 and a significant portion of the watershed is located above the recharge zone of the Edwards-Trinity Plateau aquifer.

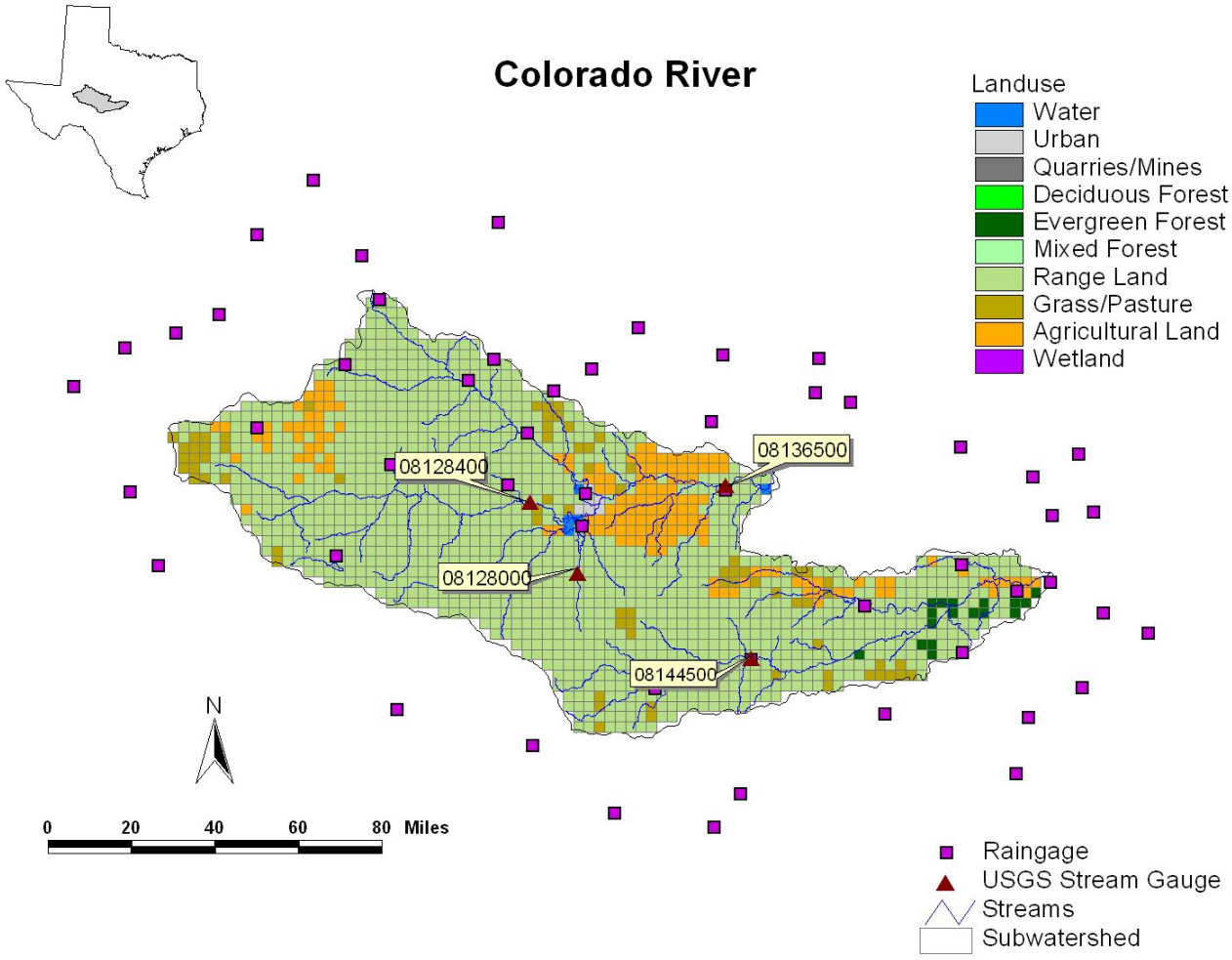

Figure 4.1 Colorado River watershed sub-basins, land use, USGS streamflow stations, and raingages.

The land use of this watershed is predominantly rangeland (83%) with some agriculture (10%) (Figure 4.1). The soil texture is predominantly clay and silty clay loam. The mean annual precipitation varies widely across the watershed with about 365mm at the west to about 708mm at the east. The average slope of the watershed is about 0.4% with a maximum slope of 1% at a few locations in the watershed.

This watershed was selected for this study because rainfall is highly variable within the watershed and often occurs as heavy showers, and comes mainly during the growing season. The watershed has minimal raingage density. Due to the erratic nature of the rainfall, the sparsely located raingages in the watershed often miss these heavy localized rainfall events. One such extreme rainfall event that happened on April 27, 2000, is shown in Figure 4.2. The raingages located within the watershed missed most of the peak storm activity with rainfall greater than 100mm. As these rainfall events supply the bulk of water that replenishes the soil water available at the root zone and the aquifer, it is essential to capture the spatial distribution of such rainfall events for agricultural drought monitoring.

NEXRAD Rainfall Data

Hourly Stage III NEXRAD rainfall data available from 1995 to 2002 were collected from the National Weather Service – River Forecasting Service (NWS-RFC) in Dallas-Ft. Worth, Texas. The hourly NEXRAD data was accumulated from 7AM to 7AM for obtaining daily NEXRAD rainfall estimates. The NEXRAD data was

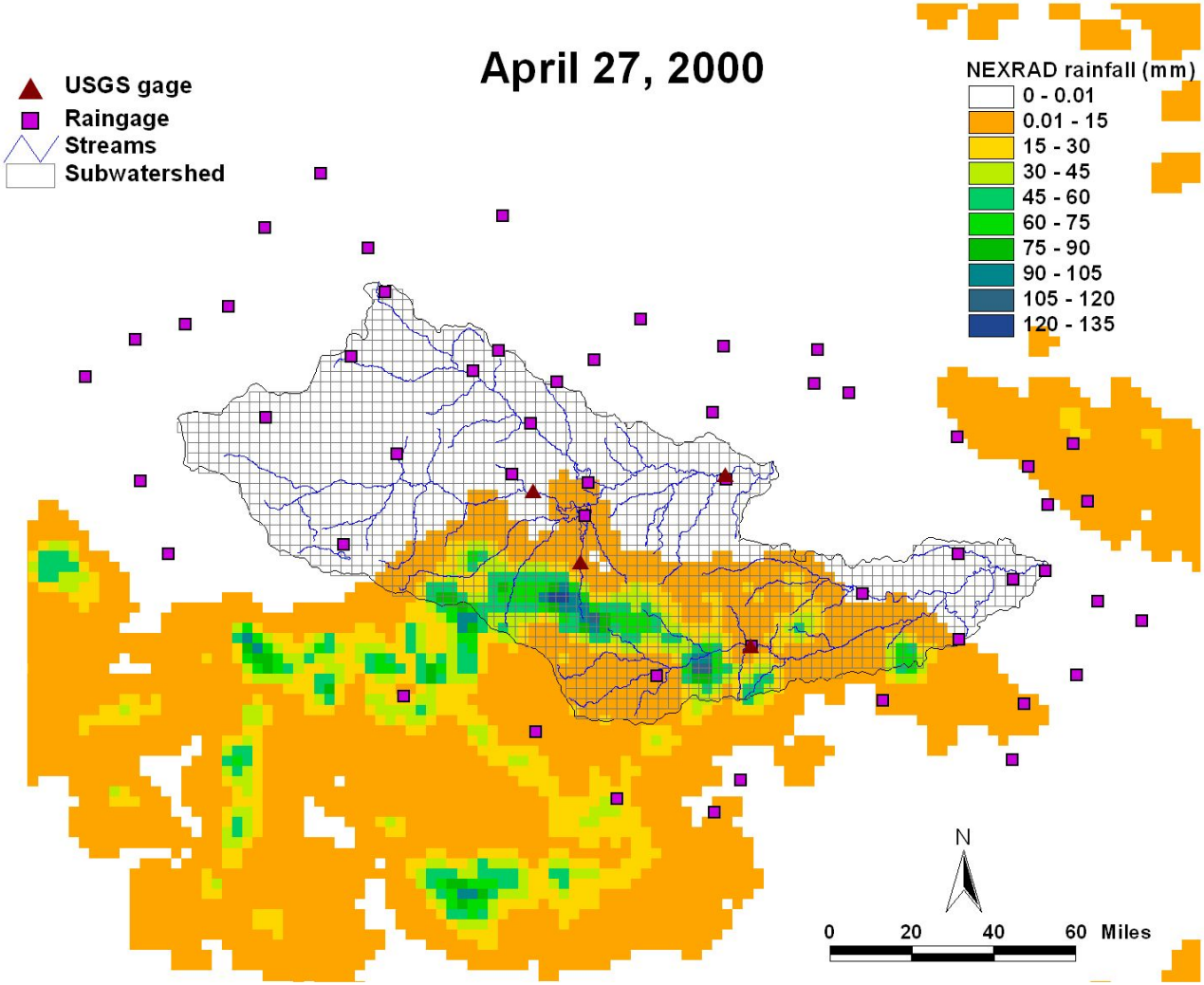

Figure 4.2 NEXRAD rainfall data on April 27, 2000.

accumulated during these hours because at most of the National Weather Service weather stations, daily rainfall data is observed at 7AM.

Jayakrishnan (2001) used daily stage III NEXRAD data with SWAT and recommended a local bias adjustment procedure for augmenting the radar data with raingage data. Hence, the local bias in the NEXARD rainfall data was adjusted by using a simple daily bias adjustment factor developed by Jayakrishnan (2001):

BAF = Daily raingage rainfall / Stage III NEXRAD rainfall (4.1)

The daily bias adjustment factor calculated at every raingage point location was then interpolated across the watershed using the Inverse Distance Weighted (IDW) technique. Using the daily BAF, the NEXRAD rainfall data was corrected using the following equation:

Bias-Adjusted Stage III NEXRAD rainfall = BAF × Stage III NEXRAD rainfall (4.2)

Thus the bias adjustment procedure corrects the NEXRAD rainfall data and makes it equal to the raingage rainfall at the raingage location, while at the same time, preserving the spatial variability of radar data (Jayakrishnan 2001).

In order to overcome the geo-referencing errors in radar data as well as in raingage locations, rainfall data from nine of the closest NEXRAD grid cells were compared with the raingage data. The NEXRAD grid cell that had the closest rainfall data to raingage data was used for calculating the BAF. Extremely high or low values of BAF are possible depending on the radar and raingage rainfall data. In order to avoid

these extreme values, BAF was constrained between an upper limit of 2.0 and a lower limit 0.5 (Jayakrishnan 2001). Further, on days with zero rainfall in raingage, the BAF was set to 1.0.

Daily NEXRAD rainfall data from 1995-2002, both before and after local bias adjustments, were compared with raingages located within 50km of the watershed boundary to evaluate the accuracy of Stage III NEXRAD data. There were about 53 raingages located within 50km of the watershed boundary. However, only 16 of the raingages measured rainfall from 7AM to 7AM. Hence, the NEXRAD rainfall data was compared with raingage data at these 16 raingages only. The comparisons were made conditional with respect to zero rainfall (i.e., only during those days when both raingage and NEXRAD recorded a rainfall event). The coefficient of determination (R^2), coefficient of efficiency (E) given by equations 2.1 and 2.2, slope and intercept of the linear regression fit were the statistics used to compare the NEXRAD and raingage rainfall data.

Hydrologic Modeling

The hydrologic model used for this study was the Soil and Water Assessment Tool (SWAT) developed by Arnold et al. (1993). SWAT is a physically based basin-scale continuous time distributed parameter hydrologic model that uses spatially distributed data on soil, land use, Digital Elevation Model (DEM), and weather data for hydrologic modeling and operates on a daily time step. Brief descriptions of the SWAT hydrologic component and model input requirements are given in Chapter II.

The Colorado River watershed was discretized into 1541 4km × 4km cells (sub-basins) for hydrologic modeling. Extraction of soil and land use parameters for these sub-basins and SWAT model setup are discussed in detail in Chapter II. Several model runs were conducted using two sources of precipitation data, raingage data and NEXRAD rainfall data, to study the effectiveness of spatially distributed rainfall data from NEXRAD. A brief description of each of these model runs are given in Table 4.1.

The SWAT model was already calibrated for the Colorado River watershed using historical rainfall data (prior to 1995) from raingages (Chapter II). However, NEXRAD rainfall data was only available from 1995 onwards. Hence, as a first step, the model was run using raingage data from 1995-2002, but using the same model parameters from the study done in Chapter II. Then, the NEXRAD rainfall data was used as the rainfall input for the model with the model parameters remaining the same. The simulated streamflow from both the model runs were compared with the observed streamflow to evaluate the model simulations in terms of spatially variable rainfall input. The R^2 and E statistics given by equations 2.1 and 2.2 were used to evaluate the model simulations.

The model was again recalibrated using NEXRAD data to study any improvement in streamflow simulations and also to investigate the changes in model parameters when using spatially distributed rainfall data. Using these new calibration parameters derived from NEXRAD rainfall data, the model was re-run using the historical rainfall data from the raingage (prior to 1995). The streamflow simulation statistics from both of the runs (Run 1 and Run 5) were then analyzed to study the

Table 4.1 Description of SWAT model runs.

Model Run	Description
Run 1	Chapter II, SWAT was calibrated and validated using raingage data prior to 1995
Run 2	SWAT was run using calibration parameters from Run 1, but using raingage data from 1995-2002
Run 3	SWAT was run using calibration parameters from Run 1, but using NEXRAD data from 1995-2002
Run 4	SWAT was recalibrated and run using NEXRAD data from 1995-2002
Run 5	Same as Run 1, but using calibration parameters from Run 4. This run was to check if the model streamflow statistics were comparable to Run 1
Run 6	SWAT was run using calibration parameters from Run 4 using raingage data from 1995-2002

relative advantage of spatially distributed rainfall data (NEXRAD) for calibration of model parameters.

Soil Moisture and Drought Index

The soil moisture and evapotranspiration data simulated from Run 5 was used to extract long-term weekly soil moisture and evapotranspiration statistics (Chapter III) for calculation of drought indices, Soil Moisture Deficit Index (SMDI) and Evapotranspiration Deficit Index (ETDI). From Run 4, weekly soil moisture was simulated using NEXRAD rainfall data from 1995-2002. For the same time period, using Run 6, weekly soil moisture was simulated from raingage data. The drought indices SMDI and ETDI were also calculated for Run 4 and Run 6 using their respective soil moisture and evapotranspiration simulations.

The model simulations from 1995-1998 were considered as model setup period to overcome any initialization errors in the model, and thus the soil moisture simulations from Run 4 (NEXRAD) and Run 6 (Raingage) were compared only from 1999-2002. The soil moisture simulations from Run 4 and Run 6 were compared for each of the 1541 sub-basins using R^2 statistics. The spatial distribution of R^2 of soil moisture was then evaluated in terms of R^2 between NEXRAD and raingage rainfall data used for model simulations and distance from raingages. The R^2 would be high for sub-basins closer to the raingage and would decrease with distance from raingages if the raingage density of the watershed was not enough to capture the spatial distribution of rainfall.

The R^2 statistics will give an integrated measure of soil moisture simulated over the entire simulation period, using two different rainfall data sources at each sub-basin.

In order to analyze the differences in spatial distribution of soil moisture simulation due to differences in spatial distribution of rainfall data at each time step over the entire watershed, spatial cross-correlation at zero lag was calculated between weekly soil moisture simulations from Run 4 and Run 6. The spatial cross-correlation between soil moisture simulations would be high if NEXRAD and raingage had similar rainfall magnitude and spatial distribution for the entire watershed. The spatial cross-correlation would be lower if the spatial distribution of rainfall data were different in NEXRAD and raingage data used from the closest raingages. Then, using total rainfall volume and standard deviations of NEXRAD and raingage rainfall events, the reasons for variations in spatial distribution of soil moisture were analyzed. Similar analysis was done on drought indices calculated from Run 4 and Run 6.

Results and Discussion

Comparison of NEXRAD and Raingage Rainfall Data

The raingage data from 16 cooperative National Weather Service (NWS) stations were compared with unadjusted and bias-adjusted NEXRAD rainfall data (Table 4.2). The coefficient of Efficiency (E) of the unadjusted NEXRAD rainfall data at the raingage locations varied between 0.15 and 0.82. The E statistics improved considerably for the bias-adjusted NEXRAD rainfall, varying between 0.52 and 0.95. The R^2 and slope of the linear regression fit also improved considerably for the bias-adjusted

NEXRAD rainfall data at all of the 16 raingage locations. The E values between NEXRAD and raingage data (Tables 4.3 and 4.4) showed that the accuracy of NEXRAD data improved considerably after 1997. In 1995 the E values between unadjusted and raingage data at the 15 operational NWS stations were less than 0.8. However, in the year 2000, out of 13 operational NWS stations, the E values between unadjusted and raingage data were greater than 0.8 at 11 stations. NEXRAD under-predicted rainfall by at least 20% in 1995 (Table 4.5). However in 2000, the NEXRAD rainfall was within 5% of the raingage data at most of the stations.

Except for three raingages - Sterling City, Duncan Wilson Ranch, and Ackerly - the overall E statistic of bias-adjusted NEXRAD rainfall was greater than 0.7 at other raingages. Analysis of the raingage data at these three stations showed, that the E was as high as 0.80 during some years and low during other years (Table 4.4). The low E during certain years could be due to changes in observation time of rainfall at these raingages. This is an inherent problem with rainfall data from cooperative weather stations, as these are manned by volunteers and strict enforcement of observation time is not done. Nevertheless, comparison of data from all the 16 raingages with NEXRAD data showed that the R^2 improved from 0.67 to 0.86 and E improved from 0.64 to 0.85 for bias-adjusted NEXRAD rainfall data (Figure 4.3).

Table 4.2 Comparison statistics conditional with respect to zero rain for unadjusted and bias-adjusted NEXRAD data (1995-2002) with raingage data at cooperative National Weather Service stations.

Station	n	Unadjusted NEXRAD rainfall				Bias Adjusted NEXRAD Rainfall			
		E	R^2	slope	Intercept	E	R^2	slope	Intercept
Ackerly 4SE	206	0.44	0.53	0.65	1.20	0.69	0.73	0.81	0.20
Center City	433	0.74	0.76	0.83	0.46	0.92	0.93	0.94	-0.37
Coleman	438	0.77	0.80	0.75	0.65	0.92	0.92	0.94	-0.56
Duncan Wilson Ranch	63	0.15	0.31	0.42	3.00	0.66	0.74	0.65	1.20
Garden City 1 E	204	0.60	0.67	0.83	-0.44	0.76	0.78	0.84	-0.19
Lampasas	460	0.54	0.59	0.72	0.95	0.85	0.86	0.88	0.00
Moss Ranch	50	0.48	0.72	0.44	2.90	0.85	0.87	0.88	-0.92
Mullin	394	0.77	0.78	0.76	1.00	0.95	0.96	0.94	-0.24
Nix Store 1 W	395	0.44	0.49	0.53	3.30	0.73	0.75	0.75	1.50
Priddy 1 NE	91	0.36	0.55	0.54	1.30	0.71	0.77	0.79	-0.40
Red Bluff Crossing	330	0.73	0.76	0.81	0.70	0.89	0.90	0.90	0.17
Richland Springs	215	0.48	0.58	0.65	1.30	0.73	0.77	0.81	0.08
Silver Valley	415	0.77	0.78	0.79	0.70	0.93	0.94	0.96	-0.56
Sterling City 8 NE	178	0.16	0.35	0.53	1.60	0.52	0.61	0.73	0.06
Water Valley	345	0.82	0.83	0.82	0.82	0.95	0.96	0.97	-0.17
Water Valley 11 NNE	261	0.74	0.78	0.79	-0.07	0.90	0.92	0.96	-0.90

Table 4.3 Coefficient of efficiency (E) between unadjusted NEXRAD rainfall and raingage data for each year.

Station	1995	1996	1997	1998	1999	2000	2001	2002	ALL
Ackerly 4SE	-1.1	0.36	0.79	0.33	0.42	0.9	-0.35	+	0.44
Center City	0.24	0.8	0.52	0.86	0.82	0.9	0.85	0.88	0.74
Coleman	-0.06	0.72	0.82	0.85	0.93	0.86	0.85	0.83	0.77
Duncan Wilson Ranch	0.04	0.3	+	+	+	+	+	+	0.15
Garden City 1 E	0.41	0.11	0.3	-2.4	0.12	0.89	0.82	0.48	0.60
Lampasas	0.47	0.66	0.61	0.68	0.8	0.64	-2.5	0.56	0.54
Moss Ranch	+	0.3	0.55	+	+	+	+	+	0.48
Mullin	0.61	0.78	0.77	0.77	0.86	0.92	0.7	+	0.77
Nix Store 1 W	0.12	0.11	0.34	0.56	0.52	0.82	0.34	0.44	0.44
Priddy 1 NE	0.2	0.63	0.35	+	+	+	+	+	0.36
Red Bluff Crossing	0.17	0.78	0.55	0.75	0.94	0.91	0.8	0.92	0.73
Richland Springs	-0.3	0.72	0.73	0.46	-0.3	0.93	0.38	-0.4	0.48
Silver Valley	0.28	0.65	0.82	0.39	0.85	0.88	0.81	0.96	0.77
Sterling City 8 NE	-0.98	0.46	0.56	-9.5	-0.07	-1.2	0.64	-0.04	0.16
Water Valley	0.57	0.84	0.8	0.48	0.76	0.94	0.96	0.81	0.82
Water Valley 11 NNE	0.17	0.75	0.72	0.82	0.9	0.91	0.66	0.8	0.74

+ National Weather Service rainfall data not available

Table 4.4 Coefficient of efficiency (E) between bias-adjusted NEXRAD rainfall and raingage data for each year.

Station	1995	1996	1997	1998	1999	2000	2001	2002	ALL
Ackerly 4SE	-0.46	0.72	0.95	0.7	0.58	1	0.38	+	0.69
Center City	0.66	0.94	0.81	1	0.97	0.97	0.98	1	0.92
Coleman	0.33	0.85	0.95	1	1	1	0.98	0.98	0.92
Duncan Wilson Ranch	0.56	0.85	+	+	+	+	+	+	0.66
Garden City 1 E	0.66	0.57	0.52	-1.5	0.42	0.98	0.87	0.66	0.76
Lampasas	0.71	0.84	0.8	0.97	0.95	0.82	0.24	0.84	0.85
Moss Ranch	+	0.69	0.92	+	+	+	+	+	0.85
Mullin	0.88	0.94	0.94	0.98	0.94	0.99	0.98	+	0.95
Nix Store 1 W	0.45	0.3	0.69	0.88	0.8	1	0.7	0.77	0.73
Priddy 1 NE	0.68	0.85	0.6	+	+	+	+	+	0.71
Red Bluff Crossing	0.62	0.97	0.72	0.97	1	0.99	0.86	1	0.89
Richland Springs	-0.02	0.82	0.95	0.78	-0.18	1	0.84	0.48	0.73
Silver Valley	0.6	0.78	0.98	0.88	1	1	0.97	1	0.93
Sterling City 8 NE	-0.63	0.88	0.84	-1.1	0.64	-0.71	0.8	0.05	0.52
Water Valley	0.9	0.96	0.97	0.54	1	0.99	1	1	0.95
Water Valley 11 NNE	0.66	0.95	0.82	1	1	1	0.82	0.89	0.90

+ National Weather Service rainfall data not available

Table 4.5 Percentage difference in annual rainfall between the bias-adjusted NEXRAD rainfall and raingage data.

Station	1995	1996	1997	1998	1999	2000	2001	2002
Ackerly 4SE	-44.0	0.3	-7.5	-4.7	-7.5	5.7	-27.0	+
Center City	-27.0	-12.0	-13.0	-4.2	12.0	-2.8	0.5	0.8
Coleman	-51.0	-12.0	-12.0	-7.4	0.1	-6.8	-5.4	-3.9
Duncan Wilson Ranch	-47.0	-0.3	+	+	+	+	+	+
Garden City 1 E	-40.0	-0.8	-12.0	-12.0	36.0	-3.0	-7.5	-8.3
Lampasas	-30.0	-15.0	-21.0	-6.9	-5.2	-4.3	60.0	-6.1
Moss Ranch	+	-24.0	-14.0	+	+	+	+	+
Mullin	-19.0	-9.4	-7.3	-13.0	-4.9	-4.0	6.0	+
Nix Store 1 W	-40.0	-16.0	-22.0	-20.0	-16.0	-2.7	-6.7	-3.0
Priddy 1 NE	-31.0	-11.0	-27.0	+	+	+	+	+
Red Bluff Crossing	-34.0	-5.5	-17.0	1.4	2.2	5.0	-2.0	0.9
Richland Springs	-53.0	-6.2	-8.8	-12.0	2.5	1.4	4.4	17.0
Silver Valley	-45.0	-14.0	-6.5	3.0	1.5	-5.0	-2.7	-0.8
Sterling City 8 NE	-42.0	10.0	-18.0	-31.0	-10.0	-32.0	4.9	-18.0
Water Valley	-57.0	-1.9	-7.0	-6.6	2.7	-1.9	-1.9	1.7
Water Valley 11 NNE	-44.0	3.7	-20.0	4.5	6.8	11.0	-9.4	-6.2

+ National Weather Service rainfall data not available

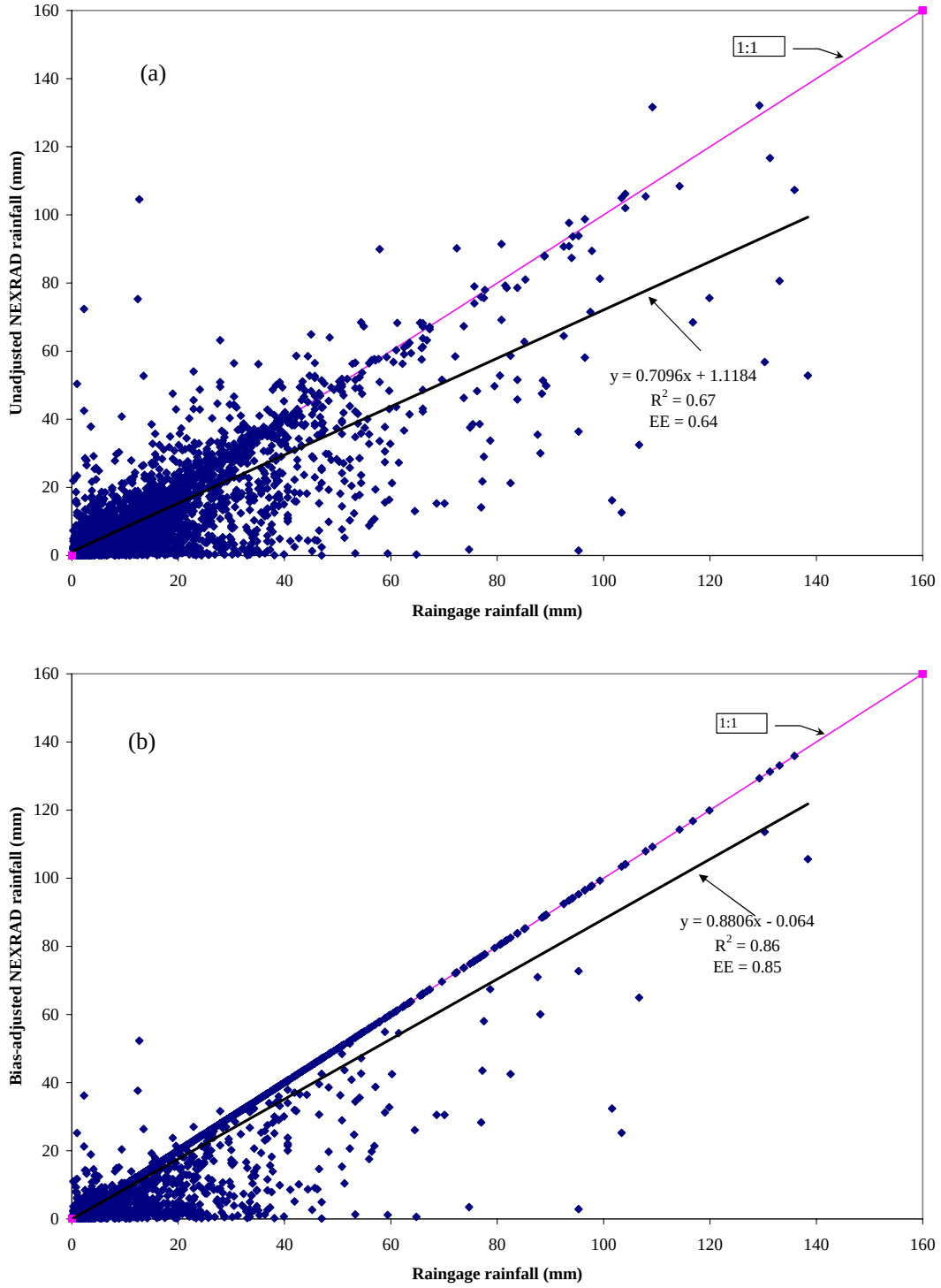

Figure 4.3 Comparison of raingage data with NEXRAD data. a) Unadjusted NEXRAD rainfall data b) Bias-adjusted NEXRAD rainfall data.

Streamflow Comparison

The model was calibrated for streamflow in Chapter II using raingage data prior to 1995 (Run 1). The R^2 and E statistic of weekly streamflow during the validation period is given in Table 4.6. Using the same model parameters from Run 1, but running the model with raingage data after 1995 (Run 2), the weekly streamflow simulations were very poor except for USGS gage 08144500 (Table 4.7). This was because the raingages completely missed some or all of the precipitation events that caused the streamflow at these USGS gages. Weekly measured and simulated streamflow at one of the USGS gages is shown in Figure 4.4. However, when bias-adjusted NEXRAD rainfall data was used (Run 3), the streamflow simulations improved considerably at all the USGS gages (Table 4.8).

In order to further improve the streamflow simulations using NEXRAD rainfall data, the model parameters were recalibrated with bias-adjusted NEXRAD rainfall data (Run 4). The model was calibrated using the non-linear auto-calibration algorithm, VAO5A (Harwell subroutine library 1974), and selected model parameters were changed within reasonable limits, as indicated in Table 2.3. The recalibrated model with bias-adjusted NEXRAD data simulated weekly streamflow much closer to the observed streamflow (Table 4.9). Weekly measured and simulated streamflow at the USGS gage 08128400 using bias-adjusted NEXRAD rainfall data (Run 4) is shown in Figure 4.5. The R^2 and E statistic were considerably high (R^2 and E ~ 0.7) for Run 4 when compared to Run 2 and Run 3. This result suggests that knowing the spatial distribution of rainfall

Table 4.6 Comparison of observed and simulated streamflow for Run 1 (Table 2.9).

USGS Gage	Years	No. of Years	R^2	E
08128000	1959	1	1	1
08128400	1986	1	0.98	0.85
08136500	1940 to 1961	22	0.78	0.74
08144500	1974 to 1975	2	0.92	0.9

Table 4.7 Comparison of observed and simulated streamflow for Run 2.

USGS Gage	Years	No. of Years	R^2	E
08128000	2001 to 2002	2	0.00085	-1.2
08128400	2001 to 2002	2	0.00061	-5.5
08136500	1999 to 2002	4	0.56	-0.24
08144500	1999 to 2002	4	0.92	0.7

Table 4.8 Comparison of observed and simulated streamflow for Run 3.

USGS Gage	Years	No. of Years	R^2	E
08128000	2001 to 2002	2	0.94	0.86
08128400	2001 to 2002	2	0.43	-0.028
08136500	1999 to 2002	4	0.67	-0.91
08144500	1999 to 2002	4	0.97	0.81

Table 4.9 Comparison of observed and simulated streamflow for Run 4.

USGS Gage	Years	No. of Years	R^2	E
08128000	2001 to 2002	2	0.92	0.83
08128400	2001 to 2002	2	0.84	0.81
08136500	1999 to 2002	4	0.7	0.67
08144500	1999 to 2002	4	0.96	0.95

Table 4.10 Comparison of observed and simulated streamflow for Run 5.

USGS Gage.	Years	No. of Years	R^2	E
08128000	1959	1	1	1
08128400	1986	1	0.92	-0.45
08136500	1940 to 1961	22	0.81	0.8
08144500	1974 to 1975	2	0.86	0.63

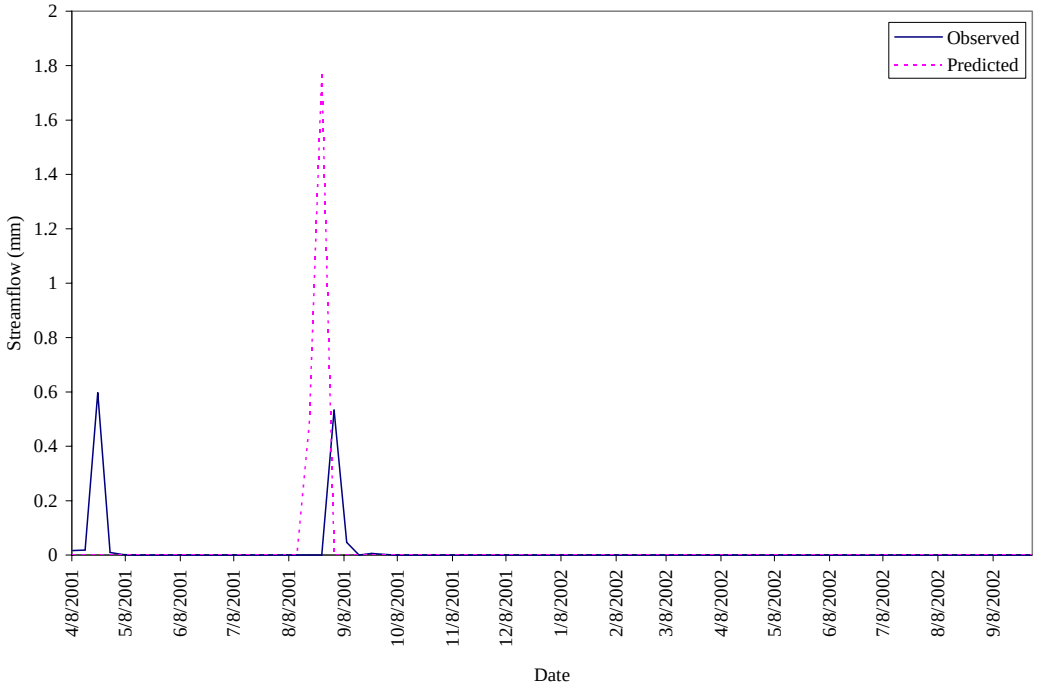

Figure 4.4 Weekly measured and simulated streamflow at USGS gage 08128400 using raingage data (Run 2).

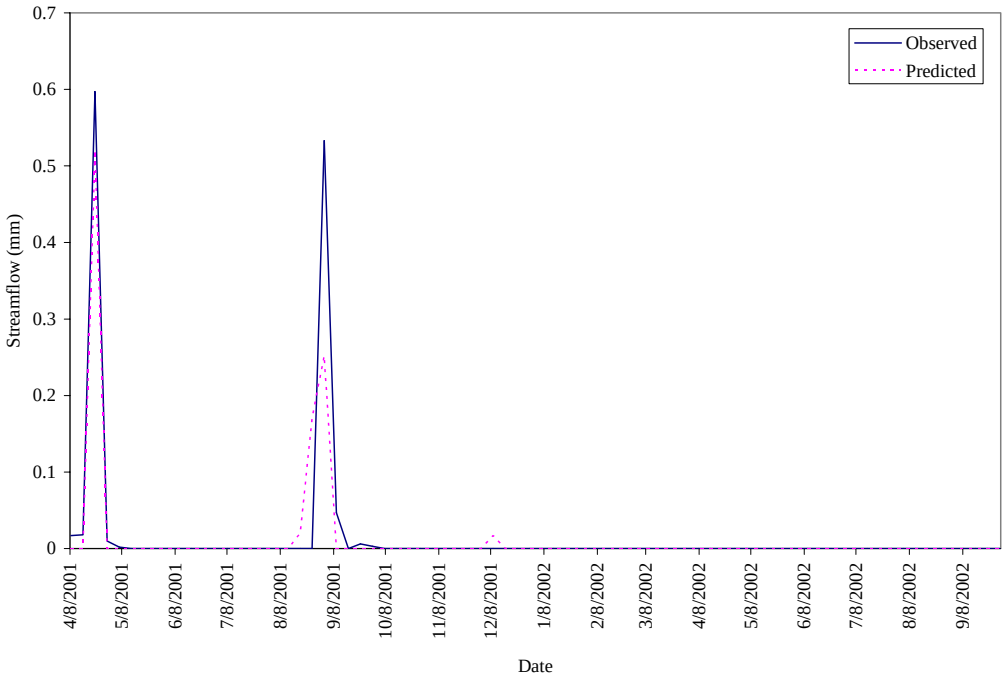

Figure 4.5 Weekly measured and simulated streamflow at USGS gage 08128400 using bias-adjusted NEXRAD rainfall data (Run 4).

is critical for streamflow simulations at semi-arid watersheds, and NEXRAD could be a useful source for obtaining spatially distributed rainfall for hydrologic modeling.

The model parameters using raingage data prior to 1995 and bias-adjusted NEXRAD data are given in Tables 4.11 and 4.12. The model parameters that showed greater sensitivity to change in rainfall data sources are CN2, ESCO, SOL_AWC, and SOL_K. Previous studies have shown that streamflow is highly sensitive to these parameters when compared to other parameters (Arnold et al. 2000; Lenhart et al. 2002; Santhi et al. 2001; Texas Agricultural Experiment Station 2000). Hence, use of spatially distributed rainfall data results in more changes to these parameters when compared to other model parameters. As the model parameters changed due to changes in the rainfall data source (raingage vs NEXRAD), a question arises as to the usefulness of a model calibrated with NEXRAD data for doing streamflow simulations using historical raingage data. This has major implications for drought related studies, as NEXRAD data has only been available since 1995, and historical simulations have to be done only with raingage data alone.

In order to study this, the model was run (Run 5) using raingage data for the same validation period as Run 1, but using model parameters from Run 4. Except for USGS gage 0812400, the R^2 and E statistic showed comparable performance in streamflow simulations between Run 1 and Run 5 (Table 4.10). SWAT simulated streamflow overestimated the measured streamflow at USGS gage 0812400; hence the E statistic was low. This could be due to a peak storm activity at the raingage location;

Table 4.11 SWAT model parameters obtained using raingage data prior to 1995 for model calibration.

SWAT Parameters	USGS streamgages			
	08128000	08128400	08136500	08144500
ESCO	0.95	0.583	0.771	0.539
GW_REVAP	0.119	0.256	0.112	0.133
RCHRG_DP	0.349	0.709	0.217	0.64
REVAPMN (mm)	0	0.175	0.305	0
GWQMN (mm)	43	41.5	20.4	22.3
CANMAX-RNGE	0	6.41	0	0.23
CN2-RNGE (% change)	-34.3	-38.9	-27.1	-29
CN2-AGRL (% change)	-	-2.43	-12.1	-
CN3-PAST (% change)	-	-	-2.29	-40
SOL_K (% change)	-1.81	-0.156	-0.117	14.4
SOL_AWC (% change)	20	7.28	-1.85	16
CH_K (mm/hr)	19.6	42.2	11.6	56.8

AGRL – Agriculture; PAST – Pasture; RNGE – Rangeland.

Table 4.12 SWAT model parameters obtained using bias-adjusted NEXRAD data from 1995-2002.

SWAT Parameters	USGS streamgages			
	08128000	08128400	08136500	08144500
ESCO	0.267	0.811	0.683	0.588
GW_REVAP	0.14	0.0624	0.147	0.338
RCHRG_DP	0.2	0.804	0.55	0.373
REVAPMN (mm)	0	1.78	0	0
GWQMN (mm)	15.4	8.42	18.2	46.6
CANMAX-RNGE	1.27	3.05	0.74	7.01
CN2-RNGE (% change)	-33.7	-31.9	-40	-39.4
CN2-AGRL (% change)	-	-13.6	-9.6	-
CN3-PAST (% change)	-	-	3.08	-21.5
SOL_K (% change)	-3.53	1.57	7.54	3.46
SOL_AWC (% change)	15.5	2.08	-0.815	6.15
CH_K (mm/hr)	28.1	19.4	31	19.6

AGRL – Agriculture; PAST – Pasture; RNGE – Rangeland.

however, the peak storm event did not occur over a large area of the watershed as indicated by the raingage data. Hence, the streamflow was over-predicted by SWAT.

Nevertheless, the streamflow simulations at other USGS gages were in close agreement with observed data. Hence, the model parameters derived using NEXRAD data was equally good for simulations using raingage data. However, when the calibration parameters obtained from raingage data were used for NEXRAD simulations (Run 3), the model statistics R^2 and E were comparatively low. This result implies that for studies involving raingage and NEXRAD rainfall data, spatially distributed NEXRAD rainfall data could be used for model calibration for obtaining reliable model parameters. These model parameters could then be used for simulations involving raingage data. However, this needs to be verified over various watersheds to make stronger conclusions.

Time Series Correlation of Weekly Soil Moisture and Drought Index Between Run 4 and Run 6

As most of the available water at the root zone was in the top two feet of soil profile, only the soil water simulated at the top two feet was compared between Run 4 and Run 6. In order to study the soil moisture simulated between Run 4 and Run 6, time series of raingage and NEXRAD rainfall data used by each of the 1541 sub-basins for simulating soil moisture were analyzed. Coefficient of Determination (R^2) was computed between cumulative weekly raingage and NEXRAD rainfall data for each sub-basin (Figure 4.6).

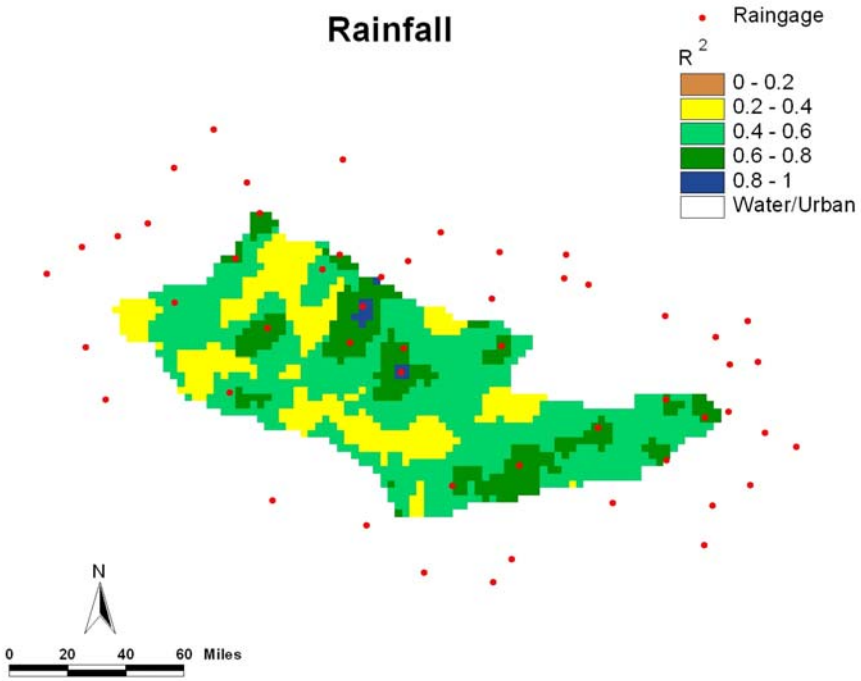

Figure 4.6 Time-series R^2 of raingage and NEXRAD rainfall data at each sub-basin.

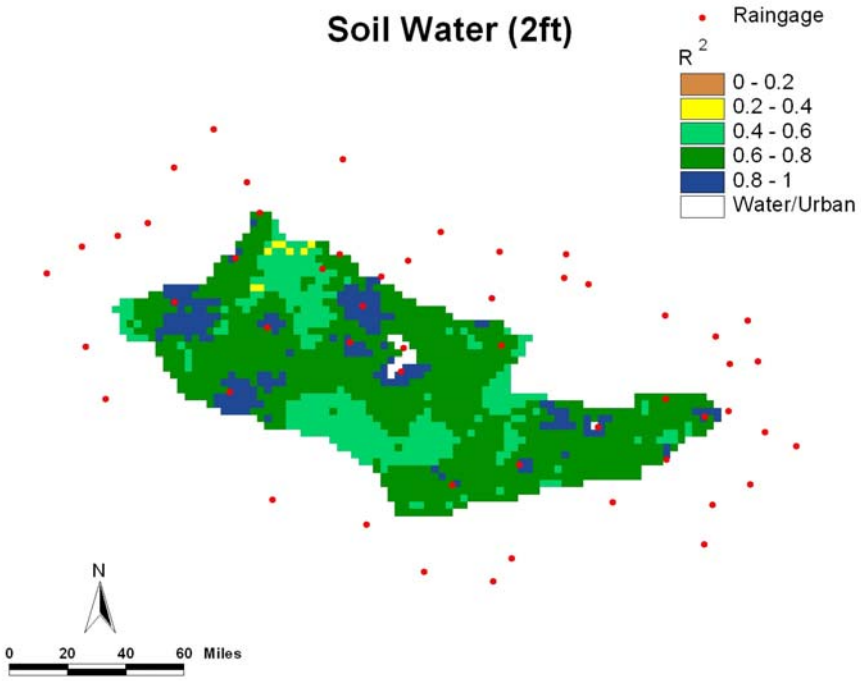

Figure 4.7 Time-series R^2 of soil water simulated using raingage and NEXRAD rainfall data at each sub-basin.

As expected, the R^2 was high (> 0.6) between raingage and NEXRAD rainfall data close to raingage locations, and the R^2 decreased with distance from raingages.

The spatial distribution of R^2 between weekly soil water (2ft) simulated using raingage and NEXRAD rainfall data also showed a similar spatial trend as that of rainfall R^2 (Figure 4.7). However, in contrast to rainfall R^2, the R^2 values of soil water were greater than 0.6 for most of the watershed and ranged between 0.4-0.6 at the furthest location from the raingages. The higher R^2 of soil water could be a result of the spatial distribution of precipitation that affects the soil moisture distribution mainly during and a few weeks after a storm event. After that the soil moisture distribution is mainly governed by the soil and land use properties. Further, this watershed is located in the semi-arid region and hence, almost all of the rainfall stored in the soil profile is lost as evapotranspiration. Hence, the R^2 values for soil water simulated were comparatively high despite the different rainfall sources.The spatial distribution of R^2 for ETDI and SMDI-2 were very similar to each other and closely followed that of soil water (Figures 4.8 and 4.9). This was expected because ETDI and SMDI are both functions of soil water. The similarities in the spatial distribution of R^2 (figures 4.6 to 4.9) suggest that consideration of spatial distribution of rainfall is critical for soil water simulations and drought monitoring. Further, the errors in soil water simulations could increase with distance from raingages due to variation in spatial distribution of rainfall.

Spatial Cross-Correlation of Weekly Soil Moisture and Drought Index Between Run 4 and Run 6

Spatial cross-correlation at zero lag was calculated between weekly soil water (2ft) simulated from raingage and NEXRAD rainfall data. The changes in spatial cross-correlation of simulated soil moisture during different weeks were analyzed using weekly total rainfall volume over the entire watershed and spatial standard deviation of raingage and NEXRAD data used in model simulations. The analysis of weekly soil water data during the year 2000 is presented here as it had some high and low precipitation events that affected the spatial cross-correlation of soil water (2ft).

The spatial cross-correlation of soil water was close to 0.7 during the week of 4/21/2000 (Figure 4.10). But the correlation dropped to 0.2 during the week of 5/5/2000. This was because of two small rainfall events that happened in between these weeks that were not fully captured by the raingage. The spatial standard deviations of these events measured by NEXRAD were different than the spatial standard deviations obtained from raingage data (Figure 4.11). Small rainfall events such as these produce more infiltration into soils than surface runoff and hence fill the soil profile to varying levels of saturation depending on the available water holding capacity. Because most of the rainfall from these events is stored in the soil profile, the spatial cross-correlation of soil water between NEXRAD and raingage data were considerably less.

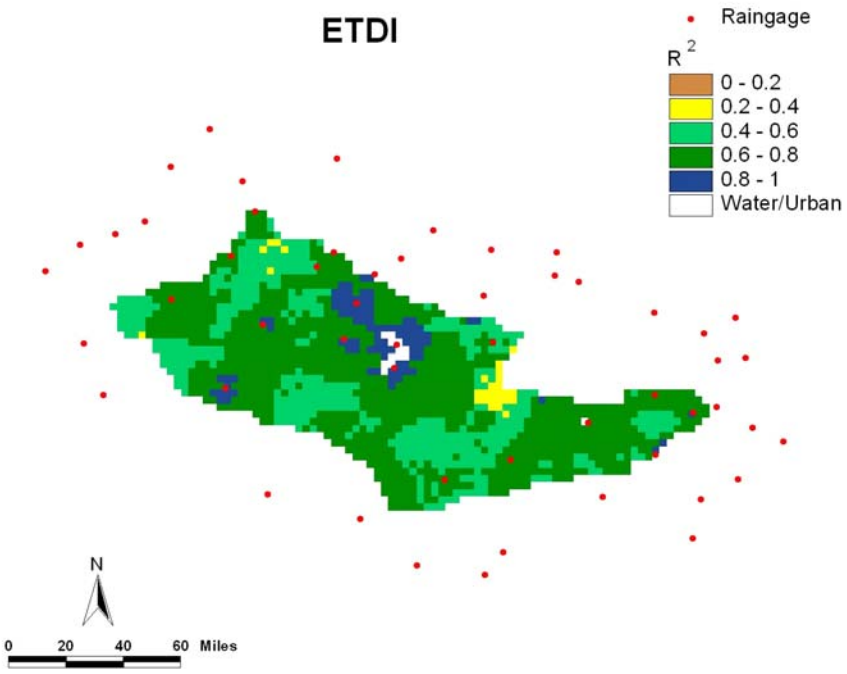

Figure 4.8 Time-series R^2 of ETDI simulated using raingage and NEXRAD rainfall data at each sub-basin.

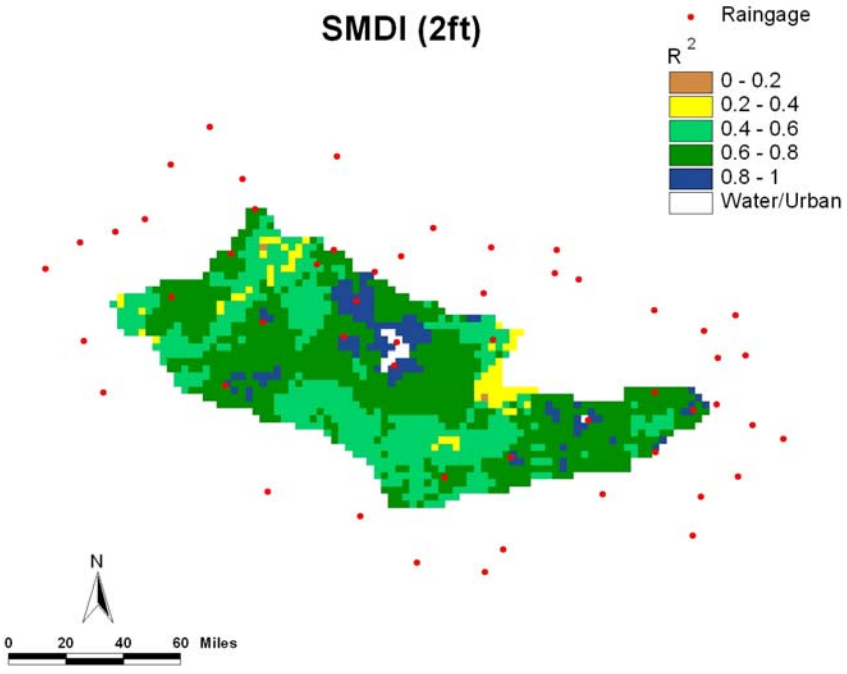

Figure 4.9 Time-series R^2 of SMDI-2 simulated using raingage and NEXRAD rainfall data at each sub-basin.

The spatial cross-correlation of soil water again increased above 0.6 during the week of 6/9/2000. This was because of two relatively high rainfall events that occurred during the weeks of 5/19/2000 and 6/9/2000. These high precipitation events fill the soil profile to saturation. Although there are differences in rainfall volumes measured by NEXRAD and Raingage, after saturation, most of the water will be lost as runoff. As the soil attained saturation in both the simulation runs, the spatial cross-correlation became high ($r \sim 0.7$).

The spatial cross-correlation became ($r \sim 0.15$) low again during the week of 7/28/2000. During the summer most of the soil became dry. However, the rainfall volume during 7/28/2000, which replenished the soil water, was different for NEXRAD and raingage data. As this precipitation event resulted in varying degrees of saturation of soil between NEXRAD and raingage simulations, the spatial cross-correlation of soil water dropped from 0.6 two weeks before to 0.15.

The spatial cross-correlation of soil water increased ($r \sim 0.7$) again during the week of 8/25/2000. This was because most of the water in the soil profile evaporated and soils became equally dry in both the simulations during two dry weeks preceding 8/25/2000. The spatial cross-correlation again reduced slightly ($r \sim 0.6$) during the week of 9/15/2000. This was due to a difference in rainfall volume measured by NEXRAD and raingage for an event that occurred during the same week.

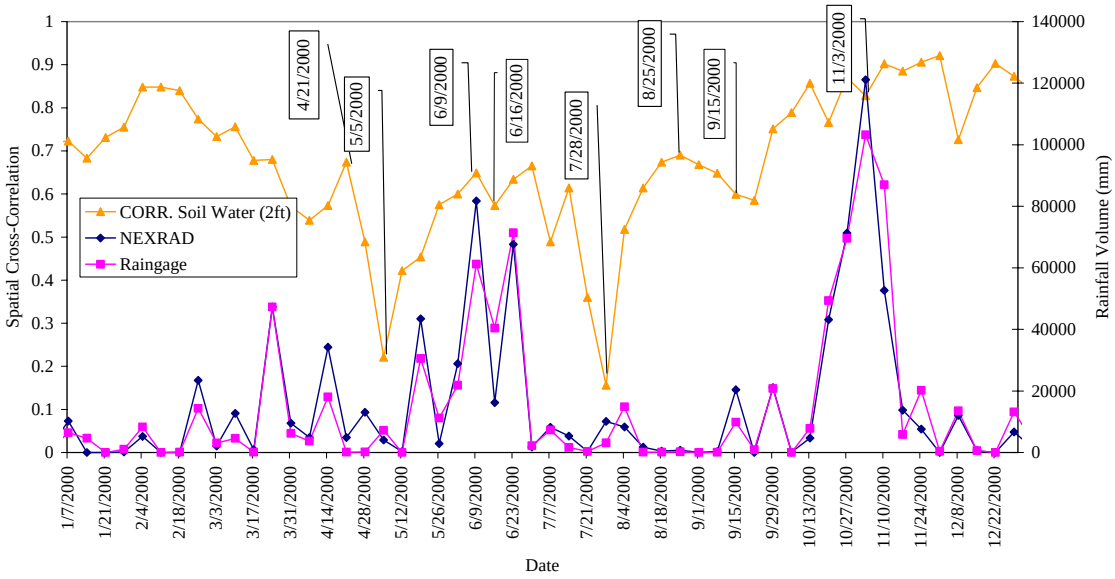

Figure 4.10 Spatial cross-correlations of soil water and rainfall volumes over the entire basin from raingage and NEXRAD.

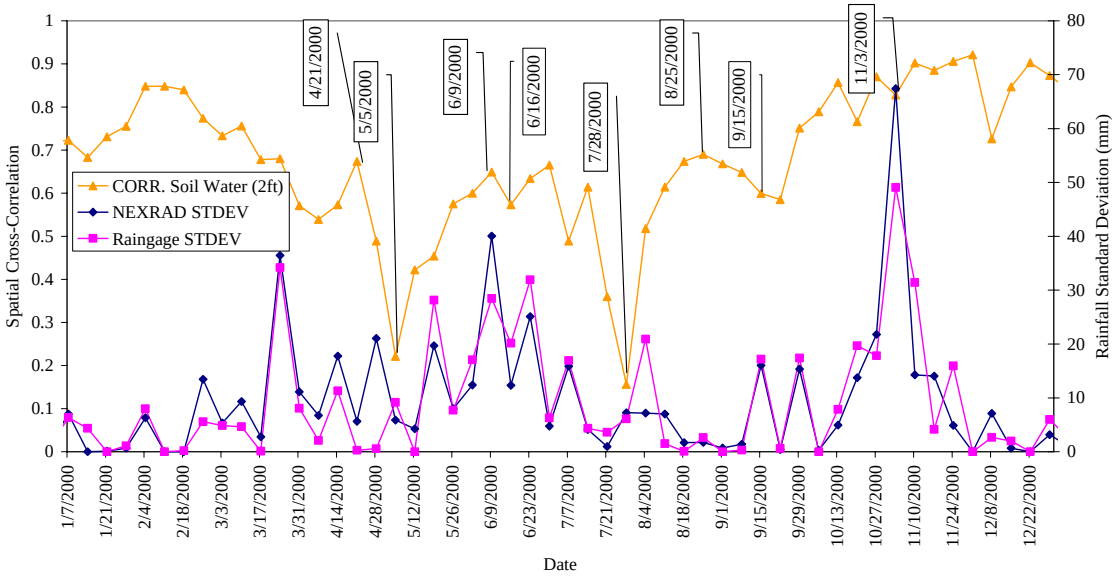

Figure 4.11 Spatial cross-correlations of soil water and standard deviations of raingage and NEXRAD rainfall data.

Following the big rainfall event (~78mm) that occurred during the week of 11/3/2000 across the entire basin, the spatial cross-correlation of soil water increased to above 0.9 as the soil profile became mostly saturated in both the model runs (Run 4 and Run 6). Even though there were differences in rainfall volumes and standard deviation measured by NEXRAD and raingage, beyond saturation, most of the water was lost as runoff and therefore, spatial cross-correlation of soil water was not affected beyond this point.

These observations were further apparent from the comparison of spatial cross-correlations of soil water with the average drought indices ETDI and SMDI-2 over the entire watershed (Figures 4.12 and 4.13). The spatial cross-correlations of soil water tend to become low during the on-set of drought (ETDI and SMDI < 0). Hence, any small, sporadic rainfall events not measured by raingage data but measured by NEXRAD, reduced the spatial cross-correlations of soil water. However, as the drought approached the maximum intensity (ETDI and SMDI ~ 3), the spatial cross-correlations increased because the soils became dry across the watershed in both the raingage and NEXRAD simulations. The spatial cross-correlations of soil water increased as the soil water increased (ETDI and SMDI > 0) following heavy rainfall events. The spatial cross-correlations increased because these heavy rainfall events that occur across most of the watershed were captured by both the raingage and NEXRAD.

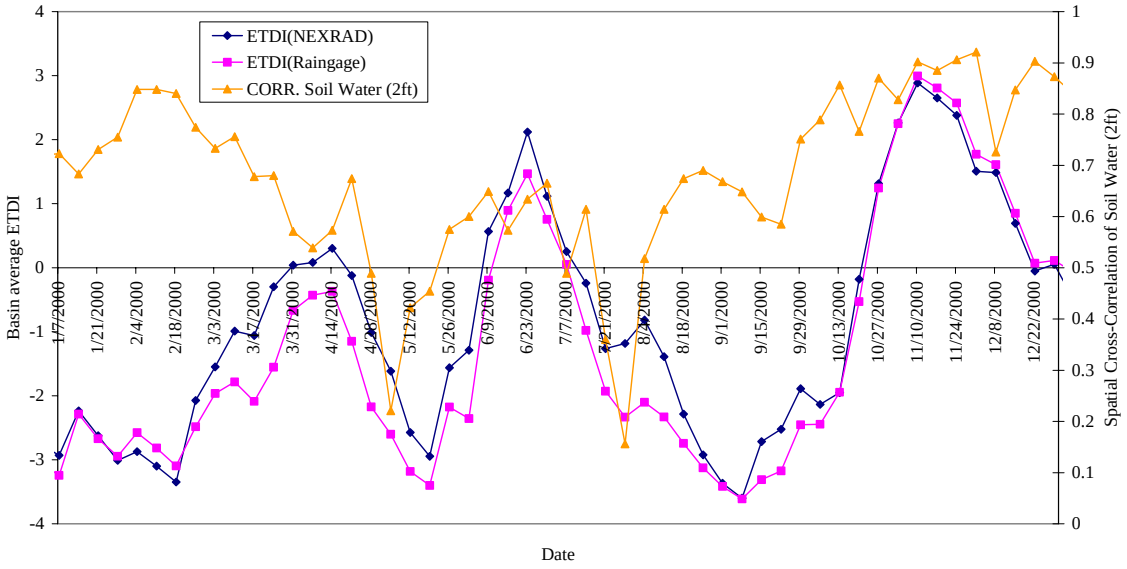

Figure 4.12 Spatial cross-correlations of soil water and mean drought index ETDI.

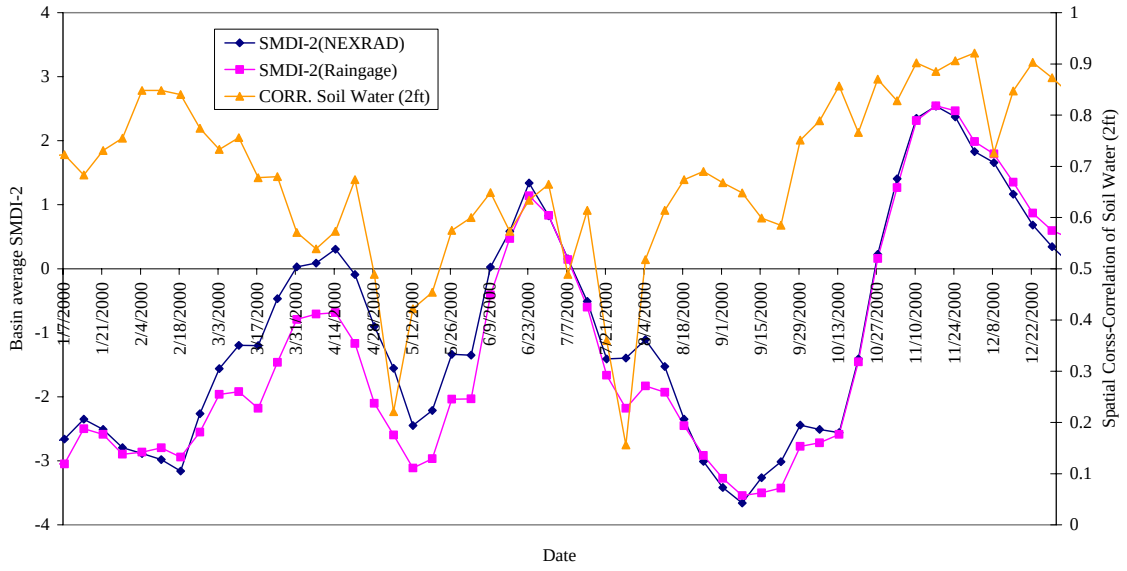

Figure 4.13 Spatial cross-correlations of soil water and mean drought index SMDI-2.

Although the means of drought index calculated over the entire watershed were similar for simulations using NEXRAD and raingage data, the spatial cross-correlations were varying due to the spatial variability of rainfall (Figure 4.14). The spatial cross-correlation of SMDI-2 and ETDI followed closely the spatial cross-correlation of soil water at two feet because the drought indices were derived as a function of soil water. Hence, rainfall events that affect the spatial cross-correlations of soil water also affect the spatial cross-correlations of drought indices. However, there was a slight lag between the spatial cross-correlations of drought indices and soil water (Figure 4.14). The lag was expected because the drought index for the current week depends on the soil water conditions and evapotranspiration of the previous weeks (Equations 3.8 and 3.11).

Summary and Conclusions

The significance of spatial variability of rainfall data for simulating streamflow, soil moisture and drought was evaluated by the hydrologic model SWAT using raingage and NEXRAD rainfall data. A local bias adjustment procedure developed by Jayakrishnan (2001) improved the accuracy of NEXRAD data considerably. The local bias adjustment of the NEXRAD data improved the R^2 and E statistic from 0.67 and 0.64 to 0.86 and 0.85, respectively. The streamflow simulations using bias adjusted

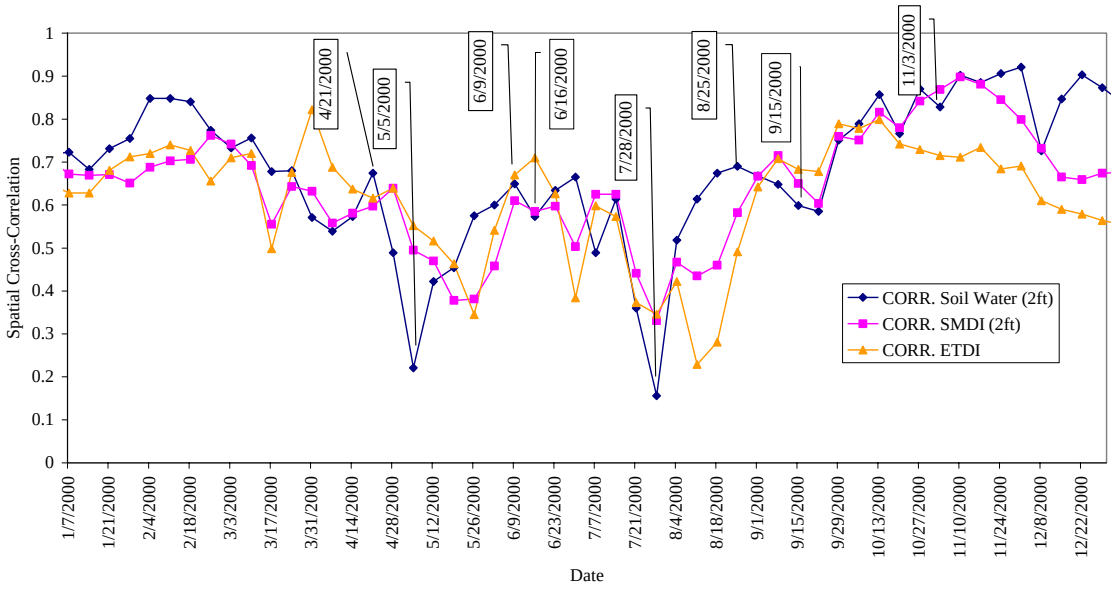

Figure 4.14 Spatial cross-correlations of soil water, ETDI and SMDI-2.

NEXRAD rainfall data more closely matched the observed streamflow (R^2 ~ 0.8 and E ~ 0.8) than the streamflow simulated using raingage data. The study also showed that certain model calibration parameters such as CN2, ESCO, SOL_AWC, and SOL_K depend on spatial distribution of rainfall. The model parameters calibrated using raingage data, when used for simulating streamflow with NEXRAD rainfall data, yielded poor statistics (for USGS gage no. 08136500, R^2: 0.67, E: -0.91). However, the same model parameters calibrated using NEXRAD data, when used with raingage data, satisfactorily simulated the streamflow (for USGS gage no. 08136500, R^2: 0.81, E: 0.80). Hence, for studies involving use of both raingage and NEXRAD rainfall data, NEXRAD rainfall data could be used for calibrating the model and the same model parameters could be used for simulation years involving raingage data.

Time series correlation analysis between soil moisture simulations using raingage and NEXRAD rainfall data showed that soil moisture simulations were affected by spatial variability of rainfall, which was not effectively characterized by raingages. The R^2 between soil moisture simulated at each grid cell using raingage and NEXRAD rainfall data was high (~ 0.8) at the location of raingage. However, the R^2 decreased (~ 0.4) with distance from the raingage, indicating the deviations in simulations due to the spatial variability of rainfall and the rainfall events missed by raingages.

Spatial cross-correlation analysis of soil moisture simulated by raingage and NEXRAD data showed a higher correlation during days of heavy precipitation events that saturated the soils in both the simulations. However, spatial variability of small

rainfall events during the dry season affected the spatial cross-correlation of soil moisture considerably. This was because small rainfall events produce more infiltration into soils than surface runoff and hence, fill the soil profile to varying levels of saturation depending on the available water holding capacity. As the drought indices SMDI-2 and ETDI were functions of soil water available at two feet, they were affected by the spatial variability of rainfall to the same extent as that of soil water. As NEXRAD rainfall data could effectively capture the spatial variability of rainfall, the use of local bias-adjusted NEXRAD rainfall data could help overcome the limitations of raingage data for simulating soil water and in the calculation of drought index for drought monitoring.

CHAPTER V

CONCLUSIONS AND RECOMMENDATIONS

Conclusions

Objective 1:" To develop a long-term record of soil moisture and evapotranspiration for different soil and land use types, using a comprehensive hydrologic and crop growth model, Soil and Water Assessment Tool (SWAT), GIS and historical weather data for Texas".

The hydrologic model SWAT was used for developing a long-term soil moisture dataset at a spatial resolution of 4km × 4km and at a weekly temporal resolution. The hydrologic model was calibrated for stream flow using an auto-calibration algorithm and validated over multiple years.

- The overall R^2 and E values for the calibration period was 0.75 and the validation period was 0.70 on weekly stream flow. Most of the differences between the measured and simulated stream flow occurred due to a lack of raingage network in the watershed.
- Due to a lack of measured evapotranspiration or soil moisture data, simulated soil moisture was analyzed using 16 years of NDVI data. Analysis showed that the simulated soil moisture was well-correlated with NDVI for agriculture and pasture land use types ($r \sim 0.6$). The correlations were as high as 0.8 during

certain years, indicating that the model performed well in simulating the soil moisture.

- There was a lag of at least one week between the simulated soil moisture and NDVI because it takes some time for the plant to respond to the water stress in the root zone.
- In high precipitation zones like Lower Trinity, NDVI was well-correlated only during the dry years because NDVI doesn't fluctuate much during normal or wet years due to high available soil moisture. Further analysis is needed to explain the NDVI response of forest and rangeland in terms of soil water or precipitation due to the well-developed root system that can extract water beyond the root zone.

Objective 2: "To develop drought indices based on soil moisture and evapotranspiration deficits and evaluate the performance of the indices for monitoring agricultural drought".

Weekly soil moisture and evapotranspiration simulated by the calibrated hydrologic model SWAT was used to develop a set of drought indices – SMDI and ETDI, respectively. The drought indices were derived from soil moisture deficit and evapotranspiration deficit and scaled between -4 and 4 for spatial comparison of drought index, irrespective of climatic conditions.

- The auto-correlation lag of the drought indices, ETDI and SMDI, were closely related to the available water holding capacity of the soil, with lag increasing as a result of increased water holding capacity.
- ETDI and SMDI-2 had the lowest auto-correlation lag because the top two feet of the soil profile very actively participate in the evapotranspiration of available soil water. Hence, ETDI and SMDI-2 could be good indicators of short-term agricultural droughts.
- The spatial variability of the developed drought indices was high with a standard deviation greater than 1.0 during most weeks in a year.
- The high spatial variability in the drought indices was mainly due to high spatial variability in rainfall distribution.
- The spatial variability (standard deviation) of the drought indices, especially ETDI, during different seasons closely followed the variability in precipitation and potential evapotranspiration across seasons.
- ETDI and SMDI's were positively correlated with PDSI and SPI's for all six watersheds. This suggests that the dry and wet period indicated by the ETDI and SMDI's were in general agreement with PDSI and SPI.
- For all six watersheds, ETDI and SMDI-2 were well-correlated with the SPI-1 ($r \sim 0.7$) month, indicating that ETDI and SMDI-2 are good indicators of short-term drought conditions suitable for agricultural drought monitoring.

- PDSI was highly correlated with SPI-9 and SPI-12 months ($r > 0.8$), suggesting that precipitation was the dominant factor in PDSI, and PDSI is an indicator of long-term weather conditions.
- The wheat and sorghum crop yields were highly correlated with the drought indices ($r > 0.75$) during the weeks of critical crop growth stages, indicating that ETDI and SMDI's can be used for agricultural drought monitoring.
- For high precipitation zones, the reduction in crop yield could not be attributed to moisture stress alone. The yield reduction could also be due to factors such as soil fertility, pests, diseases, water logging, and frost.

Objective 3: "To study the effect of spatially distributed rainfall from NEXt generation weather RADar (NEXRAD) rainfall data in the simulation of soil moisture and estimation of drought indices".

The significance of spatial variability of rainfall data for simulating streamflow, soil moisture and drought was evaluated by the hydrologic model SWAT using raingage and NEXRAD rainfall data.

- A local bias adjustment procedure developed by Jayakrishnan (2001) improved the accuracy of the NEXRAD data considerably. The local bias adjustment of the NEXRAD data improved the R^2 and E statistic from 0.67 and 0.64 to 0.86 and 0.85, respectively.

- The streamflow simulations using bias adjusted NEXRAD rainfall data more closely matched the observed streamflow (R^2 ~ 0.8 and E ~ 0.8) than the streamflow simulated using raingage data.
- Model calibration parameters such as CN2, ESCO, SOL_AWC, and SOL_K depended on spatial distribution of rainfall. Hence, for studies involving use of both raingage and NEXRAD rainfall data, NEXRAD rainfall data could be used for calibrating the model and the same model parameters could be used for simulation years involving raingage data.
- Time series correlation analysis showed that the R^2 between soil moisture simulated at each grid cell using raingage and NEXRAD rainfall data was high (~ 0.8) at the location of the raingage. However, the R^2 decreased (~ 0.4) with distance from the raingage, indicating the deviations in simulations due to the spatial variability of rainfall and the rainfall events missed by raingages.
- Spatial cross-correlation analysis of soil moisture simulated by raingage and NEXRAD data showed a higher correlation during days of heavy precipitation events that saturated the soils in both the simulations. However, spatial variability of small rainfall events during the dry season affected the spatial cross-correlation of soil moisture considerably. This was because small rainfall events produce more infiltration into soils than surface runoff and thus fill the soil profile to varying levels of saturation depending on the available water holding capacity.

- As the drought indices SMDI-2 and ETDI were functions of soil water available at two feet, they were affected by the spatial variability of rainfall to the same extent as that of soil water.
- As NEXRAD rainfall data could effectively capture the spatial variability of rainfall, the use of local bias-adjusted NEXRAD rainfall data could help overcome the limitations of raingage data for simulating soil water and in the calculation of drought index for drought monitoring.

Recommendations

1. Hydrologic models were primarily calibrated using observed streamflow data. However, for drought monitoring studies which are based on soil moisture, observed data on soil moisture and evapotranspiration under natural hydrologic conditions are lacking for ideal model calibration. Hence, a good network of observation stations that measure soil moisture and evapotranspiration would be useful in calibrating the models for simulating soil moisture and drought monitoring.
2. Microwave remote sensing data that measures the top soil moisture could be a useful source for calibrating the model simulated soil moisture. However, a good network of ground stations is needed for calibrating the microwave soil moisture data.
3. Time-stability analysis as applied by Mohanty and Skaggs (2001) could be done on the simulated soil moisture data to identify time-stable locations, which

exhibit mean behavior than other locations irrespective of the degree of wetness or dryness of the soil, for establishing a network of soil moisture monitoring stations.

4. A sensitivity analysis could be done on the drought indices to study the effect of changes in model parameters to corresponding changes in drought intensity and duration.
5. In the current study the drought indices were compared with county level crop yield data. However, if crop yield data from individual farms is available, it could be used to develop a yield forecast model based on current drought conditions.
6. Short-term and long-term weather forecasts, rainfall and temperatures, by the National Weather Service (NWS) could be used as inputs for SWAT, and drought indices ETDI and SMDI could be computed from the soil moisture for forecasting the intensity of upcoming short-term and long-term drought conditions.
7. Frequency and spatial characteristics of drought could be studied to develop an intensity-area-duration curve to characterize the spatial patterns of drought. This will help identify areas frequently affected by droughts and its spatial extent, which could be used for the development of a drought preparedness plan.
8. In the current study, due to a lack of first-order weather stations, the Cooperative Weather Station network of the National Weather Service was primarily used to correct the local bias of NEXRAD data. However, the bias adjustment could be

improved if a good network of First-order weather stations were available at the study watersheds.

REFERENCES

Akinremi, O. O., and S. M. McGinn. 1996. Evaluation of the palmer drought index on the Canadian Prairies. *Journal of Climate* 9(5): 897-905.

Akinremi, O. O., S. M. McGinn, and A. G. Barr. 1996. Simulation of soil moisture and other components of the hydrological cycle using a water budget approach. *Canadian Journal of Soil Science* 76(2): 133-142.

Allen, R. G., L. S. Pereira, D. Raes, and M. Smith. 1998. Crop evapotranspiration: Guidelines for computing crop water requirements. FAO Irrigation and Drainage Paper No. 56. Rome, Italy: Food and Agricultural Organization.

Alley, W. M. 1984. The Palmer Drought Severity Index: Limitations and assumptions. *Journal of Climate and Applied Meteorology* 23(7): 1100-1109.

Arnold, J. G., P. M. Allen, and G. Bernhardt. 1993. A comprehensive surface-groundwater flow model. *Journal of Hydrology* 143(1-4):47-69.

Arnold, J. G., and P. M. Allen. 1996. Estimating hydrologic budgets for three Illinois watersheds. *Journal of Hydrology* 176(1-4):57-77.

Arnold, J. G., R. Srinivasan, R. S. Muttiah, and J. R. Williams. 1998. Large area hydrologic modeling and assessment Part1: Model development. *Journal of the American Society of Water Resources Association* 34(1):73-89.

Arnold, J. G., R. S. Muttiah, R. Srinivasan, and P. M. Allen. 2000. Regional estimation of base flow and groundwater recharge in the Upper Mississippi River basin. *Journal of Hydrology* 227(1-4):21-40.

Bedient, P. B., B. C. Hoblit, D. C. Gladwell, and B. E. Vieux. 2000. NEXRAD radar for flood prediction in Houston. *Journal of Hydrologic Engineering* 5(3):269-277.

Bryant, E. A. 1991. *Natural Hazards.* Cambridge: Cambridge University Press.

Chaubey, I, C. T. Haan, S. Grunwald, and J. M. Salisbury. 1999. Uncertainty in the model parameters due to spatial variability of rainfall. *Journal of Hydrology* 220(1-2):48-61.

Chenault, E. A., and G. Parsons. 1998. Drought worse than 96; Cotton crops one of worst ever. http://agnews.tamu.edu/stories/AGEC/Aug1998a.htm. Accessed 9 August 2001.

Daly, C., R. P. Neilson, and D. L. Phillips, 1994: A statistical-topographic model for mapping climatological precipitation over mountainous terrain. *Journal of Applied Meteorology* 33(2):140-158.

DeFries, R., M. Hansen, and J. Townsheld. 1995. Global discrimination of land cover types from metrics derived from AVHRR pathfinder data. *Remote Sensing of Environment* 54(3):209-222.

Demarée, G. 1982. Comparison of techniques for the optimization of conceptual hydrological models. *Mathematics and Computers in Simulation* 24(2):122-130.

Di Luzio, M., R. Srinivasan, and J. G. Arnold. 2002a. Integration of watershed tools and SWAT model into basins. *Journal of the American Water Resources Association* 38(4):1127-1141.

Di Luzio, M., R. Srinivasan, J. G. Arnold, and S. L. Neitsch. 2002b. Soil and water assessment tool. ArcView GIS interface manual: Version 2000. TWRI TR-193, College Station, TX: Texas Water Resources Institute.

Dugas, W. A., M. L. Heuer, and H. S.Mayeux. 1999. Carbon dioxide fluxes over Bermudagrass, Native Prairie, and Sorghum. *Agricultural and Forest Meteorology* 93(2): 121-139.

Eckhardt, K., and J. G. Arnold. 2001. Automatic calibration of a distributed catchment model. *Journal of Hydrology* 251(1-2): 103-109.

Economic Research Service. 2000. United States fact sheet. http://www.ers.usda.gov/facts. Accessed September 11, 2003.

Engman, E. T. 1991. Applications of microwave remote sensing of soil moisture for water resources and agriculture. *Remote Sensing of Environment* 35(2-3):213-226.

Farrar, T. J., S. E. Nicholson, and A. R. Lare. 1994. The influence of soil type on the relationships between NDVI, rainfall, and soil moisture in semiarid Botswana. II. NDVI response to soil moisture. *Remote Sensing of Environment* 50(2):121-133.

Faurès, J, D. C. Goodrich, D. A. Woolhiser, and S. Sorooshian. 1995. Impact of small-scale spatial rainfall variability on runoff modeling. *Journal of Hydrology* 173(1-4):309-326.

FEMA. 1995. *National Mitigation Strategy: Partnerships for Building Safer Communities.* Washington, DC: Federal Emergency Management Agency.

Goklany, I. M. 2002. Comparing 20th century trends in U. S. and global agricultural water and land use. *International Water Resources Association* 27(3): 321-329.

Goodrich, D. C., J. Faurès, D. A. Woolhiser, L. J. Lane, and S. Sorooshian. 1995. Measurement and analysis of small scale convective storm rainfall variability. *Journal of Hydrology* 173(1-4): 283-308.

Green, W. H., and G. A. Ampt. 1911. Studies on soil physics 1: The flow of air and water through soils. *Journal of Agricultural Sciences* 4(1):1-24.

Guttman, N. B. 1998. Comparing the Palmer Drought Index and the Standardized Precipitation Index. *Journal of the American Water Resources Association* 34(1): 113-121.

Hane, D. C., and F. V. Pumphrey. 1984. *Crop Water Use Curves for Irrigation Scheduling.* Corvallis, OR: Agricultural Experiment Station, Oregon State University.

Hargreaves, G. H., and Z. A. Samani. 1985. Reference crop evapotranspiration from temperature. *Applied Engineering in Agriculture* 1(2):96-99.

Harmel, R.,D., C. W. Richardson, and K. W. King. 2000. Hydrologic response of a small watershed model to generated precipitation. *Transactions of the ASAE* 43(6): 1483-1488.

Harwell Subroutine Library. 1974. Harwell Library Subroutine VAO5A (FORTRAN computer program). Oxon, England: Hyprotech UK Ltd.

Huang, J., H. M. Van Den Dool, and K. P. Georgakakos. 1996. Analysis of model-calculated soil moisture over the United States (1931-1993) and applications to long-range temperature forecasts. *Journal of Climate* 9(6):1350-1362.

Jackson, T. J., J. Schmugge, and E. T. Engman. 1996. Remote sensing application in hydrology: Soil moisture. *Journal of Hydrologic Sciences* 41(4): 517-530.

Jayakrishnan, R. 2001. Effect of rainfall variability on hydrologic simulation using WSR-88D (NEXRAD) data. Ph.D. Dissertation, College Station, TX: Texas A&M University.

Jensen, M. E., R. D. Burman, and R. G. Allen. 1990. Evapotranspiration and irrigation water requirements. ASCE Manuals and Reports on Engineering Practice No. 70. New York, NY: American Society of Civil Engineers.

Johnson, D., M. Smith, V. Koren, and B. Finnerty. 1999. Comparing mean aerial precipitation estimated from NEXRAD and raingage networks. *Journal of Hydrologic Engineering* 4(2):117-124.

Keyantash, J., and J. A. Dracup. 2002. The quantification of drought: An evaluation of drought indices. *Bulletin of the American Meteorological Society* 83(8):1176-1180.

Krajewski, W. F., and J. A. Smith. 2002. Radar hydrology: Rainfall estimation. *Advances in Water Resources* 25(8-12):1387-1394.

Lenhart, T., K. Eckhardt, N. Fohrer, and H. G. Frede. 2002. Comparison of two different approaches of sensitivity analysis. *Physics and Chemistry of the Earth* 27(9-10):645-654.

McKee, T. B., N. J. Doesken, and J. Kleist. 1993. The relationship of drought frequency and duration to time scales. In *Proc. 8th Conference on Applied Climatology*, 179-184, 17-22 January, Anaheim, CA. Boston, MA: American Meteorological Society.

Mohanty, B. P., and T. H. Skaggs. 2001. Spatio-temporal evolution and time-stable characteristics of soil moisture within remote sensing footprints with varying soil, slope, and vegetation. *Advances in Water Resources* 24(9-10): 1051-1067.

Monteith, J. L. 1965. Evaporation and environment. In *Proc. The State and Movement of Water in Living Organisms, 19th Symposia of the Society of Experimental Biology*, 205-234, Swansea, UK. Cambridge, UK: Cambridge University Press.

Nash, J. E., and J. V. Sutcliffe. 1970. River flow forecasting through conceptual models part I - A discussion of principles. *Journal of Hydrology* 10(3): 282-290.

Neitsch, S. L., J. G. Arnold, J. R. Kiniry, J. R. Williams, and K. W. King. 2002. Soil and water assessment tool. Theoretical documentation: Version 2000. TWRI TR – 191. College Station, TX: Texas Water Resources Institute.

Palmer, W. C. 1965. Meteorological drought. Research Paper 45. Washington, D.C.: U.S. Department of Commerce, Weather Bureau.

Palmer, W. C. 1968. Keeping track of crop moisture conditions, nationwide: The new crop moisture index. *Weatherwise* 21(4):156-161.

Priestley, C. H. B., and R. J. Taylor. 1972. On the assessment of surface heat flux and evaporation using large-scale parameters. *Monthly Weather Review* 100(2):81-92.

Ritchie, J. T. 1972. A model for predicting evaporation from a row crop with incomplete cover. *Water Resources Research* 8(5):1204-1213.

Riggo, R. F., G. W. Bomar, and T. J. Larkin. 1987. Texas drought: Its recent history (1931-1985). Report No: LP 87-04. Austin, TX: Texas Water Commission.

Saleh, A., J. G. Arnold, P. W. Gassman, L. M. Hauck, W. D. Rosenthal, J. R. Williams, and A. M. S. McFarland. 2000. Application of SWAT for the Upper North Bosque River watershed. *Transactions of the ASAE* 43(5):1077-1087.

Santhi, C., J. G. Arnold, J. R. Williams, W. A. Dugas, R. Srinivasan, and L. M. Hauck. 2001. Validation of the SWAT model on a large river basin with point and non-point sources. *Journal of American Water Resources Association* 37(5): 1169-1188.

Sellers, P. J., Y. Mintz, Y. C. Sud, and A. Dalcher. 1986. A simple biosphere model (SiB) for use within general circulation models. *Journal of the Atmospheric Sciences* 43(6): 505-531.

Seo, D.-J., J. P. Breidenbach, and E. R. Johnson. 1999. Real-time estimation of mean field bias in radar rainfall data. *Journal of Hydrology* 223(1-4):131-147.

Shafer, B. A., and L. E. Dezman. 1982. Development of surface water supply index (SWSI) to assess the severity of drought conditions in snow pack runoff areas. In *Proc. 50th Western Snow Conference*, 164-175. Reno, NV. Fort Collins, CO: Colorado State University Press.

Sharp, J. 1996. *Texas and the 1996 Drought.* Austin, TX: Texas Comptroller of Public Accounts.

Smith, J. A., D.-J. Baeck, M. Baeck, and M. D. Hudlow. 1996. An intercomparison study of NEXRAD precipitation estimates. *Water Resources Research* 32(7):2035-2045.

Sophocleous, M., and S. P. Perkins. 2000. Methodology and application of combined watershed and ground-water models in Kansas. *Journal of Hydrology* 236(3-4):185-201.

Spruill, C.A., S. R. Workman, and J. L. Taraba. 2000. Simulation of daily and monthly stream discharge from small watersheds using the SWAT model. *Transactions of the ASAE* 43(6): 1431-1439.

Srinivasan, R., and J. G. Arnold. 1994. Integration of a basin-scale water quality model with GIS. *Journal of the American Water Resources Association* 30(3):453-462.

Srinivasan, R., J.G. Arnold, and C. A. Jones. 1998a. Hydrologic modeling of the United States with the soil and water assessment tool. *International Journal of Water Resources Development* 14(3):315-325.

Srinivasan, R., T. S. Ramanarayanan, J. G. Arnold, and S.T. Bednarz. 1998b. Large area hydrologic modeling and assessment part II: Model application. *Journal of the American Water Resources Association* 34(1): 91 – 101.

Tannehill, I. R. 1947. *Drought: Its Causes and Effects.* Princeton, NJ: Princeton University Press.

TASS. 2003. Texas Agricultural Statistics Service: 2002 county estimates. http://www.nass.usda.gov/tx/index.htm. Accessed Nov.18 2003.

Texas Agricultural Experiment Station. 2000. Brush management/water yield feasibility studies for eight watersheds in Texas. TWRI TR-182. College Station, TX: Texas Water Resources Institute.

Thornthwaite, C. W. 1948. An approach toward a rational classification of climate. *Geographical Review* 38(January):55-94.

USDA Soil Conservation Service. 1972. *National Engineering Handbook.* Hydrology Section 4, Chapters 4-10. Washington, DC: GPO.

USDA Soil Conservation Service. 1992. *States Soil Geographic Database (STATSGO) Data User's Guide.* No. 1492, Washington, DC: GPO.

USGS. 1993. Digital Elevation Model guide. http://edc.usgs.gov/guides/dem.html. Accessed May 4, 2004.

Van Griensven, A., and W. Bauwens. 2001. Integral water quality modelling of catchments. *Water Science and Technology* 43(7): 321-328.

Verigo, S. A., and L. A. Razumova. 1966. *Soil Moisture and Its Significance in Agriculture*. Jerusalem: Israel Program for Scientific Translations.

Vogelmann, J.E., S.M. Howard, L. Yang, C. R. Larson, B. K. Wylie, and J. N. Van Driel. 2001. Completion of the 1990's national land cover data set for the conterminous United States. *Photogrammetric Engineering and Remote Sensing* 67(6):650-662.

Wilhite, D. A. 2000. Drought as a natural hazard: concepts and definitions. In *Drought: A Global Assessment (Vol. I)*, ed. Donald A. Wilhite, ch.1, 3-18, New York: Routledge.

Wilhite, D. A., and M. H. Glantz. 1985. Understanding the drought phenomenon: the role of definitions. *Water International* 10(3):111-120.

Williams, J. R., C. A. Jones, and P. T. Dyke. 1984. A modeling approach to determining the relationship between erosion and soil productivity. *Transactions of the ASAE* 27(1):129-144.

Zazueta, F.S., and J. Xin. 1994. Soil moisture sensors. Bulletin no.292. Gainesville, FL: Florida Cooperative Extension Service, University of Florida.

VITA

Balaji Narasimhan
Spatial Sciences Lab,
1500 Research Parkway Suite B223
College Station, Texas 77845.
Tel. 979-468-8051; Fax. 979-862-2607
E-mail: balaji_nn@hotmail.com

Educational Background:
Ph.D., Agricultural Engineering, 2004, Texas A&M University, College station, USA.
M.S., Agricultural Engineering, 1999, University of Manitoba, Winnipeg, Canada.
B.E., Agricultural Engineering, 1997, Tamil Nadu Agricultural University, Trichy, India.

Experience:
1999 – Present Graduate Research/Teaching Assistant, Texas A&M University, USA.
1997 – 1999 Graduate Research/Teaching Assistant, University of Manitoba, Canada.

Refereed Journal Articles:

Narasimhan, B., R. Srinivasan, and A. D. Whittaker. 2003. Estimation of Potential Evapotranspiration from NOAA-AVHRR Satellite. *Applied Engineering in Agriculture* 19(3): 309-318.

Chen, P. Y., R. Srinivasan, G. Fedosejevs, and B. Narasimhan. 2002. An Automated Cloud Detection Method for Daily NOAA-14 AVHRR Data for Texas, U.S.A. *International Journal of Remote Sensing* 23(15): 2939-2950.

Narasimhan, B. and Sri Ranjan, R. 2000. Electrokinetic Barrier to Prevent Subsurface Contaminant Migration: Theoretical Model Development and Validation. *Journal of Contaminant Hydrology* 42(1):1-17.

Selected Conference Proceedings:

Narasimhan, B., and R. Srinivasan. 2003. Developing an Agricultural Drought Assessment System Using Hydrologic Model SWAT and GIS. ASAE meeting Paper No. 032118. St. Joseph, Mich.: ASAE.

Narasimhan, B., and R. Srinivasan. 2002. Development of a Soil Moisture Index for Agricultural Drought Monitoring Using a Hydrologic Model (SWAT), GIS and Remote Sensing. Texas Water Monitoring Congress. September 9-11, 2002. Austin, TX.

Srinivasan, R., and Narasimhan, B. 2001. Estimation of Drought Index (KBDI) in Real-Time Using GIS and Remote Sensing Technologies. ASAE meeting Paper No. 013054. St. Joseph, Mich.: ASAE.